BIODEGRADATION OF PARAFFIN WAX

by

Fabien Marino

Department of Chemical Engineering
McGill University, Montréal

December, 1998

A thesis submitted to the Faculty of Graduate Studies and Research in partial fulfilment of the requirements of the degree of Master of Engineering.

ABSTRACT

Nineteen bacteria were tested for growth on paraffin wax as the sole source of carbon. Paraffin wax is a solid mixture of hydrocarbons including *n*-alkanes ranging from $C_{18}H_{38}$ to $C_{37}H_{76}$. Of the nineteen bacteria tested, four bacteria (*Arthrobacter paraffineus* ATCC 19558, *Mycobacterium* OFS, *Pseudomonas fluorescens* Texaco and *Rhodococcus* IS01) grew well on paraffin wax. However, only one, *Rhodococcus* IS01, was found to rapidly and completely degrade a mixture of paraffin wax liquefied with hexadecane using the Self-Cycling Fermentation (SCF) technology. This strain was able to degrade *n*-alkanes ranging from dodecane to heptatriacontane as well as highly branched hydrocarbons such as pristane and hepta-methyl-nonane.

Kinetic studies performed with *Rhodococcus* IS01 growing on mixtures of *n*-alkanes showed that the hydrocarbons were degraded in ascending order of chain length: shortest to longest chain. The short lag period between the biodegradation of the different *n*-alkanes suggested that the growth of *Rhodococcus* IS01 on mixtures of *n*-alkanes followed some form of diauxie. Further kinetic studies were conducted growing *Rhodococcus* IS01 on individual and various mixtures of n-alkanes; these showed that the initial first-order oxidation constant decreased with increasing chain length. This trend is suspected to be due to an enzyme specificity constraint rather than to a mass transfer limitation. In addition, it was also observed that the maximum specific growth rate constant (μ_{max}) increased with increasing *n*-alkane chain length.

Rhodococcus IS01 was also found to produce a cell-associated biosurfactant.

RÉSUMÉ

Dix-neuf bactéries ont été testées afin de déterminer si elles pouvaient utiliser de la cire de parrafine comme unique source de carbone. La paraffine est un mélange solide d'hydrocarbures comprenant des *n*-alcanes allant de $C_{18}H_{38}$ à $C_{37}H_{76}$. Des dix-neuf bactéries testées, quatre souches bactériennes (*Arthrobacter paraffineus* ATCC 19558, *Mycobacterium* OFS, *Pseudomonas fluorescens* Texaco et *Rhodococcus* IS01) ont put être cultivé avec de la paraffine. Cependant, une seule de ces souches bactériennes, *Rhodococcus* IS01, a pu dégrader rapidement et complètement un mélange de cire liquéfié avec de l'hexadécane en utilisant la technologie de la Fermentation Auto-Cyclique (FAC). Cette souche a l'abileté de biodégrader des *n*-alcanes allant du dodécane au heptatriacontane ainsi que des hydrocarbures fortement embranchés tels que le pristane et le hepta-méthyl-nonane.

Les études cinétiques performées avec *Rhodococcus* IS01 cultivé sur des mélanges de *n*-alcanes ont démontrées que les hydrocarbures furent dégradés dans un ordre croissant de longueurs des chaînes d'hydrocarbures: de la plus courte à la plus longue chaîne. Le court délai entre la biodégradation des différents *n*-alcanes a suggéré que la croissance du *Rhodococcus* IS01 sur des mélanges de *n*-alcanes est charactérisée par une certaine forme de diauxie. D'autres études cinétiques réalisées avec *Rhodococcus* IS01 cultivé sur des mélanges de *n*-alcanes ainsi que sur des *n*-alcanes individuels ont démontré que la constante d'oxydation initiale de premier ordre a diminué avec l'augmentation de la longueur des chaînes des *n*-alcanes. Il est possible que cette tendance soit attribuée à une contrainte de spécificité des enzymes plutôt qu'à une limitation du transfert de masse des hydrocarbures. Il a également été constaté que la constante spécifique de croissance maximum (μ_{max}) a augmenté avec l'augmentation de la longueur des chaînes des *n*-alcanes.

Rhodococcus IS01 a produit un biosurfactant associé aux cellules lors de sa culture sur hydrocarbures.

ACKNOWLEDGEMENTS

The past two years have been fruitful, I became a Ninja and I got a Master's degree! It was fun but it's time to go, I've realized that I can't keep on wasting my good looks and brawniness in academia like this.

First and foremost, I would like to express my most sincere gratitude and appreciation to the almighty Dr. D.G. Cooper. Thank you for your support, extraordinary patience, advice, infinite knowledge and teachings over the years. Another mission accomplished for you!

Special thanks to my superstar girlfriend Aphrodite for her immense support, love (if you know what I mean!) and exuberance♥. Yes the name is real! One question: "Does going out with a superstar make you a superstar? I would like to think so!".

Huge thanks also go to all the members of the Falcon group: Wayne Brown, Scot Hughes, Stefan Muller, John Crosman, Frank Godin, Rob Pinchuk, Mike May, Jonathan Webber, Yin Choi Lim, Jeff Barriga, Bill McCaffrey. And also to the summer students: Jeff Karp, Gregan Dunn, Timmy DiStefano, Sandro Nalli, Mike Silverberg, Jimmy Gartshore and Declan Brady. We did some crazy and juicy stuff! I now know what it is like to live in a zoo!

I would also like to say thank you to the faculty and staff of the department of Chemical Engineering at McGill for their precious help during the last 24 months. Very special thanks to Dr. Berk, Dr. Rey, Dr. Weber, Anne Prihoda, Barbara Hanley, Louise Miller, Joanne Terrasi, Pat Fong and Mike Harrigan. Nine words, "never underestimate the power of the administrative staff, ever"!

Thank you to my parents who never had a clue what I was doing but always encouraged me and always believed in me! Warm thanks to all my friends for keeping my sanity intact all this time. Thanks to Felix Hinojosa and Mitch "The predator" Cyl, the ambassadors of JKD. Thanks for understanding why I don't want to become a professional kickboxer!

In Bruce Lee's immortal words "Take what is useful and discard the rest"! Ok, must go now... must get to platform... mothership is waiting! 👽

TABLE OF CONTENTS

1.0 INTRODUCTION **1**

1.1 BIOREMEDIATION OF LONG CHAIN *N*-ALKANES 1
1.2 PROBLEMS ASSOCIATED WITH THE BIODEGRADATION OF SOLID *N*-ALKANES 5
1.2.1 Modes of insoluble substrate uptake *5*
1.2.2 Microbial metabolism of long-chain n-alkanes *7*
1.3 FERMENTATION METHODS 11

2.0 OBJECTIVES **14**

3.0 MATERIALS AND METHODS **15**

3.1 MICROORGANISMS 15
3.2 MEDIA AND CULTURE CONDITIONS 16
3.3 SCREENING OF PARAFFIN WAX DEGRADING BACTERIA 16
3.3.1 Modified Kiyohara method *17*
3.3.2 Shake-flasks experiments *17*
3.4 SELF-CYCLING FERMENTATIONS 17
3.5 BIOMASS MEASUREMENT 18
3.5.1 End of cycle biomass *18*
3.5.2 Intracycle biomass *18*
3.6 HYDROCARBON MEASUREMENT 19
3.7 SURFACE TENSION MEASUREMENT 21
3.8 EMULSION TEST 21
3.9 pH DETERMINATION 21
3.10 DETERMINATION OF K_LA 21
3.11 DETERMINATION OF THE PARAMETERS OF THE MONOD EQUATION 23

4.0 EXPERIMENTAL APPARATUS **25**

4.1 BALANCE *VERSUS* DIFFERENTIAL PRESSURE (DP) CELL 26
4.2 OXYGEN TRANSFER 30

5.0 RESULTS **31**

5.1 SELECTION OF MICROORGANISMS 31
5.2 SELF-CYCLING FERMENTATIONS 33
5.2.1 Self-Cycling Fermentation with Mycobacterium OFS *33*
5.2.2 Self-Cycling Fermentation with Arthrobacter paraffineus ATCC 19558 ..... *36*
5.2.3 Self-Cycling Fermentation with Pseudomonas fluorescens Texaco *39*
5.2.4 Self-Cycling Fermentation with *Rhodococcus* IS01 ..... *41*
5.3 ABIOTIC RUN 55
5.4 FIRST-ORDER OXIDATION RATE CONSTANTS K 56
5.5 MAXIMUM SPECIFIC GROWTH RATE μ_{MAX} 57
5.6 HYDROCARBON METABOLITE 61

6.0 DISCUSSION **67**

6.1 BIOREMEDIATION OF PARAFFIN WAX 67
6.2 METABOLITES 69
6.3 KINETIC STUDIES 70
6.3.1 First-order oxidation rate constant *72*
6.3.2 Maximum specific growth rate constant *77*
6.4 METABOLISM OF *N*-ALKANES 79

7.0 CONCLUSION **81**

8.0 REFERENCES **82**

9.0 APPENDIX A: INTRACYCLE BIOMASS MEASUREMENT TECHNIQUE **89**

10.0 APPENDIX B: MODELING OF RUN#7 WITH A GENETIC ALGORITHM **94**

LIST OF TABLES

Table 3-1: Name, source and optimum temperature of tested microorganisms. 15
Table 3-2: Media formulations. 16
Table 3-3: GC Operating conditions for hydrocarbon analysis. 19
Table 3-4: Hydrocarbon GC retention times. 20

Table 5-1: Growth of tested microorganisms after 7 days. 32
Table 5-2: Initial substrate concentrations and Ks values for run#7. 56

Table 10-1: Values of parameters obtained with GA. 97

LIST OF FIGURES

Figure 1-1: Chromatograms of crude oil and paraffin wax. 2

Figure 3-1: Calibration curves for hexadecane and eicosane. 20

Figure 4-1: Schematic of the cyclone SCF reactor set-up with DP transducer. 28

Figure 4-2: Schematic of the cyclone SCF reactor set-up with balance. 29

Figure 5-1: Concentration of hexadecane(○) and wax (◊) *versus* time: run #3, cycle 9, *Mycobacterium* OFS. 35

Figure 5-2: Dissolved oxygen trace: run#3, *Mycobacterium* OFS. 35

Figure 5-3: Concentration of hexadecane (□) and wax (○) *versus* time: run #4, cycle 27, *Arthrobacter paraffineus* ATCC 19558. 37

Figure 5-4: Concentration of paraffin wax (○) *versus* time: run #4, cycle 27 , *Arthrobacter paraffineus* ATCC 19558. 37

Figure 5-5: Dissolved oxygen trace: run#4, *Arthrobacter paraffineus* ATCC 19558. 38

Figure 5-6: Surface tension measurements for *Arthrobacter paraffineus* ATCC 19558. Data for this work (□) and Duvniak *et al.*'s work (○). 38

Figure 5-7: Dissolved oxygen trace: run#6, *Pseudomonas fluorescens* Texaco. 40

Figure 5-8: Dissolved oxygen trace: cycles with pristane, run#7, *Rhodococcus* IS01. 42

Figure 5-9: Dissolved oxygen trace: cycles with hexadecane, run#7, *Rhodococcus* IS01. 43

Figure 5-10: Concentration of biomass (◆), hexadecane (□) and wax (○) *versus* time: run #7, cycle 36, *Rhodococcus* IS01. 43

Figure 5-11: Concentration of hexadecane (□) and wax (○) *versus* time: run #7, cycle 36, *Rhodococcus* IS01. 44

Figure 5-12: Concentration of *n*-alkanes $C_{20}H_{42}$ (▲), $C_{21}H_{44}$ (□), $C_{22}H_{46}$ (●),$C_{23}H_{48}$ (Δ),$C_{24}H_{50}$ (■), $C_{25}H_{52}$ (○), run #7, cycle 36, *Rhodococcus* IS01. 44

Figure 5-13: Concentration of *n*-alkanes $C_{26}H_{54}$ (●),$C_{27}H_{56}$ (□),$C_{28}H_{58}$ (▲),$C_{29}H_{60}$ (○),$C_{30}H_{62}$ (■),$C_{31}H_{64}$ ()), run #7, cycle 36, *Rhodococcus* IS01. 45

Figure 5-14: Concentration of *n*-alkanes $C_{32}H_{66}$ (○),$C_{33}H_{68}$ (■),$C_{34}H_{70}$ (Δ),$C_{35}H_{72}$ (●),$C_{36}H_{74}$ (□),$C_{37}H_{76}$ (▲), run #7, cycle 36, *Rhodococcus* IS01 45

Figure 5-15: Concentration of hexadecane (■) and biomass (Δ), run #7, cycle 5, *Rhodococcus* IS01. 47

Figure 5-16: Concentration of hexadecane (■), dodecane (○) and biomass (Δ), run #7, cycle 11, *Rhodococcus* IS01. 47

Figure 5-17: : Concentration of hexadecane (■), heptadecane (○) and biomass (Δ), run #7, cycle 16, *Rhodococcus* IS01. 48

Figure 5-18: Concentration of hexadecane (■), eicosane (●) and biomass (Δ), run #7, cycle 22, *Rhodococcus* IS01. 48

Figure 5-19: Concentration of hexadecane (■), pentacosane (◆) and biomass (Δ), run #7, cycle 28, *Rhodococcus* IS01. 49

Figure 5-20: Concentration of dodecane (○), hexadecane (■), heptadecane (□), eicosane (●), pentacosane (◆) and biomass (Δ),run #7, cycle 32, *Rhodococcus* IS01. 49

Figure 5-21: Concentration of dodecane (○) and pristane (□), run #7, cycle 38, *Rhodococcus* IS01. 51

Figure 5-22: Concentration of hexadecane (○) and pristane (□), run #7, cycle 43, *Rhodococcus* IS01. 51

Figure 5-23: Concentration of eicosane (○) and pristane (□), run #7, cycle 48, *Rhodococcus* IS01. 52

Figure 5-24: Concentration of pentacosane (○) and pristane (□), run #7, cycle 52, *Rhodococcus* IS01. 52

Figure 5-25: Concentration of mixture #1 of dodecane (○), heptadecane (■), eicosane (●), pentacosane (◆), pristane (□) and biomass (Δ), run #7, cycle 57, *Rhodococcus* IS01. 53

Figure 5-26: Concentration of mixture #2 of dodecane (○), heptadecane (■), eicosane (●), pentacosane (◆) and pristane (□), run #7, cycle 62, *Rhodococcus* IS01. 53

Figure 5-27: Concentration of eicosane (●), pentacosane (◊), triacontane (○) and pristane (□), run #7, cycle 66, *Rhodococcus* IS01. 54

Figure 5-28: Carbon dioxide evolution for pristane and $C_{16}H_{34}$ run and pristane and $C_{20}H_{42}$, run#7, *Rhodococcus* IS01. 54

Figure 5-29: Concentration of dodecane (○), hexadecane (■), heptadecane (□), eicosane (●), pentacosane (◆) and pristane (Δ), Abiotic run 55

Figure 5-30: First-order oxidation rate constants *versus*. carbon number. Pristane and individual *n*-alkanes (□), pristane and mixture of $C_{12}H_{26}$, $C_{17}H_{36}$, $C_{20}H_{42}$ & $C_{25}H_{52}$ #1 (●),pristane and mixture of $C_{12}H_{26}$, $C_{17}H_{36}$, $C_{20}H_{42}$ & $C_{25}H_{52}$ #2 (◊), pristane and mixture of $C_{20}H_{42}$, $C_{25}H_{52}$ and $C_{30}H_{62}$ (▲)..... 58

Figure 5-31: First-order oxidation rate constants *versus*. carbon number. Hexadecane and individual *n*-alkanes (□), hexadecane with mixture of $C_{12}H_{26}$, $C_{17}H_{36}$, $C_{20}H_{42}$ & $C_{25}H_{52}$ (○). 58

Figure 5-32: First-order oxidation rate constants *versus*. carbon number. Hexadecane and individual *n*-alkanes from paraffin wax (○), run #7, cycle 36, *Rhodococcus* IS01 . 59

Figure 5-33: Maximum specific growth rate μ_{max} *versus*. carbon number. Pristane and individual *n*-alkanes (□), pristane and mixture of $C_{12}H_{26}$, $C_{17}H_{36}$, $C_{20}H_{42}$ & $C_{25}H_{52}$ #1 (●), pristane and mixture of $C_{12}H_{26}$, $C_{17}H_{36}$, $C_{20}H_{42}$ & $C_{25}H_{52}$ #2 (◊), pristane and mixture of $C_{20}H_{42}$, $C_{25}H_{52}$ and $C_{30}H_{62}$ (□). 59

Figure 5-34: Maximum specific growth rate μ_{max} *versus* carbon number. Hexadecane and individual *n*-alkanes (□), hexadecane with mixture of $C_{12}H_{26}$, $C_{17}H_{36}$, $C_{20}H_{42}$ & $C_{25}H_{52}$ (○). 60

Figure 5-35: Gas chromatogram of paraffin wax, run#7, cycle 36, sample 2, *Rhodococcus* IS01. 62

Figure 5-36: Gas chromatogram of paraffin wax, run#7, cycle 36, sample 9, *Rhodococcus* IS01. The unknown peak appears at 19.132 minutes..... 63

Figure 5-37: Unknown peak concentration over time, run#7, cycle 36, *Rhodococcus* IS01. 63

Figure 5-38: Concentration of unknown peak during growth on hexadecane and pentacosane, run #7, cycle 28, *Rhodococcus* IS01. 64

Figure 5-39: Concentration of unknown peak during growth on dodecane, hexadecane, heptadecane, eicosane and pentacosane, run #7, cycle 32, *Rhodococcus* IS01. 64

Figure 5-40: Concentration of unknown peak during growth on mixture #1 composed of dodecane, heptadecane, eicosane, pentacosane and pristane, run #7, cycle 57, *Rhodococcus* IS01..... 65

Figure 5-41: Concentration of unknown peak during growth on pentacosane and pristane, run #7, cycle 52, *Rhodococcus* IS01..... 65

Figure 5-42: Mass spectrograph of unknown compound 66

Figure 6-1: Example of a concave-down profile fit with two first-order fits. 74

Figure 10-1: Biomass and hexadecane concentrations *versus* time. Experimental data (o), model prediction (—)..... 98

Figure 10-2: Eicosane to heptacosane concentrations *versus* time. Experimental data (o), model prediction (—)..... 99

Figure 10-3: Octacosane to pentatriacontane concentrations *versus* time. Experimental data (o), model prediction (—). 100

Figure 10-4: Hexatriacontane and heptatriacontane concentrations *versus* time. Experimental data (o), model prediction (—)..... 101

1.0 INTRODUCTION

With the recent spill of the *Sea Empress* off the coast of Wales, the Gulf War, the 1989 spill of more than 200 000 barrels of crude oil from the oil tanker *Exxon Valdez* in Prince William Sound, Alaska and other unreported spills, the hydrocarbon contamination of the marine environment is a clear and present problem[85]. It is estimated that between 1.7 and 8.8 million metric tons of petroleum per year ends up in our ecosystem[21]. As soon as it is introduced in the marine environment, chemical, physical and biological processes act on the petroleum[11]. Microbial degradation of these hydrocarbons by indigenous population of microorganisms is considered an essential step by which petroleum and other hydrocarbon pollutants are eliminated[11].

Oil spills have traditionally been tackled using dispersant chemicals, or by removing the oil physically. The problem is that the chemicals must be added immediately after the spill before the volatile component evaporate and the oil weathers to a tar-like consistency, at which point the cleaning becomes more troublesome[85].

1.1 Bioremediation of long chain *n*-alkanes

The mineralization, or complete biodegradation, of an organic molecule in waters and soil is almost always a consequence of microbial activity[84]. In general, the biodegradation of aliphatic pollutants is affected by biological and physico-chemical factors. Biological factors include the enzymatic activity of the microorganisms on the alkanes and the transport limitation of the substrate across the membrane[68]. The rate of mineralization of the pollutant is a function of the availability of the chemicals and the quantity of the active microbes[13]. The physico-chemical factors include the fermentation conditions and the substrate characteristics such as its water solubility, viscosity, diffusivity and surface tension[68].

Various studies have been made on the microbial degradation of hydrocarbons from ecological viewpoints and several have dealt with the isolation of microorganisms capable of growing on *n*-paraffins. Information on the biodegradation of long chains *n*-alkanes such as paraffin wax is interesting for bioremediation technology since heavy oil

sediments contain appreciable proportions of such alkanes (see figure 1-1). Paraffin wax is a cheap petroleum component that is composed mainly of solid *n*-paraffins ($C_{18}H_{38}$ to $C_{37}H_{76}$) and is obtained as a by-product during the production of lubricating oils[87]. Solid *n*-alkanes are a distinct class of *n*-paraffins found in different environmental aspects from crude oil spillage to plant cuticular wax[92]. At present paraffin wax is mainly used for candles and damp-proofing paper.

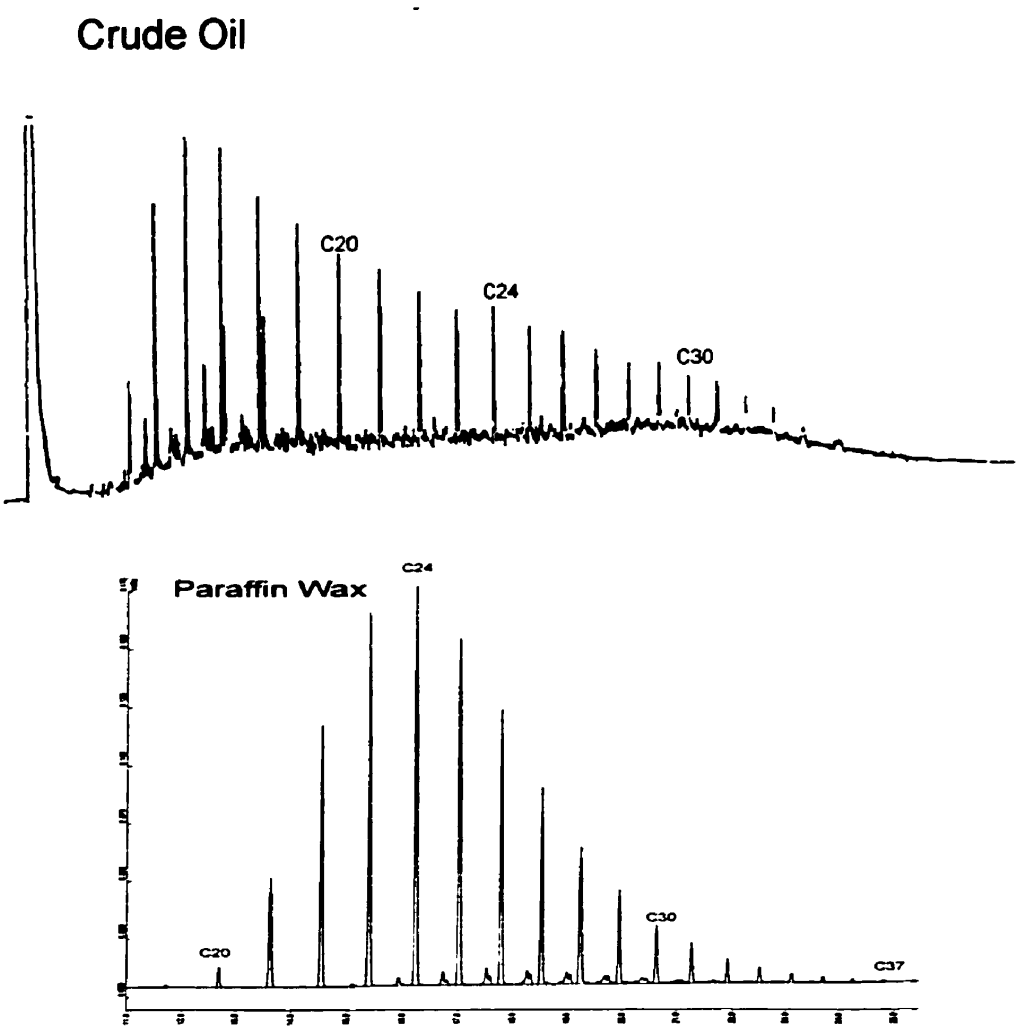

Figure 1-1: Gas chromatograms of crude oil and paraffin wax.

Growth of microorganisms (monera and fungi kingdom) on *n*-alkanes and hydrocarbons is documented extensively in the literature[1,8,9,10,13,15,19,34,45,47,48,50,55,62,63,66,68]. Studies have been performed with mixed and axenic cultures utilizing individual, or mixtures of, hydrocarbons as substrates.

At the macroscopic level, yeasts, molds and bacteria are all invisible to the eye and can be grossly characterized as simple biocatalysts. However, there are fundamental differences between yeasts, molds and bacteria. In the literature, it is common to see comparisons between results reported for experiments conducted with yeasts and results for studies conducted with bacteria for example. Yeasts and bacteria are both microorganisms and have some similarities but they differ greatly in other aspects such as their mode of reproduction, their internal structure and more importantly for this work, their modes of nutrient absorption. Yeasts are eukaryotic organisms (the DNA is contained within a nucleus) while bacteria are prokaryotic (the DNA lies loose inside the cell). The difference between bacteria could even be brought down to the Gram level. It is well known that Gram-positive and Gram-negative bacteria are similar in some features and very different in other features (e.g. cell surface, which could be of importance for hydrocarbon transport through the cell). The work presented here only deals with bacteria. References to results involving fungi will be clearly stated.

Before bioremediation of hydrocarbons became the most urgent aspect of hydrocarbon biodegradation, as early as the 1950's, growth of the microorganisms on hydrocarbons was gaining significance[15,16]. For example, single cell protein production from crude oil was widely examined[15,16]. It quickly became evident that growth on alkanes had several other advantages such as the production of commercially useful secondary metabolites[19]. Microorganisms growing on alkanes have been reported to produce amino acids, carbohydrates, nucleic acids, lipids, organic acids, vitamins, coenzymes, antibiotics and biosurfactants to name a few[19].

Biodegradation in a solid medium (*i.e.* soil bioremediation) is gaining popularity but bioremediation of hydrocarbons in aqueous environment still remains the more researched topic. To allow bioremediation to occur, microorganisms require a water

activity between 0.9 and 1.0[82]. Two types of carbon sources can be encountered in the environment: water soluble (e.g. glucose) and water insoluble (e.g. hexadecane). One rate limiting step of any biodegradation process is the carbon availability[1].

The main goal of this study was to biodegrade paraffin wax, a solid mixture of long chain *n*-alkanes varying from 18 to 37 carbons (melting point≈65°C), using it as the sole carbon source. Paraffin wax is insoluble and is solid at room temperature. Suitable growth substrates are usually assumed to be liquid rather than solid long-chain *n*-alkanes. With a solid substrate an important problem is its availability for biodegradation by the microbial community. It has been shown that the solid hydrocarbons tend to agglomerate together thereby making it harder for the cells to access it[15]. Lower available surface area results in slower growth rates[28].

A wide variety of microbes are able to use long chains hydrocarbons as their sole source of carbon and energy[88]. Microorganisms can utilize both liquid and solid hydrocarbons if they are dissolved in the medium. Linear growth has been reported for cells growing on solid hydrocarbons while exponential growth has been reported for growth on liquid hydrocarbons[2,17,18]. However, it was demonstrated that if the solid substrate was dissolved by a biodegradable or non-biodegradable solvent, the rate of oxidation greatly increased and showed exponential growth[2,15,17]. The microorganisms used solid *n*-paraffins to a large extent when they were dissolved in an organic phase. The use of such a solvent increased the substrate's solubility and its available surface area. This increase in surface area accelerated the mineralization of the hydrocarbon pollutants[15]. Pristane, a branched hydrocarbon has been used as a solvent to accelerate the biodegradation of solid hydrocarbons[15,16,17]. The authors demonstrated that the cell yield was unaffected by pristane. In the presence of hexadecane, the utilization of pristane appeared to be suppressed suggesting that the microbes were using the substrate that was easier to degrade preferentially (which makes sense on an energetic point of view)[15]. The range of *n*-alkanes that can be dissolved in pristane is, of course, limited by their solubility in pristane. Hepta-methyl nonane, another branched hydrocarbon could also potentially be used as a solvent. It has also been demonstrated that when exposed to water insoluble substrates, some microorganisms have the ability to produce

biosurfactants. These biosurfactants lower the medium's surface tension, thus increasing the surface area available to the microbes[14].

1.2 Problems associated with the biodegradation of solid *n*-alkanes

There are two problems associated with the biodegradation of hydrocarbons by microorganisms. First, the insoluble substrate cannot enter the cells and second, the cells do not produce the necessary enzymes needed to metabolize the hydrocarbons. Microbes able to grow on hydrocarbons have shown the ability to accumulate the paraffinic substrate intracellularly in inclusion bodies[22]. The uptake of the solid *n*-alkanes by microorganisms is believed to occur through transport across the cell membrane[22]. This passage through the cells is a crucial step for the catabolism of these chemicals. It has been shown that it can even be limiting for very long chains (up to 36 carbons)[34]. To be able to catabolize the long-chain hydrocarbons, a microorganism must have the phenotype allowing it to do so by producing the degrading enzymes.

1.2.1 Modes of insoluble substrate uptake

The exact mode of uptake of hydrocarbons by microorganisms is unclear. Three mechanisms are generally accepted as possible mechanisms for the uptake of insoluble hydrocarbon by bacteria and yeasts[27,35,40,42]. 1) The cells utilize the hydrocarbons dissolved in the aqueous phase. 2) The cells utilize "solubilized/pseudosolubilized" or "accommodated" submicron droplets of hydrocarbon. 3) The cells utilize the substrate through a direct contact with large hydrocarbon drops.

Early workers with yeasts assumed that cells could not grow directly on the liquid hydrocarbon and could not grow on solid hydrocarbon by directly growing on the solid phase of the substrate[2]. They argued that cells grew on the substrate dissolved in the aqueous medium[24]. *N*-alkanes have extremely low solubility in water. The solubility of dodecane in distilled water is 3.7 ppb, hexadecane is 0.9 ppb, eicosane is 1.9 ppb and hexacosane is 1 ppb[26]. Several studies demonstrated that the rates of dissolution of

hydrocarbons were not sufficient to support growth of the cells. The microbes were using more hydrocarbons during growth than the amount that was dissolved or diffused in the aqueous phase[24,33]. Some researchers postulated that the cells needed a chemical that helped them dissolve additional substrate to grow. The theory of submicron droplets adsorbing to cells for growth not limited by transport came about[24,33]. These pseudosolubilized or accommodated submicron droplets were formed by cellular and/or extracellular lipids that acted as surfactants to create micro or macroemulsions[22,33,43]. There has been evidence that the interfacial area between water and oil increased as some fermentations proceeded due to extracellular products such as lipids (maybe in the form of micelles), fatty acids or the cells themselves which were directly responsible for pseudosolubilization of the hydrocarbon substrate[27,38]. Surface active materials have been shown to increase the specific growth rate of cells[1,36,39]. Velankar *et al.* proposed that the hydrocarbon surface area is a growth limiting factor while the number of micelles mediating the hydrocarbon transport is a rate limiting factor[38]. They also suggested that if the substrate mass transfer occurred by direct contact between the microbes and hydrocarbon large droplets (>1 :m) different length *n*-alkanes should have been used up at the same rate which was not the case for their study. They argue that short chains are solubilized faster into micelles than long chains. Therefore, the rates of degradation are faster for shorter chain hydrocarbons[38]. However, nowhere do they mention or talk about enzyme specificity. EDTA can inhibit pseudosolubilization because it can bind the Ca^{++} ions needed for pseudosolubilization activity. Also, in the case of pseudosolubilization, the agitation rates have no effect on growth rates[35].

Another mode of transport, that has been suggested, is the microbial transfer of insoluble hydrocarbon occurring through direct contact between the organisms and the insoluble hydrocarbons[25]. It is unclear whether this mode of uptake is mediated by facilitated diffusion or be active transport at the point of contact[35,41]. However, it is clear that this mode of uptake is dependent on the interfacial area between the cells and the hydrocarbons[27,38,29]. A high interfacial surface area correlated with a high cell productivity[25]. The surface area and hence the rate of mass transfer can be increased by increased agitation intensity and/or by the presence of bioemulsifiers or

biosurfactants[27,35,38,39,40]. Cells that were able to grow on hydrocarbons demonstrated the ability to strongly adhere to the hydrocarbons while cells that were unable to utilize insoluble hydrocarbons did not[22]. The adherence of microorganism is important for growth on oil[32]. Bacterial adherence, the mechanism by which cells adsorb to the surface of large insoluble hydrocarbon drops, seems to be the mechanism by which most substrate is transported inside the cells[28,29,39]. Adherence is directly related to the hydrophobicity of the microorganisms[29,32]. Changes in the cell's hydrophobicity during growth has been reported frequently. Lipid like compounds have been suggested to be involved in the hydrophobic nature of certain microbes. Some experiments showed that the concentration of specific fatty acids, lipids or glycolipids (depending on the study) reached a maximum early in the fermentation and then the concentration in the broth decreased with further fermentation while other studies showed the opposite[1,27,30,31,32]. High cell surface hydrophobicity determines if cells will adhere to the oil but it does not determine the ability to grow on it[32]. While non-adherent cells can grow under laboratory conditions, adherence is an important factor for hydrocarbon degrading microbes in the environment[32]. Thin fimbriae are believed to help cells to adhere[32,44]. Husain *et al.* showed that a *Pseudomonas nautica* strain adapted to growth on solid *n*-alkane (eicosane) by morphological changes such as filamentous structures allowed a 3-fold increase in the adherence of the cells[37]. Lipopolysacharide moiety on the cell surfaces are also believed to be involved in the affinity of the cells for alkanes[83]. One study showed that two different species of *Pseudomonas* used different modes of hydrocarbon uptake[35]. It is still unclear whether microbes use one, two or all the mechanisms mentioned above. Another possible mechanism could be the production of chaperon molecules (protein) that could scavenge hydrocarbon and bring it back to the cells.

1.2.2 Microbial metabolism of long-chain n-alkanes

Two pathways have been proposed for the oxidation of long chain *n*-alkanes. 1) The monoterminal oxidation pathway yielding an alcohol intermediate which is oxidized further to an aldehyde and then to an acid[50]. 2) The monoterminal oxidation yielding a

n-alkyl hydroperoxide which is then converted to a peroxy acid, an aldehyde and finally to an acid[51].

The first pathway is the most popular pathway in its acceptance. The *n*-alkane undergoes an oxygen-dependent oxidation to an alcohol catalyzed by a monooxygenase. The alcohol is then oxidized further by an alcohol dehydrogenase to an aldehyde. Then, an aldehyde dehydrogenase transforms the aldehyde to a fatty acid. The fatty acid finally undergoes β-oxidation during which two carbons are cleaved from the organic acid to give acetyl-CoA and a fatty acid-CoA two carbon units shorter than the initial *n*-alkane (see fig.1-2)[45,46,48,49,50]. Three different types of induced aldehyde dehydrogenases ($NADP^+$ and NAD^+ dependent and nucleotide independent) and 2 different types of constitutive alcohol dehydrogenases have been identified ($NADP^+$ and NAD^+ dependent)[45,46]. The aldehyde dehydrogenases have been found associated with hydrocarbon vesicles and bound to the cytoplasmic membrane with the active center of the enzyme in the direction of the periplasmic space[45]. This suggest that there could be two separate destinations for the products such as β-oxidationand wax ester synthesis by aldehyde reductases (used as carbon reserves when the cells are under carbon limitation)[46,49]. Work with yeast by Ludvik, showed that the cytoplasmic membrane underwent physiological changes when growing on hydrocarbons[54]. The membrane became thicker and showed deep invaginations indicating that the membrane could be involved in both transport and metabolism of the substrate. It was also demonstrated that V_{max} and K_m for this enzyme decreased with chain length[46].

The second pathway not involving alcohols intermediate was proposed by Finnerty in 1962. The *n*-alkane is first oxidized to an *n*-alkyl hydroperoxide by a dioxygenase. The *n*-alkyl hydroperoxide is sequentially converted to a peroxy acid, then to an aldehyde and finally to a fatty acid before undergoing β-oxidation (see figure 1-3)[48,51]. The dioxygenases isolated thus far were found in the cytoplasm of bacteria and did not need any co-enzymes[49]. When grown in the presence of long chain hydrocarbons (hexadecane and up), they were more active toward solid than liquid *n*-alkanes[49].

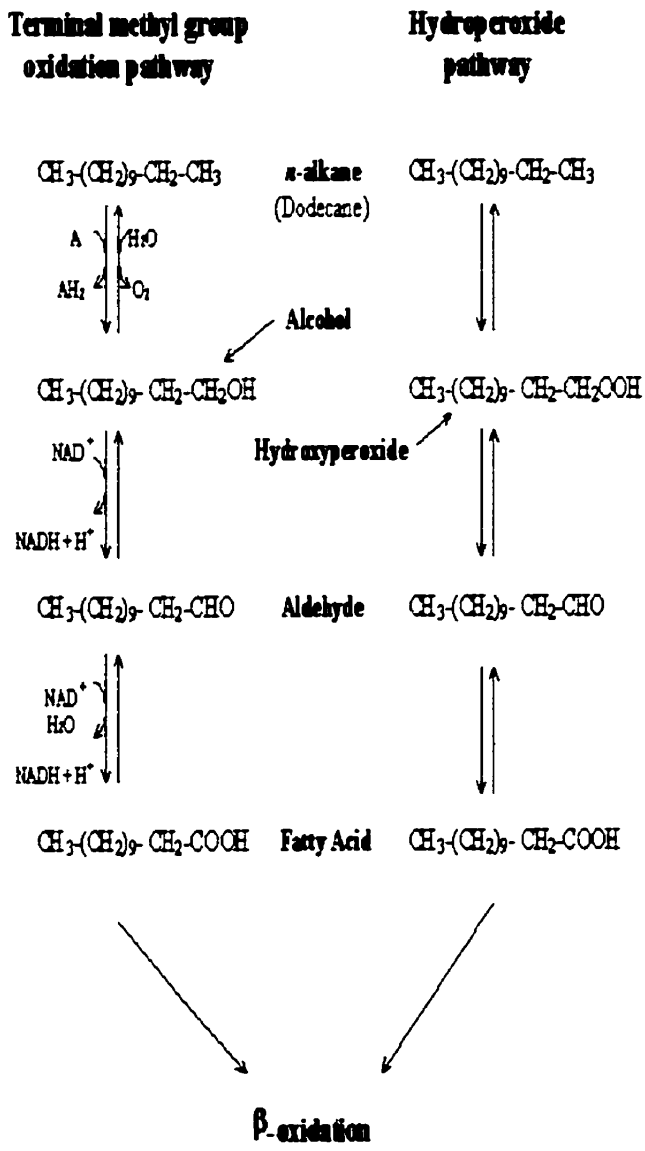

Figure 1-2: *n*-alkane metabolic pathways [82].

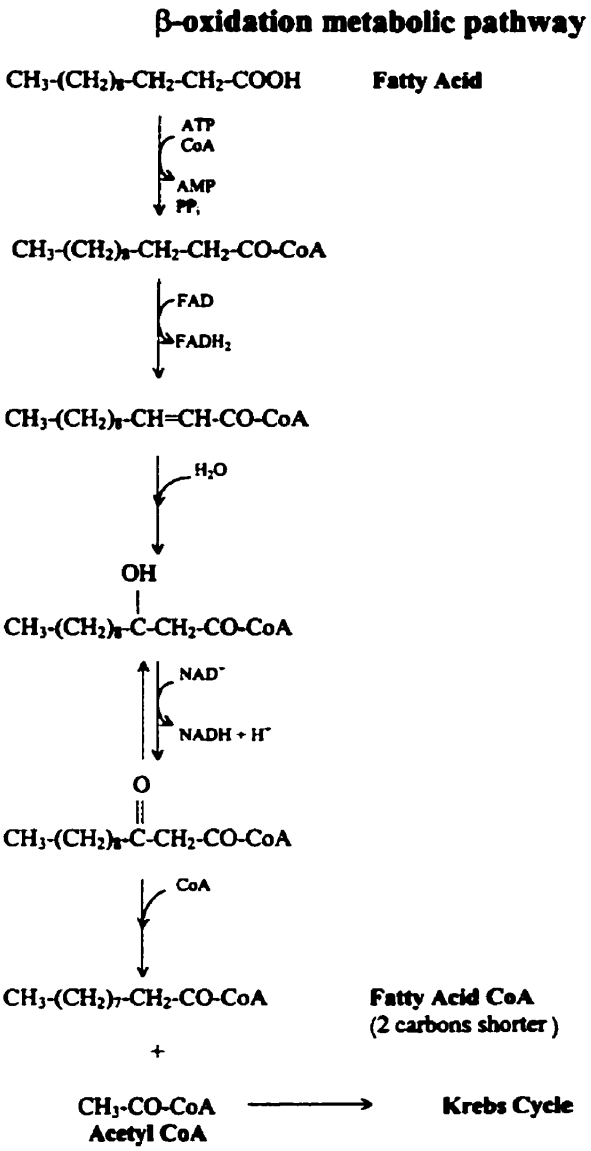

Figure 1-3: β-oxidation metabolic pathway [82].

Enzymatic studies have shown that increased lipid synthesis was activated by hydrocarbons[41]. Total cellular lipid in solid *n*-alkane grown cells increased two and a half times[92]. When the substrate was changed abruptly from glucose to hexadecane in yeast fermentations, the cells were unable to instantaneously utilize the hexadecane[41]. Before the hexadecane could be used, the lipid concentration of the cells was doubled. Therefore the authors argued that the lipids acted as solvents for the transfer of alkanes from the cell surface to the site of enzymatic action[41].

1.3 Fermentation methods

The "fermentation" term is a misnomer. Strictly speaking, a fermentation consists of the anaerobic oxidation of compounds by cells. An organic compound is the electron receptor. Therefore involving no oxygen or respiratory pathway. However, the biotechnology jargon refers to fermentation as the growth (aerobic, anoxic or anaerobic) of microorganisms in a biological reactor. Several methods of fermentation have been documented. The following section describes three of them: batch, continuous and self-cycling fermentations.

Batch fermentation consists in a closed system in which a liquid medium is inoculated with fresh living cells. The process is left to go to completion without removing or adding anything to the system. This type of fermentation allows complete utilization of the limiting nutrient. Batch systems are simple to implement. However one major drawback of this cultivation method is that it does not give very reproducible results from batch to batch.

Continuous fermentations are carried out in continuous-flow stirred-tank reactor (CSTR). Under nutrient limitation, this type of set-up is often referred to as *chemostat*. In this system, a continuous feed of substrate enters the fermenter while an equal volume of broth is removed from the reactor. Usually, ideal mixing is assumed and the concentration in any region of the fermentor is the same as the concentration of the culture coming out of the reactor. Complete utilization of the limiting substrate is not

achieved with this type of fermentation. Continuous systems tend to show more reproducible data since the environment in the reactor is more or less constant.

Self-Cycling Fermentation (SCF) is a technique in which sequential batch fermentations are performed using a computerized feedback control scheme[86]. In this method, a growth parameter (e.g. dissolved O_2) is monitored during the course of the fermentation. As the cells grow, the growth parameter changes (e.g. the dissolved O_2 decreases). When the limiting nutrient becomes depleted, the cells stop to grow and a sharp change in the monitored parameter is observed (e.g. sharp increase in dissolved O_2). At this point, half of the reactor volume is removed and replaced by fresh medium and the process starts again, this action is called phasing. The time between two successive phasing is termed cycle. The cycle time has been shown to be equal to the doubling time of the cells. It has also been demonstrated that the SCF technique results in synchronized cell population where all cells are of approximately the same age. Previous work has shown that this technique allows for complete utilization of the limiting nutrient while providing high rates of biomass production and substrate consumption. The data obtained with this method have shown to be highly reproducible making this technique a very useful tool for the study of biological systems. Typical profiles for biomass concentration, substrate concentration and dissolved oxygen concentration in a SCF fermenter are shown in figure 1-4.

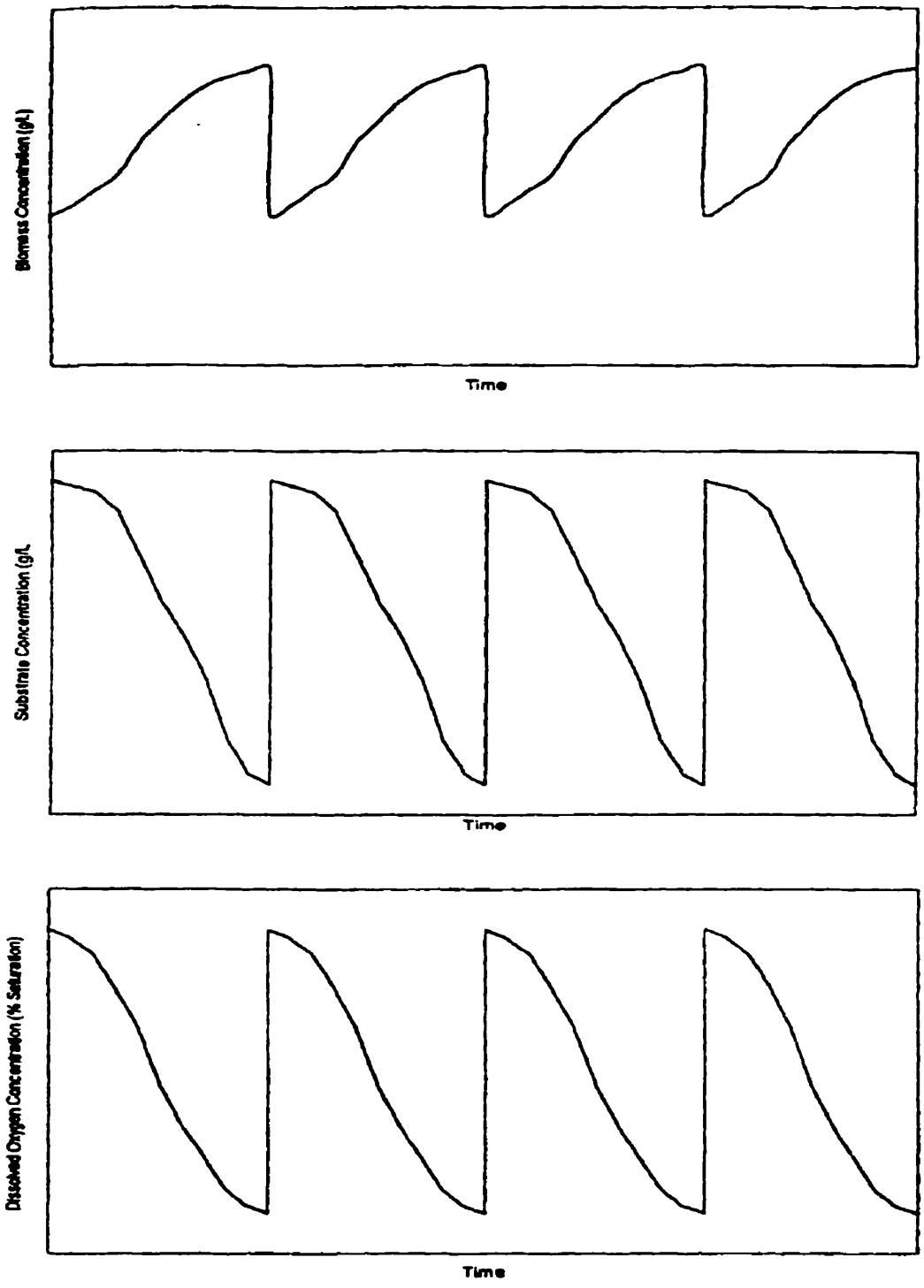

Figure 1-4: Idealized biomass concentration, limiting substrate concentration and DO profiles in the SCF.

2.0 OBJECTIVES

This work was part of the on-going research effort in which the main objective is to bioremediate contaminated soils, ground water, sediments, surface water and air contaminated with hazardous and toxic chemicals. The specific objectives of this work were: first, to find a microorganism displaying the phenotype needed to degrade paraffin wax. Second, to determine if paraffin wax could be biodegraded using the Self-Cycling Fermentation technique, and finally, to characterize the kinetics of long-chain *n*-alkanes biodegradation.

3.0 MATERIALS AND METHODS

3.1 Microorganisms

Nineteen bacteria were tested for growth on paraffin wax:

Table 3-1: Name, source and optimum temperature of tested microorganisms.

Bacterium	Source	°C
Acinetobacter ID38	J. Oudot, France	30
Acinetobacter calcoaceticus RAG-1	D.G. Cooper, Canada	34
Arthrobacter paraffineus ATCC 19558	D.G. Cooper, Canada	30
Arthrobacter nicotianae KCCB35	S.S. Radwan, Kuwait	30
Arthrobacter paraffineus ATCC 21220	D.G. Cooper, Canada	30
Corynebacterium alkanalyticum ATCC 21511	D.G. Cooper, Canada	30
Corynebacterium sp. 21744	D.G. Cooper, Canada	37
Mycobacterium OFS	J.J. Perry, USA	37
Pseudomonas aeruginosa PAO1	D.G. Cooper, Canada	30
Pseudomonas fluorescens ATCC 31125	D.G. Cooper, Canada	30
Pseudomonas fluorescens Texaco	H. Leskovsek, Slovenia	30
Pseudomonas fluorescens	C. Gaylarde, Brazil	30
Pseudomonas putida (Slovenia)	H. Leskovsek, Slovenia	30
Pseudomonas putida ATCC 12633	D.G. Cooper, Canada	26
Pseudomonas putida ATCC 44955	D.G. Cooper, Canada	26
Pseudomonas putida IR32	J. Oudot, France	30
Rhodococcus erythropolis ATCC 4277	D.G. Cooper, Canada	26
Rhodococcus IS01	J. Oudot, France	37
Rhodococcus rhodochrous ATCC 21766	D.G. Cooper, Canada	30

All of the above cultures were maintained on nutrient agar (Difco Bacto 0001-14) plates and on agar slants at 4°C. Samples of each microorganism were frozen at -70°C in a Revco freezer.

Rhodococcus IS01, *Mycobacterium* OFS (a.k.a. *Mycobacterium convolutum* R22 ATCC 29671 or *Rhodococcus sp.* ATCC 29671), *Arthrobacter paraffineus* ATCC 19558 and *Pseudomonas fluorescens* Texaco were used in the Self-Cycling Fermenter experiments. These four bacteria were maintained in shake-flasks and on nutrient agar

plates. Pure colonies were transferred to fresh petri-dishes monthly and stored at 4°C to maintain viability.

3.2 Media and culture conditions

Two media were used throughout this work: the inorganic basal medium (IBM) of Sorkoh *et al.*[6] and a modified mineral salts medium (MMSM)(Table 3-2). The limiting nutrients for all fermentations were hydrocarbons. The paraffin wax was obtained from Consumex inc. and all the other hydrocarbons (i.e. *n*-alkanes, pristane and hepta-methyl-nonane) were obtained from Sigma-Aldrich.

Table 3-2: Media formulations.

IBM				**MMSM**	
Compound	g/L	*Trace elements*	g/L	*Compound*	g/L
$NaNO_3$	0.85	EDTA	1.0	NH_4NO_3	4.0
KH_2PO_4	0.56	$ZnSO_4 \bullet 7H_2O$	2.08	KH_2PO_4	4.0
Na_2HPO_4	0.86	$MnSO_4 \bullet 4H_2O$	1.78	Na_2HPO_4	6.0
K_2SO_4	0.17	H_3BO_3	0.56	$MgSO_4 \bullet 7H_2O$	0.2
$MgSO_4 \bullet 7H_2O$	0.37	$CuSO_4 \bullet 5H_2O$	1.0	$CaCl_2 \bullet 2H_2O$	0.01
$CaCl_2 \bullet 6H_2O$	0.0007	$Na_2MoO_4 \bullet 2H_2O$	0.39	$FeSO_4 \bullet 7H_2O$	0.01
Fe_{III}·EDTA	0.004	KI	0.664	Na_2EDTA	0.014
+		$FeSO_4 \bullet 7H_2O$	0.4		
Trace elements	2.5 mL	$NiCl_2 \bullet 6H_2O$	0.004		

3.3 Screening of paraffin wax degrading bacteria

To screen for paraffin wax degrading bacteria, the nineteen bacteria mentioned above were grown in shake-flasks and on agar plates using a modification of the Kiyohara method[75].

3.3.1 Modified Kiyohara method

Agar plates containing no carbon source were prepared. The plates were then inoculated with bacteria by stabbing the plates with toothpicks previously inoculated by dipping them in bacterial colonies. Immediately thereafter, the plates were sprayed using an atomizer with a solution of paraffin wax dissolved in diethyl ether (about 10% (*w/v*)). The solvent was let to evaporate and the plates were incubated at the optimum growth temperature of the bacteria. Colonies showing degradation were surrounded with clear zones on the opaque plates.

3.3.2 Shake-flasks experiments

One hundred mL of IBM medium was added to 500 mL Erlenmeyer flasks. The flasks were plugged with foam plugs and autoclaved (AMSCO 3021-S autoclave) at 121°C and 1.2 bar for 30 minutes. The flasks were then supplemented with 10 g/L of paraffin wax. The shake-flasks were inoculated with a 1% inoculum of the desired culture previously grown on nutrient agar. The flasks were finally incubated at the appropriate temperatures (see table 3-1) in a gyratory incubator shaker (New Brunswick Scientific Co., model G25) at 250 rpm.

3.4 Self-Cycling Fermentations

Rhodococcus IS01, *Mycobacterium* OFS, *Arthrobacter paraffineus* ATCC 19558 and *Pseudomonas fluorescens* Texaco were used in the Self-Cycling Fermenter experiments. The IBM medium was used during the screening test but all the Self-Cycling Fermentations were performed using MMSM medium. The cyclone reactor had a working volume of 1.0 L. All media and apparatus were autoclaved. The 10 L medium bottles (Nalgene) were sterilized for 2.5 hours and all the components of the fermenter were sterilized for 3.5 hrs.

For all experiments, the reactor was inoculated with 2% of acclimated cells growing in shake-flasks containing MMSM, 5 g/L of paraffin wax and 5g/L of hexadecane. The wax and the hexadecane were also autoclaved for 45 minutes prior to injection in the reactor.

3.5 Biomass measurement

3.5.1 End of cycle biomass

End of cycle biomass were measured using a standard dryweight analysis[76]. Triplicate 20 mL samples were put in 30 mL Pyrex centrifuge tubes. The samples were centrifuged for 15 minutes at 5000 rpm at 4°C. The film of frozen hydrocarbons was carefully removed with tweezers. The supernatant was decanted. The pellet was washed twice with 10 mL of distilled water. The final solution was poured in a tarred aluminum weighing dish which had been previously dried in the oven for 24 hrs. The dishes were placed in an oven (Fisher Isotemp Oven 100 series, model 126G) at 105 °C and dried to constant weight for 48 hours. The dishes were cooled in a dessicator before weighing. The biomass measurements were obtained by weighing the aluminum pan with an analytical balance (Mettler, model AE 160). The biomass was determined by calculating the difference in the weight of the full and empty pans. The final biomass concentrations were reported as grams of dry biomass per liter of fermentation broth.

3.5.2 Intracycle biomass

Intracycle biomass measurements were obtained using the Marino *et al.* Method[77] (see appendix A). Intracycle biomass measurements were only obtained for experiments with *Rhodococcus* IS01. The adhesion factor (AF) was 0.62 and was more or less constant during the SCF.

3.6 Hydrocarbon measurement

The following procedure was performed to measure the hydrocarbon concentration during all the experiments. A sample of 2 mL of the culture broth were obtained from the shake-flasks or the cyclone reactor using a glass syringe (Becton Dickinson & Co. Multifit syringe). The sample was then transferred to a test tube containing 5 mL of an internal standard solution. The internal standard solution consisted of 0.01% pentadecane dissolved in chloroform. The extraction of the hydrocarbon from the sample was performed by vortexing (Vortex Genie, Fisher model K-550-G) the test tube for 2 minutes for samples containing liquid hydrocarbons and 10 minutes for samples containing solid hydrocarbons. One mL of the organic phases (bottom layer) was transferred to a microcentrifuge tube. Half a μL was injected into a gas chromatograph (GC)(HP5890 Series II) connected to a Varian Star chromatography workstation for all the experiments performed with *Rhodococcus* IS01 and connected to a peak integrator (HP3395 series II) for the rest of the experiments. The column used was an SPB-5 by Supelco. Settings on the GC are summarized in table 3-3.

Table 3-3: GC Operating conditions for hydrocarbon analysis.

Operating conditions	Value
Injection temperature	250°C
Initial column temperature	65°C
Rate	10°C /min
Final column temperature	350°C
Detector temperature	370°C
Initial time	2.5 min
Final time	0.1 min

Calibration curves for every hydrocarbon studied were obtained by plotting the hydrocarbon concentration (g/L) *versus* the area ratio of the peaks (hydrocarbon peak divided by internal standard peak) using samples of known concentrations in water. Some calibration curves are shown in figure 3-1. Table 3-4 shows the retention times of the hydrocarbons studied.

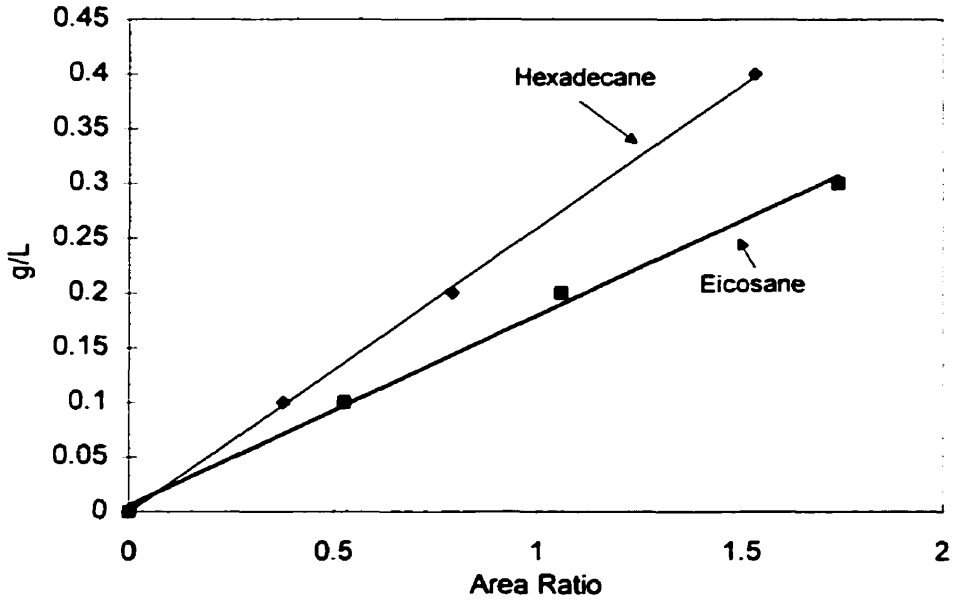

Figure 3-1: Calibration curves for hexadecane and eicosane.

Table 3-4: Hydrocarbon GC retention times.

Hydrocarbon	**Retention time (min)**	**Hydrocarbon**	**Retention time (min)**
Dodecane	3.866	Unknown compound	19.131
Pentadecane	8.169	Heptacosane	19.447
Hexadecane	9.388	Octacosane	20.166
Heptadecane	10.533	Nonacosane	20.861
Pristane	10.629	Triacontane	21.501
Eicosane	13.586	Hentriacontane	22.182
Heneicosane	14.546	Dotriacontane	22.814
Docosane	15.443	Tritriacontane	23.427
Triacosane	16.306	Tetratriacontane	24.024
Tetracosane	17.135	Pentatriacontane	24.605
Pentacosane	17.910	Hexatriacontane	25.143
Hexacosane	18.704	Heptatriacontane	25.720

3.7 Surface tension measurement

Surface tension measurements were taken using an Autotensiomat surface tension analyzer (Fisher, model 215) which used the DeNouy method. A 6.0 cm platinum-iridium alloy ring with an R/r value of 53.75 was used. All measurements were taken at room temperature (22°C). Five mL samples were poured in 3.5 cm diameter petri dishes and the surface tension was obtained by lowering the sample until the ring broke through the sample-air interface. The ring was cleaned by heating it with a Bunsen burner. Surface tension measurements were obtained in mN/m.

3.8 Emulsion test

The emulsion test procedure was the same used by Barriga[78]. Four mL of samples was added to 6 mL of iso-octane at pH=6.1 in a stoppered test tube. The height of the initial iso-octane phase was recorded. The mixture was vortexed for 3 minutes at maximum speed. The mixture was left to stand for 60 minutes and the final height of the iso-octane phase was measured. The percent phase emulsified is equal to the difference between the initial height and the final height divided by the initial height times 100.

3.9 pH determination

pH measurements were obtained using a Fisher pH electrode (Model 13-620-252) in conjunction with an Orion Research analog pH meter (model 301).

3.10 Determination of K_LA

Knowledge of the liquid mass transfer coefficient, K_La, is important for aerobic biodegradation. The K_La of the SCF system was measured using the standard "gassing-in, gassing out" procedure of Benedek and Heideger[89]. The procedure was adapted to the

cyclone reactor as explained by Sheppard[90]. The medium in the reactor circulated in the reactor at a velocity of 27 m/min and the entrainment of bubbles near the probe was negligible. The following procedure was followed: 1 L of medium was added to the cyclone reactor and the recirculating pump was started. Then, the nitrogen was introduced into the reactor at a rate of 1L/min until the dissolved oxygen in the liquid was depleted as indicated by a stable 0% saturation on a previously calibrated DO amplifier. The recirculating pump was turned off and the flow of nitrogen was stopped. Air was introduced into the reactor above the surface of the liquid in the cyclone at a rate of 1.8 L/min with a tube introduced into the cyclone. This was necessary to ensure that the head space above the surface of the medium in the cyclone was completely filled with air and not nitrogen. After five minutes, the pump was turned on and the percentage saturation of dissolved oxygen was recorded by a computer. Finally, when the reactor was saturated with dissolved oxygen and the saturation value reached a stable value, the experiment was stopped. This procedure was repeated with different air flow rates and different media. The temperature in the reactor was controlled at 27°C for all experiments.

The equation governing the process is:

$$(1) \qquad \frac{dC}{dt} = K_L a \cdot (C^* - C)$$

where

C is the concentration of oxygen in liquid as measured by the probe (mol/m^3).

C* is the dissolved oxygen in equilibrium with the concentration of oxygen in the gas leaving the reactor (mol/m^3).

The probe time constant, τ_p, was determined as explained by Brown[91]. The mass transfer coefficient was estimated from equation (2) by minimizing the sum of squares between the calculated data and the experimental data. Equation (2) was obtained from Brown[91]. Values obtained were similar to those determined by Sheppard[90].

(2) $$\frac{(C^* - C)}{(C^* - C_o)} = \left(\frac{\tau - \tau_p}{\tau}\right) \cdot \left[e^{\frac{-t}{\tau}} - \left(\frac{\tau_p}{\tau}\right) \cdot e^{\frac{-t}{\tau_p}}\right]$$

where

Co is the initial concentration of dissolved oxygen (mol/m^3).

τ_p is the probe time constant (s).

τ is given by $1/K_La$ (s^{-1}).

3.11 Determination of the parameters of the Monod equation

The Robinson method was used to fit the Monod kinetic parameters to the experimental data obtained with the SCF[70]. Using the Monod model, the rate of change of substrate consumption by bacteria in a batch reactor may be described as:

$$\frac{dS}{dt} = -\left[\frac{\mu\max \cdot S}{(Ks + S)}\right] \cdot \frac{X}{Y} \qquad (1)$$

where μ_{max} is the maximum specific growth rate, Ks is the half-saturation constant for growth, and Y is the yield coefficient. The variable S is the substrate and the variable X is the biomass concentration. If X is eliminated from equation 1 by using:

$$X = Y \cdot (So - S) + Xo \qquad (2)$$

Equation 1 becomes:

$$\frac{dS}{dt} = -\left[\frac{\mu\max \cdot S}{(Ks + S)}\right] \cdot \frac{[Y \cdot (So - S) + Xo]}{Y} \qquad (3)$$

which may be integrated to give:

$$C_1 \cdot \ln\left\{\left(\frac{[Y \cdot (So - S) + Xo]}{Xo}\right) - C_2 \cdot \ln\left(\frac{S}{So}\right)\right\} = \mu \max \cdot t \qquad (4)$$

where $C_1 = \frac{(Ks \cdot Y + So \cdot Y + Xo)}{(Y \cdot So + Xo)}$ and $C_2 = \frac{Ks \cdot Y}{(Y \cdot So + Xo)}$

So is the initial substrate, t is the time and Xo is the initial biomass. For the purpose of this work, Xo was assumed to be 50% of the end of cycle biomass obtained at the end of the cycle under study. The yield Y was easily calculated using equation 2. The rest of the variables, μ_{max} and Ks, were calculated using GraphPad Prism™. GraphPad Prism™ is a statistical package that can perform non-linear regression rapidly and easily. To corroborate the results obtained by the non-linear regression, the model was also fit with a Genetic Algorithm (GA) using the SUGAL Genetic Algorithm package[74]. Both methods gave very similar results for the 4 first sets of data. Since the non-linear regression method was faster and easier to use than the GA it was used to fit the model to the rest of the experimental data.

4.0 EXPERIMENTAL APPARATUS

The experimental apparatus used for the self-cycling fermentations with *Mycobacterium* OFS and *Arthrobacter paraffineus* ATCC 19558 was similar to that described by May[79]. Minor changes were made to the location of the dissolved oxygen (DO) probe and to the air supply system. A schematic of the apparatus is shown in figure 4-1.

The main part of the reactor set-up consisted of a glass cyclone. The temperature inside the reactor was controlled by a recirculating water bath (Haake, model FE2) and a glass water jacket heat exchanger. A Friedrich's condenser was used at the air outlet of the fermenter to prevent evaporation. All the reactor's openings were isolated from the atmosphere with Nalgene air filters (Millipore Millex-FG50, 0.2 μm). The broth was recirculated through the fermenter loop with a 0.2 hp centrifugal pump (March, model MDX). The hydrocarbon was added to the reactor using a syringe pump (Orion, model 341B) and a 30cc Luer-lock glass syringe (Becton, Dickinson & Co.) connected to the reactor with Masterflex Tygon fuel and lubricant tubing (6401-13, 0.8 mm ID). In order to inject solid hydrocarbon at room temperature, the syringe and the injection tubing were heated with a tape heater (Glas-Col apparatus, Det-1-10, 700 watts, 115 volts) to 55°C.

The DO concentration was monitored using an Ingold polarographic oxygen sensor (model IL 531). The signal from the probe was amplified with a Cole-Parmer amplifier (model 01971-00) and sent to a data acquisition board and to a strip chart recorder (Linear 1200). The carbon dioxide concentration was measured with a CO_2 sensor apparatus by Columbus Instruments controlled by the Oxymax software. In the past, biomass would occasionally cover the tip of the DO probe and disrupt the signal. To remedy this problem the DO probe was set-up in an upright position instead of a flat position. No clogging of the tip was reported after this minor change. The air inlet was controlled by a solenoid valve and the air flowrate was controlled using a rotameter (Brooks Sho-Rate, model 1355 BIBIAAA).

The liquid level in the fermenter was monitored using a differential pressure (DP) transducer (Omega, model PX170). A valve was added to the air supply system to minimize any disturbances that could affect the signal of the DP transducer cell during phasing. The DP cell was not autoclavable and therefore was isolated from the fermenter by a filter (0.45 micron Milipore filter in a Milipore Swinnex-25 Nalgene filter holder).

The SCF was controlled using an IBM compatible 8088 PC interfaced with a data acquisition board (Data Translation Model DT-2801). Most of the control program was similar to the one used by May[79] except for the phasing algorithm which was borrowed from Brown[80,91].

Upon detection of a minimum in DO, the computer would turn off the pump and the air. The liquid level in the reactor had to be static for the DP cell to gather accurate signals. The harvesting valve would open and drain half (500 mL) the broth in the reactor to an overflow container. Then the dosing valve would open and add 500 mL of fresh medium to the reactor. The harvest was collected in one of 7 sampling ports and the rest of the harvest was discarded to waste.

4.1 Balance *versus* Differential Pressure (DP) cell

The experimental apparatus used for the studies with *Pseudomonas fluorescens* Texaco and *Rhodococcus* IS01 was modified from the set-up mentioned above. This set-up used a balance instead of a DP cell. Two problems were associated with stopping the pump between cycles: First, the hydrocarbon would settle at the surface of the medium in the reactor and second, if the cells were highly hydrophobic, they would stick to the insoluble carbon source and settle on top of the reactor with the hydrocarbon. These two problems would not result in homogeneous sampling and in removing half the bacteria from the SCF. The solution lied in using a balance instead of a DP cell to keep the pump going during the harvesting. Figure 4-2 shows a schematic of the fermenter set-up using a balance. The cyclone part of the reactor was held with clamps and supported by a ring stand placed on the balance. The ring stand was secured to the wooden platform on which the entire reactor set-up was standing. The rest of the reactor (heat exchanger, tubing, DO probe, etc.) were fixed on the wood support attached to the wooden platform. Before the

balance was used, an attempt was made to use a load cell (Transducer Techniques MLP-25). The load cell was placed between two metal supporting plates (kindly lent by Dr. John Sheppard) on which the reactor was resting. The signal to noise ratio was too small and no stable and precise signal could be obtained.

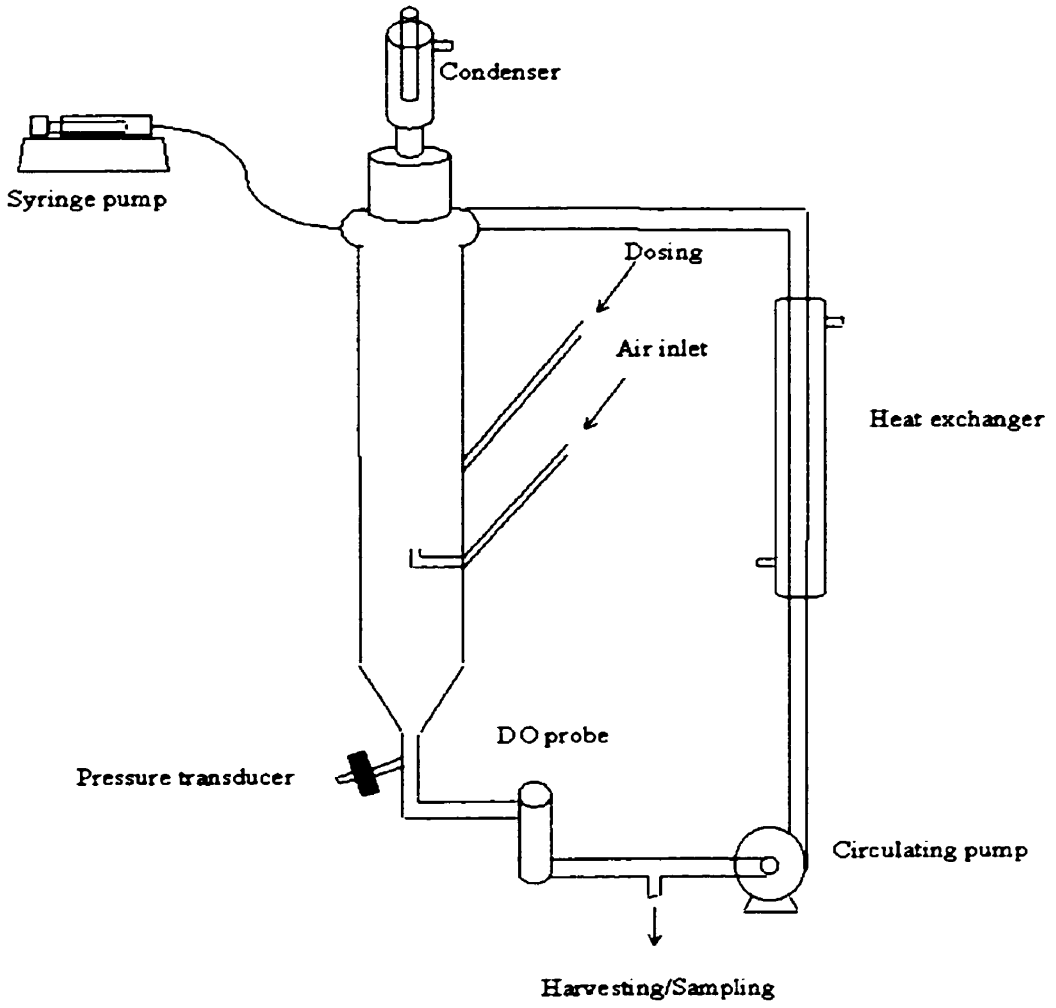

Figure 4-1: Schematic of the cyclone SCF reactor set-up with DP transducer.

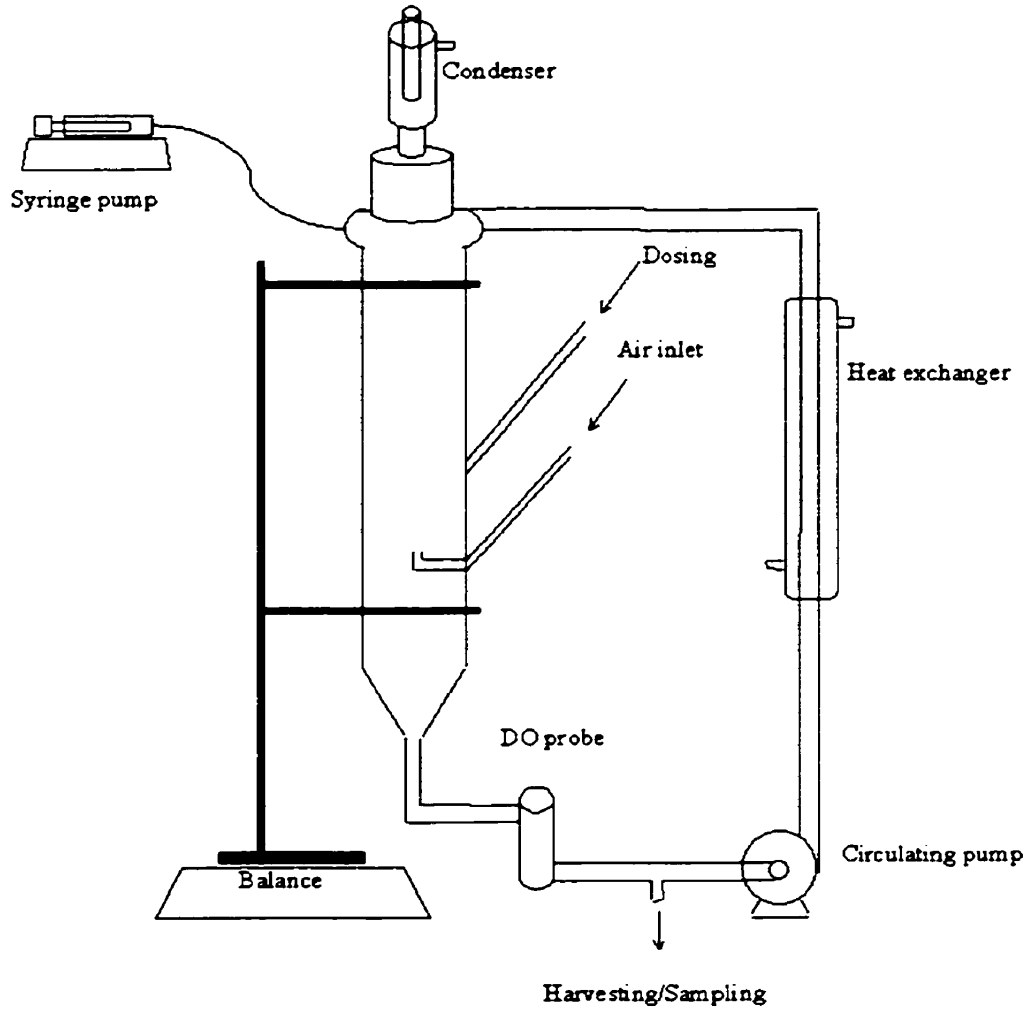

Figure 4-2: Schematic of the cyclone SCF reactor set-up with balance.

4.2 Oxygen transfer

Most of the oxygen mass transfer occurred at the walls of the cyclone reactor. When the medium was recirculating in the reactor, the air transfer occurred between the air in the reactor and the thin continuously flowing film of liquid covering the interior of the glass cyclone. The oxygen mass transfer, K_La, in the SCF system was 90.7 $hour^{-1}$ at an air flow rate of 0.56 L/min, 119.9 $hour^{-1}$ at 2.16 L/min and 164 $hour^{-1}$ at 7.84 L/min.

5.0 RESULTS

5.1 Selection of microorganisms

Nineteen bacteria were tested for growth on paraffin wax using the Kiyohara screening method. The plates were incubated at the respective bacteria's optimum temperature for 7 days. Table 1 summarizes the results of the screening. Six bacteria showed growth on the agar plates. The Kiyahara test served as a crude but rapid preliminary screening process. To corroborate the Kiyohara test results and to determine if some of the bacteria did not grow because of the nature of the screening test, all bacteria were also grown on inorganic basal medium (IBM) containing 10 g/L of paraffin wax in shake-flask. As indicated by table 1, a total of 11 bacteria grew. Seven of these bacteria showed minimal growth (light turbidity) while 4 of them showed heavy growth (denser turbidity). The best candidates for further study were: *Arthrobacter paraffineus* ATCC 19558, *Mycobacterium* OFS, *Pseudomonas fluorescens* Texaco and *Rhodococcus* IS01. All four microbial candidates were grown in the SCF with a mixture of paraffin wax and hexadecane as substrate.

Table 5-1: Growth of tested microorganisms after 7 days.

Bacterium	Growth on paraffin wax	
Legend: - No growth + Light growth ++ Heavy growth		
	Plate	**Shake-flask**
Acinetobacter ID38	-	-
Acinetobacter calcoaceticus RAG-1	-	-
Arthrobacter nicotianae KCCB35	-	+
Arthrobacter paraffineus ATCC 19558	+	++
Arthrobacter paraffineus ATCC 21220	-	+
Corynebacterium alkanalyticum ATCC 21511	-	-
Corynebacterium sp. ATCC 21744	+	+
Mycobacterium OFS	+	++
Pseudomonas aeruginosa PA01	-	+
Pseudomonas fluorescens ATCC 31125	-	-
Pseudomonas fluorescens	-	-
Pseudomonas fluorescens Texaco	+	++
Pseudomonas putida (from Slovenia)	-	-
Pseudomonas putida ATCC 12633	-	+
Pseudomonas putida ATCC 44955	-	-
Pseudomonas putida IR32	-	-
Rhodococcus erythropolis ATCC 4277	-	+
Rhodococcus IS01	+	++
Rhodococcus rhodochrous ATCC 21766	+	+

5.2 Self-Cycling Fermentations

Four runs of SCF were performed using paraffin wax and hexadecane as substrate. Run#3 was performed with *Mycobacterium* OFS, run#4 with *Arthrobacter paraffineus* ATCC 19558, run#6 with *Pseudomonas fluorescens* Texaco and run#7 with *Rhodococcus* IS01. Run#3 and run#4 were performed using the differential pressure (DP) transducer cell as the cycling device. When the DP cell was used, the pump of the SCF had to stop during the harvesting segment on the phasing procedure. This can be easily seen on the DO traces (fig.5-2 and 5-5): after each cycle, the DO drops to zero when the pump stops and increases back up when the pump starts again after the harvest. Two problems were associated with stopping the pump between cycles: 1) the hydrocarbon would settle at the surface of the medium in the reactor, and 2) if the cells were highly hydrophobic, they would adhere to the insoluble carbon source and settle at the surface of the reactor with the hydrocarbon. These two problems did not result in homogeneous sampling and in consistently removing half the biomass from the SCF. The solution lay in using a balance instead of a DP cell to keep the pump going during the harvesting. Run#6 and #7 were performed using the balance.

5.2.1 Self-Cycling Fermentation with Mycobacterium OFS

Self-Cycling Fermentation of *Mycobacterium* OFS in 1 liter of MMSM medium containing 5 g/L of paraffin wax was attempted in the cyclone reactor at 37°C. The first attempt was a failure. The wax was added as a liquid using the syringe pump, but the wax solidified upon contact with the cooler circulating medium. It formed a solid ball of paraffin that floated on top of the medium. Also, wax disabled the monitoring of the dissolved oxygen in the reactor by coating the tip of the DO probe. Hence no stable cyclic pattern could be obtain and the run was aborted. Attempts to perform SCF with solid wax were without success because of the slow growth of the cells and because the solid state of the wax was disrupting the reactor. Therefore the wax had to be solubilized to be successfully degraded. A solvent of choice was hexadecane because it is an *n*-alkane widely used in the literature, paraffin wax can readily be dissolved in it (1 to 5 ratio at 30°C) and it was biodegradable. At 37°C, a mixture of 20% (w/v) wax in

hexadecane was a liquid. Figure 5.1 shows the variation of concentrations of hexadecane and wax in the reactor within one typical cycle over time. Initially, a mixture of 0.65 g/L of hexadecane and 0.15 g/L of wax were initially added to the reactor until a cyclic steady state concentration of 1.2 g/L of hexadecane and 0.28 g/L of wax was reached after 8 cycles. At the end of the 9th cycle, after 7.1 hrs, the residual hexadecane and wax were 0.54 g/L and 0.13g/L respectively. *Mycobacterium* OFS degraded 55% of the hexadecane and 54% of the wax. Cycle 9 was prolonged for an extra 5 hours until the DO was 30% above its initial level at the beginning of the cycle. The concentrations of hexadecane and wax at that point reached 0.202 g/L and 0.087 g/L respectively. Eighty three percent of the hexadecane and 69% of the wax had been biodegraded. It can be argued that if the fermentation had been pursued for a longer time the substrate would have been completely degraded but no such evidence was gathered. In preliminary shake-flasks experiments, surface tensions as low as 29 mN/m were measured when *Mycobacterium* OFS was grown in MMSM medium containing 3g/L of wax. However, the average surface tension throughout the SCF run was 57 mN/m.

Figure 5.2 shows the DO profiles for 2 cycles during run#3. The air flowrate was 30 STD mL/min. The dissolved oxygen (DO) profile for this fermentation showed a steady increase in the oxygen demand initially and a leveling of the demand in the middle (after 4 hrs) of the cycle. The minimum DO was reached after approximately 5 hrs, the end of cycle was reached when the computer detected a 5% increase in the DO above the minimum. The DO did not increase sharply after the minimum was reached as it is often seen when a nutrient becomes limiting. For the work presented here, this profile is typical for SCF fermentations that have residual hydrocarbons remaining at the end of every cycle.

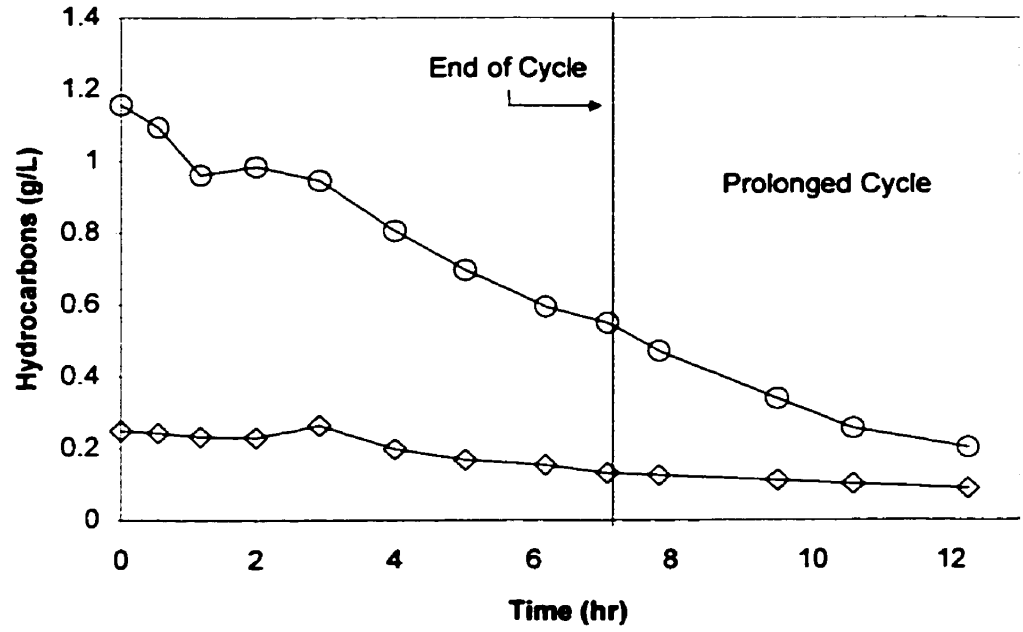

Figure 5-1: Concentration of hexadecane (O) and wax (◊) *versus* time: run #3, cycle 9, *Mycobacterium* OFS.

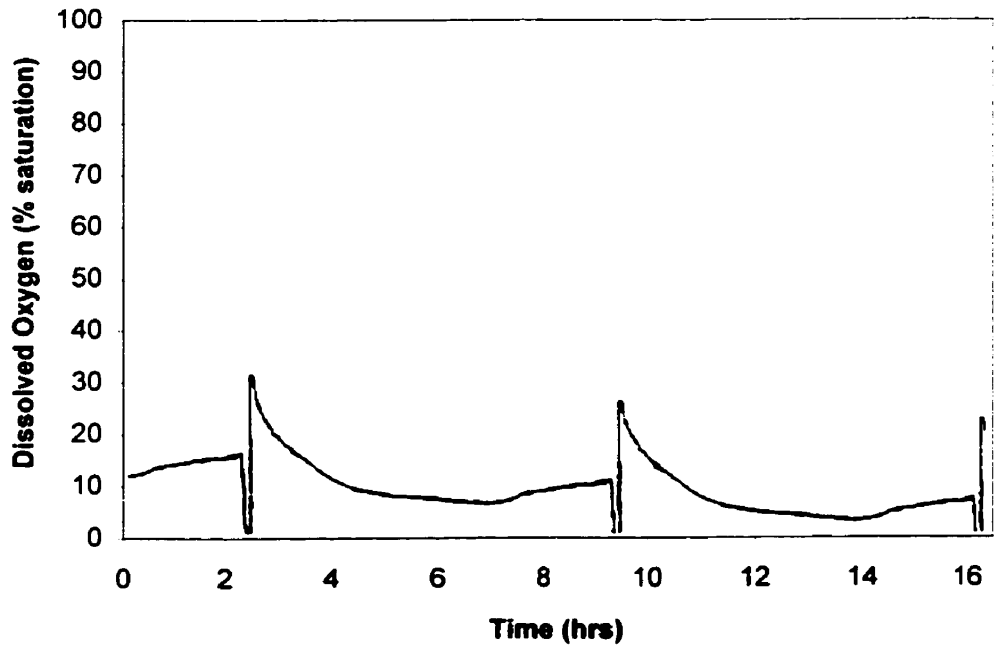

Figure 5-2: Dissolved oxygen trace: run#3, *Mycobacterium* OFS.

5.2.2 *Self-Cycling Fermentation with Arthrobacter paraffineus* ATCC 19558

Arthrobacter paraffineus ATCC 19558 was grown in the SCF with MMSM at 30 °C. A mixture of 0.85 g/L of hexadecane and 0.15 g/L of wax was added at the beginning of each cycle to the reactor until a steady state concentration of 1.22 g/L of hexadecane and 0.27 g/L of wax were reached after 14 cycles. Figure 5-3 shows the biodegradation of $C_{16}H_{34}$ and wax over time for run#4, cycle 27 and figure 5-4 only shows the paraffin wax degradation over time for the same cycle. At the end of the 27th cycle, 69% of the hexadecane and 53% of the wax had been degraded. The concentration of the hydrocarbons decreased steadily until the end of cycle was reached. The average cycle time for run#4 was 181 minutes. The concentrations of $C_{16}H_{34}$ and wax followed a similar trend. At first we observe a steady and rapid oxidation. After 100 minutes, the rate of degradation seem to slow down for the $C_{16}H_{34}$ and level off for the wax. The residual amounts of hydrocarbons for this cycle were 0.375 g/L of $C_{16}H_{34}$ and 0.133 g/L of wax. Once again complete oxidation of the hydrocarbons was not observed.

Figure 5-5 shows the DO traces of 3 cycles for run#4. The DO profile was typical (for this work) of fermentations showing incomplete removal of the limiting carbon source at the end of the cycles. As the oxygen demand increased, the DO decreased steadily until just before the end of cycle. After reaching its minimum at around 170 min, the DO trace began to increase until the computer initiated the phasing procedure. The increase is sharper than for run#3 but is still not characteristic of the disappearance of a limiting nutrient. The air flow rate was 1.1 L/min.

Originally *Arthrobacter paraffineus* ATCC 19558 was selected because of its alkane chains and because of its reported surface active properties[20]. Duvniak *et al.* reported surface tensions as low as 31 mN/m when *Arthrobacter paraffineus* ATCC 19558 was grown in MMSM and hexadecane suggesting the production of a biosurfactant. However all attempts to reproduce these results were in vain. Figure 5-6 shows the surface tension results after following the procedure described by Duvniak *et al.* During run#4 the surface tension was more or less constant at 61 mN/m .

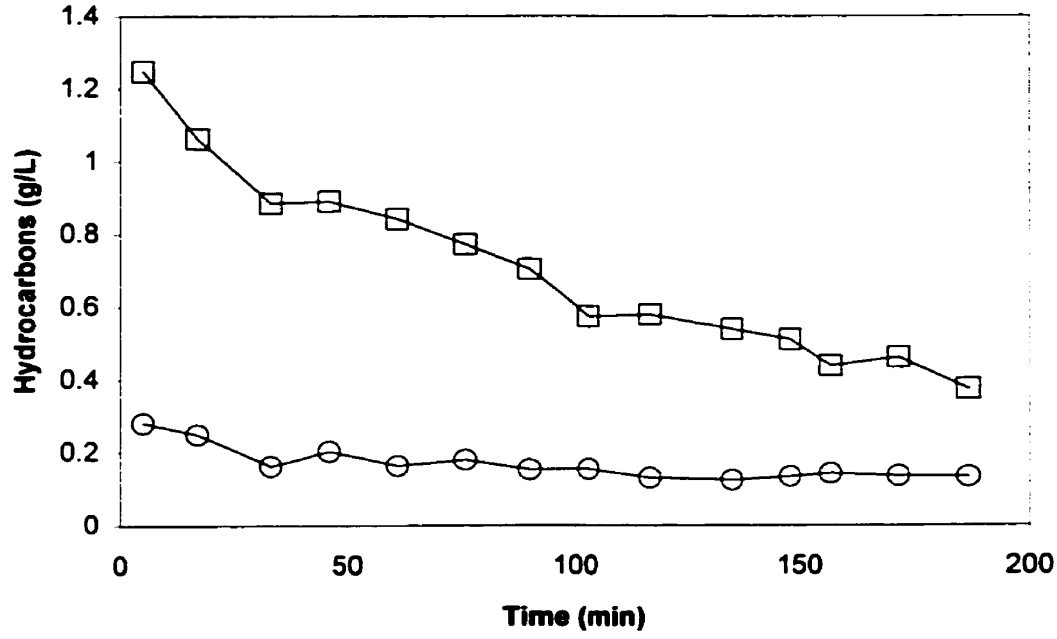

Figure 5-3: Concentration of hexadecane (□) and wax (O) *versus* time: run #4, cycle 27, *Arthrobacter paraffineus* ATCC 19558.

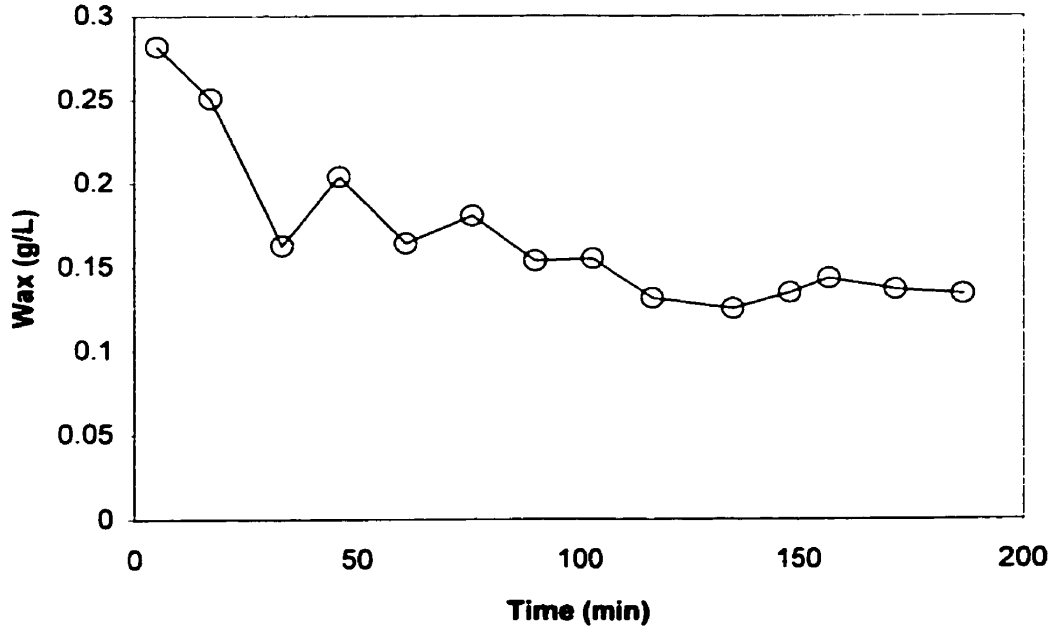

Figure 5-4: Concentration of paraffin wax (O) *versus* time: run #4, cycle 27 , *Arthrobacter paraffineus* ATCC 19558.

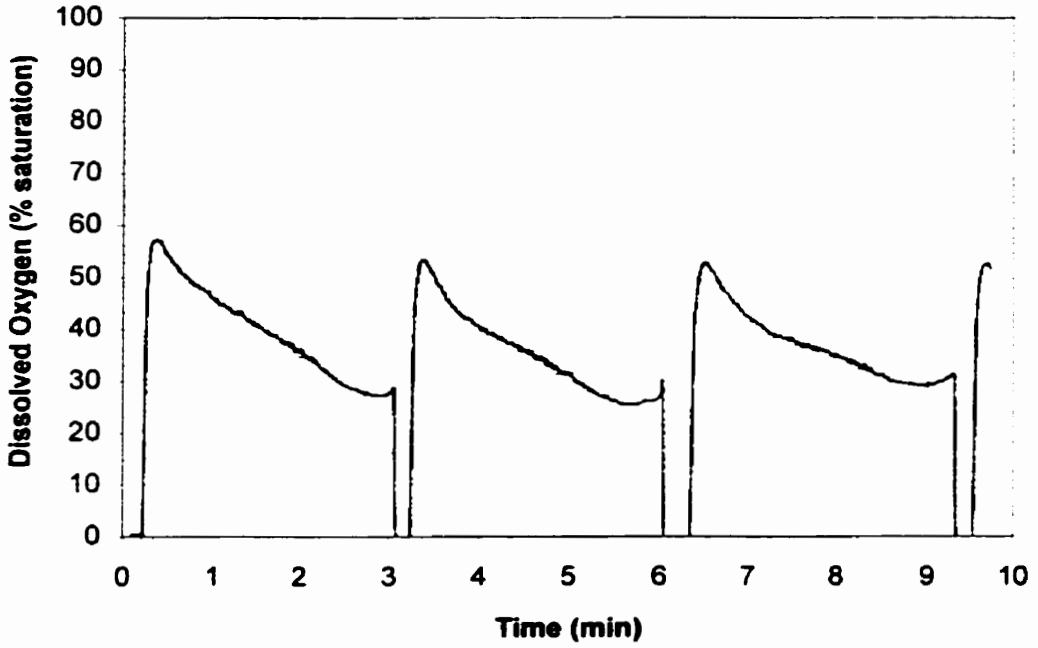

Figure 5-5: Dissolved oxygen trace: run#4, *Arthrobacter paraffineus* ATCC 19558.

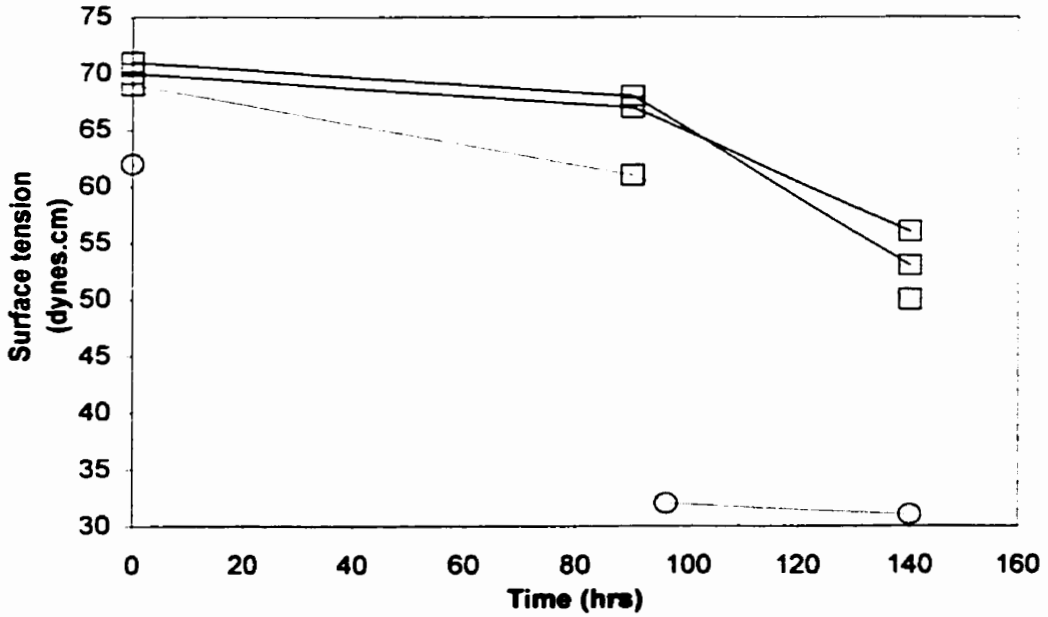

Figure 5-6: Surface tension measurements for *Arthrobacter paraffineus* ATCC 19558. Data for this work (□) and Duvniak *et al.*'s work (○).

5.2.3 Self-Cycling Fermentation with Pseudomonas fluorescens Texaco

Preliminary shake-flasks experiments showed that *Pseudomonas fluorescens* Texaco successfully degraded mixtures of $C_{16}H_{34}$ and wax as well as wax alone when growing on IBM at 30 °C. A lag phase of 5 to 8 days was usually observed. Fermenations with *Pseudomonas fluorescens* Texaco showed no surface active properties. Of the four best candidates (*Arthrobacter paraffineus* ATCC 19558, *Mycobacterium* OFS, *Pseudomonas fluorescens* Texaco and *Rhodococcus* IS01), *Pseudomonas fluorescens* Texaco was the only one that did not grow on hepta-methyl nonane (HMN) (it did grow on pristane however). All the other bacteria tested grew on HMN and pristane.

Run#6 with *Pseudomonas fluorescens* Texaco was unsuccessful. The medium used was IBM. The fermentation temperature was 30 °C. Eight g/L of $C_{16}H_{34}$ and 1 g/L of hepta-methyl nonane (HMN) were added at the beginning of every cycle. HMN was used as a solubilizing agent for the subsequent additions of solid hydrocarbons. Figure 5-7 shows the DO trace for cycle 5 (middle cycle). The length of the cycles averaged 23hrs and the difference in DO between the beginning and the end of the cycle was only 5% suggesting that the growth of *Pseudomonas fluorescens* Texaco was occurring very slowly. Attempts to grow the bacteria with hexadecane alone also failed.

The medium was changed to MMSM in an attempt to rescue this run because MMSM contains the essential nutrients the bacteria needed in excess and had a better buffering capacity. It was unsuccessful, the cycles were still 23 hours long. Intracycle pH measurements were taken to try to elucidate the situation. The pH at the beginning of the run was 7, after 12 hours the pH was 5.3 and after 21 hours was down to 3.5. Such a low pH inhibits bacterial growth. No further attempt to rescue the run were pursued. Since no useful stable DO profiles were obtained, no intracycle measurements of the residual hydrocarbons were taken.

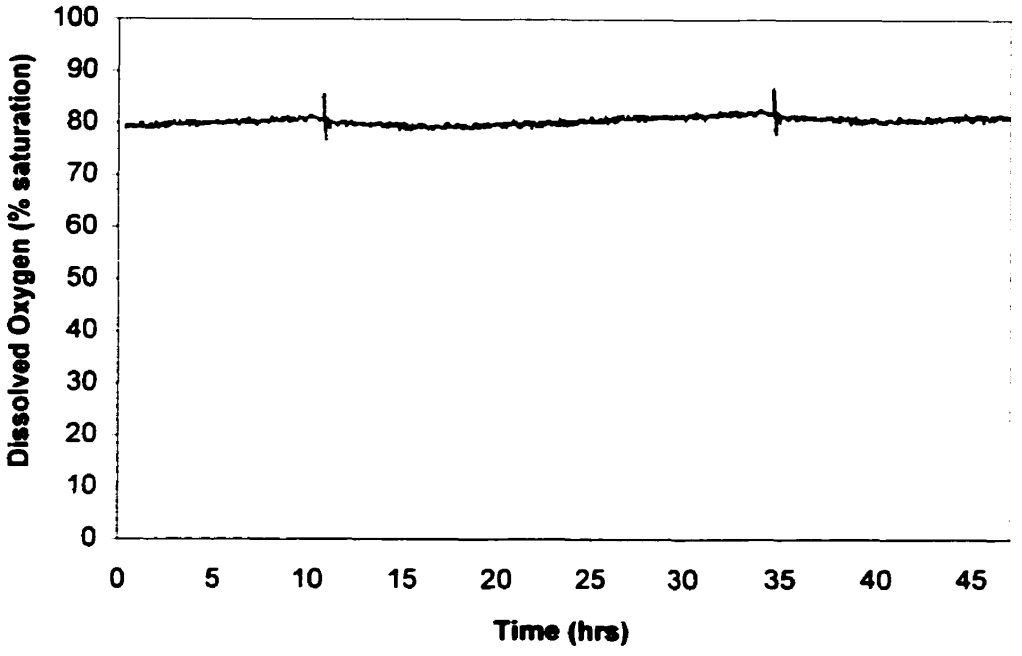

Figure 5-7: Dissolved oxygen trace: run#6, *Pseudomonas fluorescens* Texaco.

5.2.4 *Self-Cycling Fermentation* with *Rhodococcus* IS01

Preliminary shake-flask experiments with *Rhodococcus* IS01 were very promising. This bacterium grew quickly (24 hrs) on mixtures of $C_{16}H_{34}$ and wax as well as on wax alone. An interesting macroscopic feature of *Rhodococcus* IS01, while growing on wax alone, was that after 36 hrs, the wax was transformed from a solid hydrocarbon disk floating on top of the medium to broken smaller pieces of paraffin dispersed throughout the medium. This observation could imply the production of a secondary metabolite having surface active properties. Surface tension measurements were taken with *Rhodococcus* IS01 growing on 8 g/L of $C_{16}H_{34}$. Surface tensions as low as 26 mN/m were recorded for the whole broth (medium and cells). After centrifuging the cells out of the broth, the supernatant showed a surface tension of 70 mN/m suggesting that the biosurfactant was cell associated. Further studies demonstrated that the biosurfactant was only present in significant quantities when the cells were grown on excess hydrocarbons as a sole carbon source (>8 g/L).

Figure 5-8 shows a typical DO profile for 3 cycles of the system growing on pristane for run#7. Figure 5-9 shows the DO traces of two cycles and a half with on $C_{16}H_{34}$ for run#7. The average cycle time was 271 min (4.5 hrs) for growth on $C_{16}H_{34}$ and other *n*-alkanes and 182 min (3 hrs) for growth on pristane and other *n*-alkanes. The air flowrate was 0.2 L/min. The DO decreased steadily until the maximum oxygen demand was reached after 180 min, at which point the DO trace suddenly increased sharply causing the computer to terminate the cycle. This trace is typical (for this work) for fermentations in which the limiting nutrient was completely exhausted. Note that, unlike the previous SCF runs, run#7 was performed using a balance to determine the amount of broth removed during the emptying phase and the amount of fresh medium added during the filling phase instead of a differential pressure transducer cell (DP cell). This is important because it was not necessary to stop the circulation of the broth by turning off the pump during cycling. This ensured homogeneity of the volume removed in the harvesting step.

Figure 5-10 shows the intracycle concentrations of the biomass, $C_{16}H_{34}$ and wax for cycle 36. Half a g/L of $C_{16}H_{34}$ and 0.15 g/L of wax were added to reactor at the beginning

of each cycle. The biomass concentration increased as the *n*-alkanes concentrations decreased and reached a constant value when the $C_{16}H_{34}$ and the wax had been completely oxidized. Figure 5-11 also shows the disappearance of $C_{16}H_{34}$, but the wax concentrations are presented with a larger scale. The $C_{16}H_{34}$ was completely oxidized approximately 100 minutes before the wax disappeared. At about 200 minutes, there was a step like decrease in the concentration of paraffin wax as the hexadecane disappeared.

Figure 5-12 through 5-14 shows the concentrations of the individual *n*-alkane components of paraffin wax over time for cycle 36

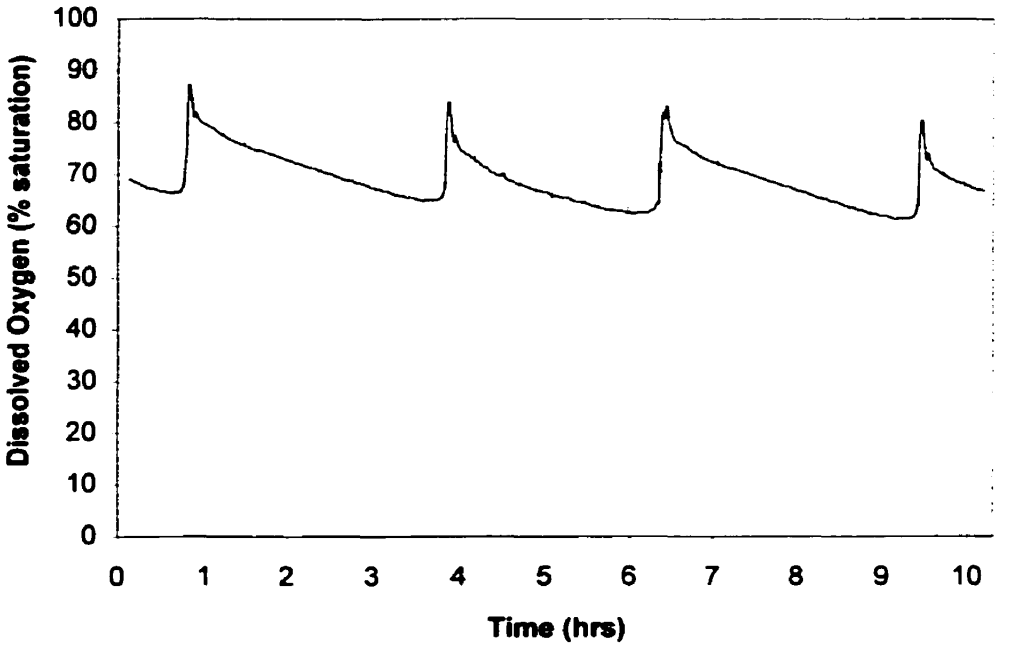

Figure 5-8: Dissolved oxygen trace: cycles with pristane, run#7, *Rhodococcus* IS01.

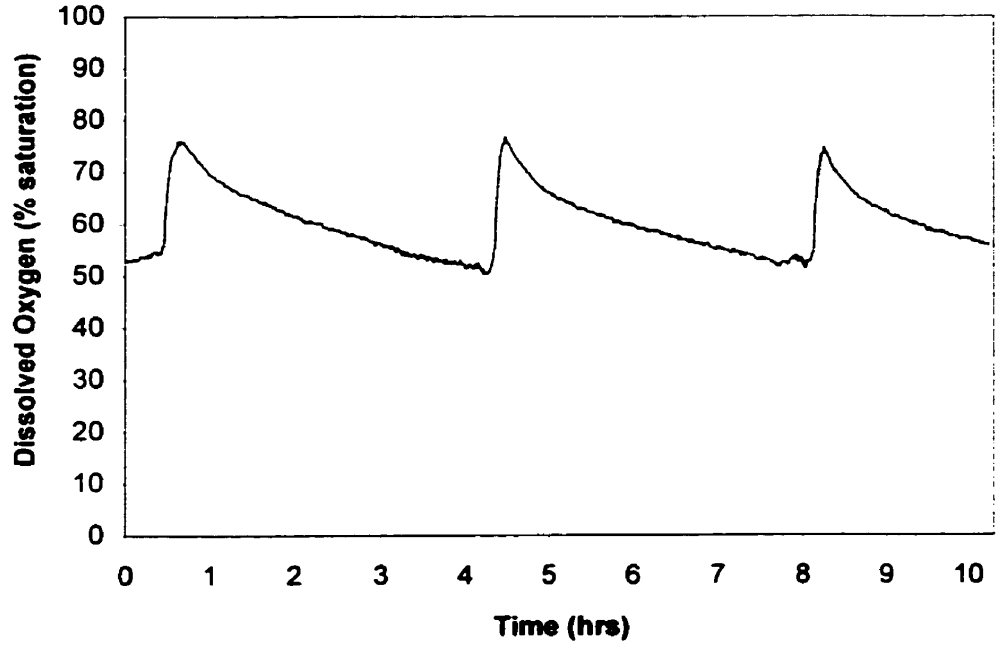

Figure 5-9: Dissolved oxygen trace: cycles with hexadecane, run#7, *Rhodococcus* IS01.

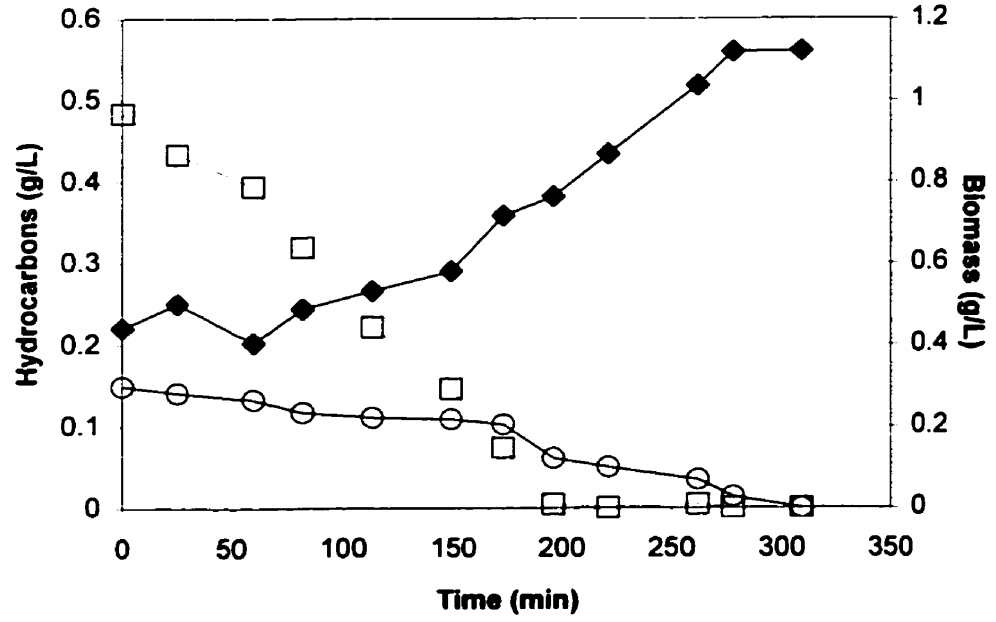

Figure 5-10: Concentration of biomass (◆), hexadecane (□) and wax (○) *versus* time: run #7, cycle 36, *Rhodococcus* IS01.

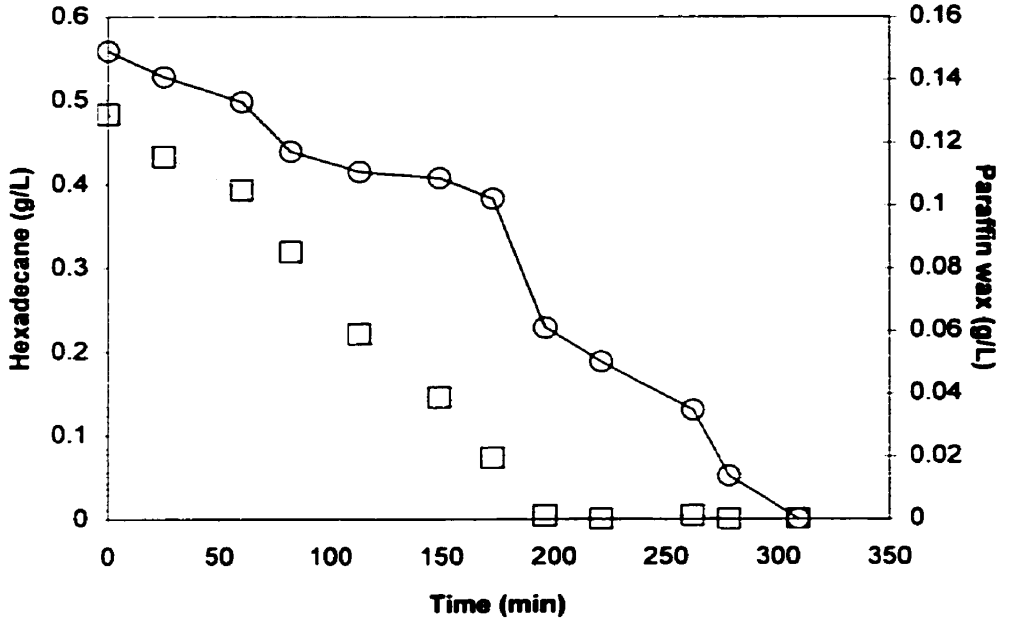

Figure 5-11: Concentration of hexadecane (□) and wax (○) *versus* time: run #7, cycle 36, *Rhodococcus* IS01.

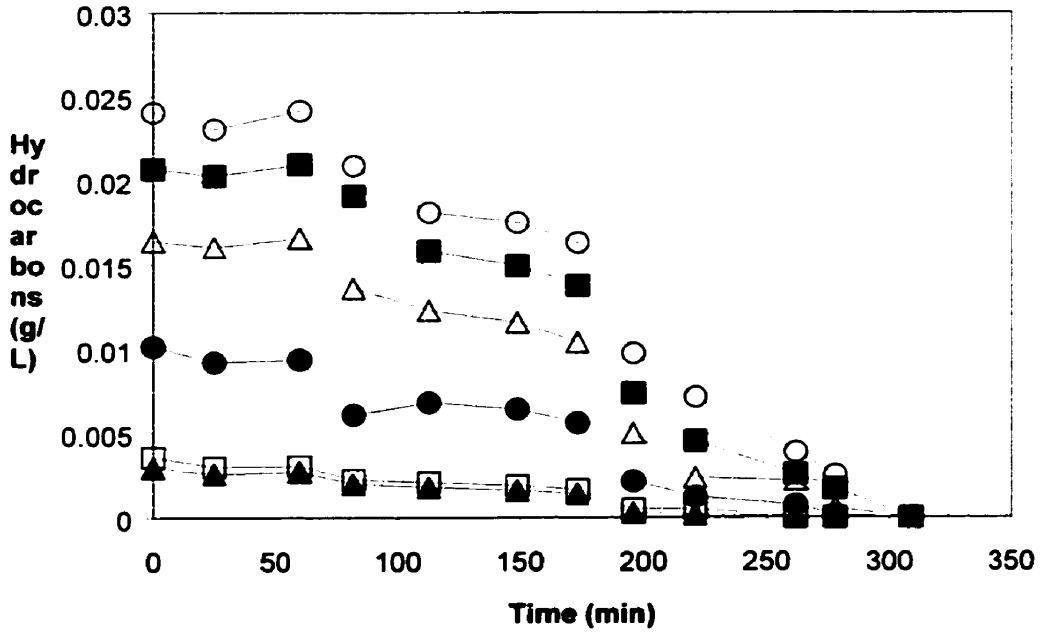

Figure 5-12: Concentration of *n*-alkanes $C_{20}H_{42}$ (▲), $C_{21}H_{44}$ (□), $C_{22}H_{46}$ (●),$C_{23}H_{48}$ (Δ),$C_{24}H_{50}$ (■), $C_{25}H_{52}$ (○), run #7, cycle 36, *Rhodococcus* IS01.

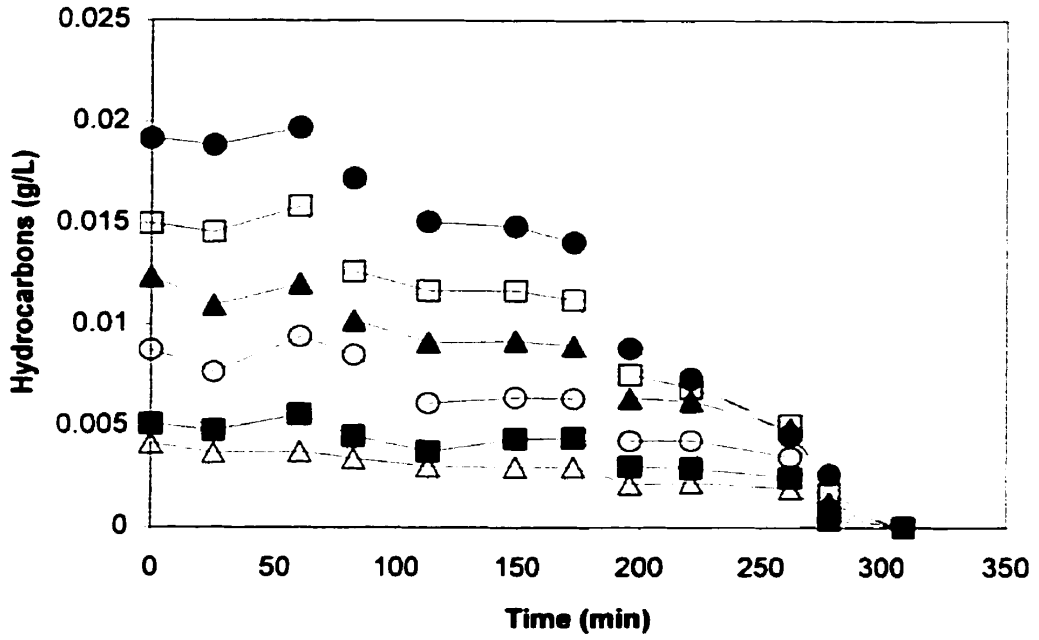

Figure 5-13: Concentration of *n*-alkanes $C_{26}H_{54}$ (●), $C_{27}H_{56}$ (□), $C_{28}H_{58}$ (▲), $C_{29}H_{60}$ (○),$C_{30}H_{62}$ (■), $C_{31}H_{64}$ (Δ), run #7, cycle 36, *Rhodococcus* IS01.

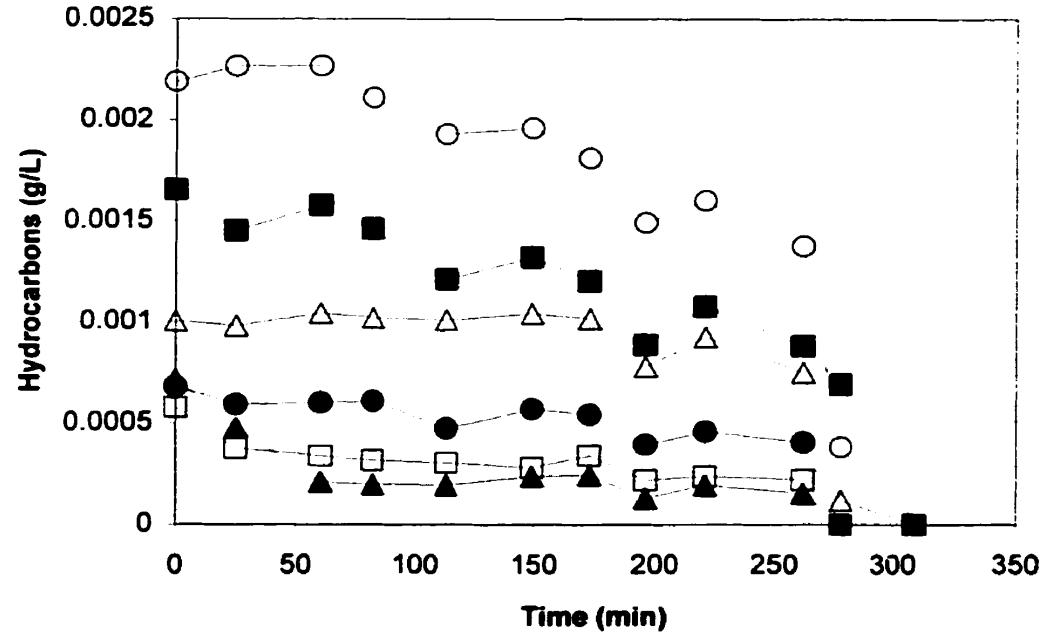

Figure 5-14: Concentration of *n*-alkanes $C_{32}H_{66}$ (○), $C_{33}H_{68}$ (■), $C_{34}H_{70}$ (Δ), $C_{35}H_{72}$ (●), $C_{36}H_{74}$ (□),$C_{37}H_{76}$ (▲), run #7, cycle 36, *Rhodococcus* IS01.

To study the kinetics of biodegradation of *n*-alkanes in the SCF, two sets of experiments were performed. The first set of experiments consisted of the Self-Cycling-Fermentation using $C_{16}H_{34}$ as the solubilizing hydrocarbon and the second set consisted of Self-Cycling-Fermentation using pristane as the solubilizing agent. For both sets of fermentations, it required an average of 4 cycles between each set of experiments (i.e. changes in the carbon source) before the SCF cycles returned to stable and repeatable patterns.

The results of the first set of experiments performed using hexadecane as the constant hydrocarbon in each fermentation is presented next. Figure 5-15 shows the concentrations of the biomass and hexadecane for cycle 5 of run#7. The $C_{16}H_{34}$ was completely exhausted. Figure 5-16 shows the concentrations of the biomass, $C_{12}H_{26}$ and $C_{16}H_{34}$ for cycle 11 of the same run. Figure 5-17 shows the evolution of the biomass, $C_{16}H_{34}$ and $C_{17}H_{36}$ for cycle 16. Figure 5-18 shows the concentrations of the biomass, $C_{16}H_{34}$ and $C_{20}H_{42}$ for cycle 22. Figure 5-19 shows the concentrations of the biomass, $C_{16}H_{34}$ and $C_{25}H_{52}$ for cycle 28. The results for the experiment of this set, growing *Rhodococcus* IS01 on a mixture of $C_{12}H_{26}$, $C_{16}H_{34}$, $C_{17}H_{36}$, $C_{20}H_{42}$ and $C_{25}H_{52}$, are presented in figure 5-20 (cycle 32). All hydrocarbons were completely oxidized. The last fermentation involved in growing the cells on $C_{16}H_{34}$ and nonane (C_9H_{20}). Nonane was toxic to the cells. In less than 30 minutes most of the cells died. This death was characterized by a sudden clearing of the biomass in the cyclone reactor (the medium went from a turbid appearance to a light, transparent yellow color).

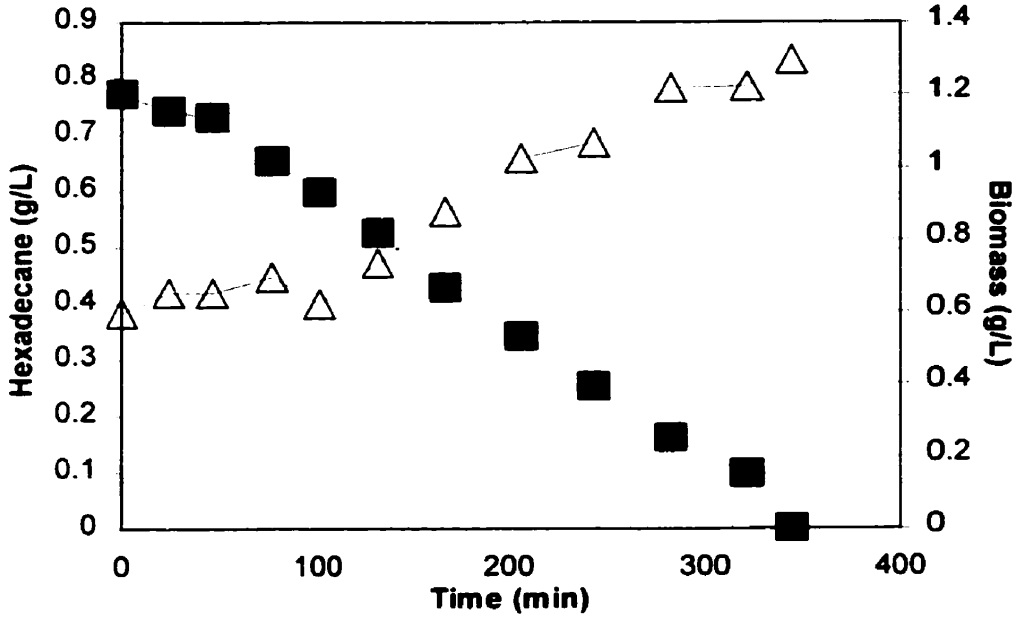

Figure 5-15: Concentration of hexadecane (■) and biomass ()), run #7, cycle 5, *Rhodococcus* IS01.

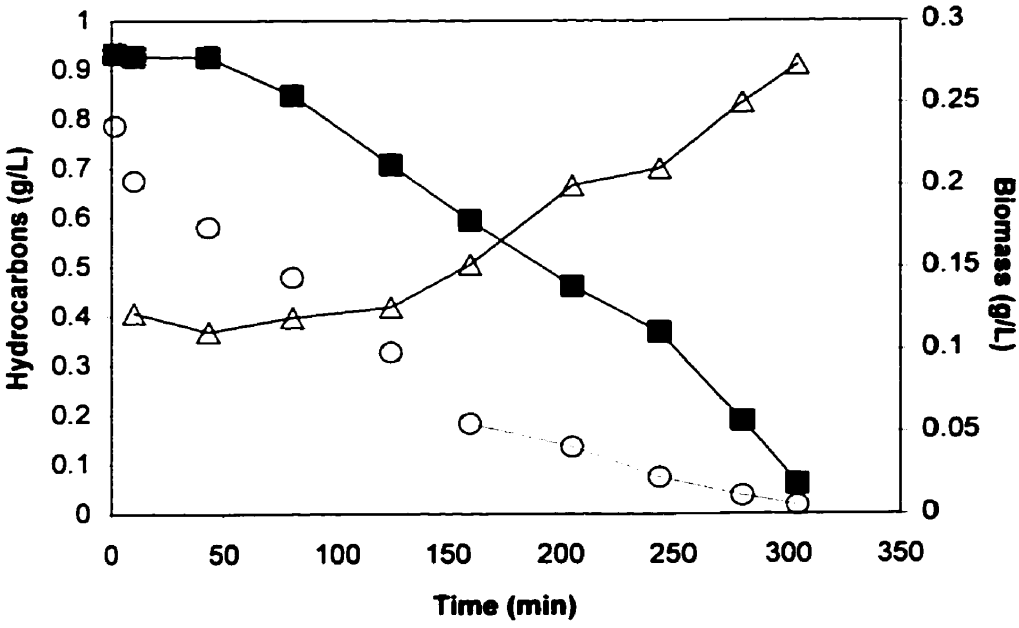

Figure 5-16: Concentration of hexadecane (■), dodecane (O) and biomass (Δ), run #7, cycle 11, *Rhodococcus* IS01.

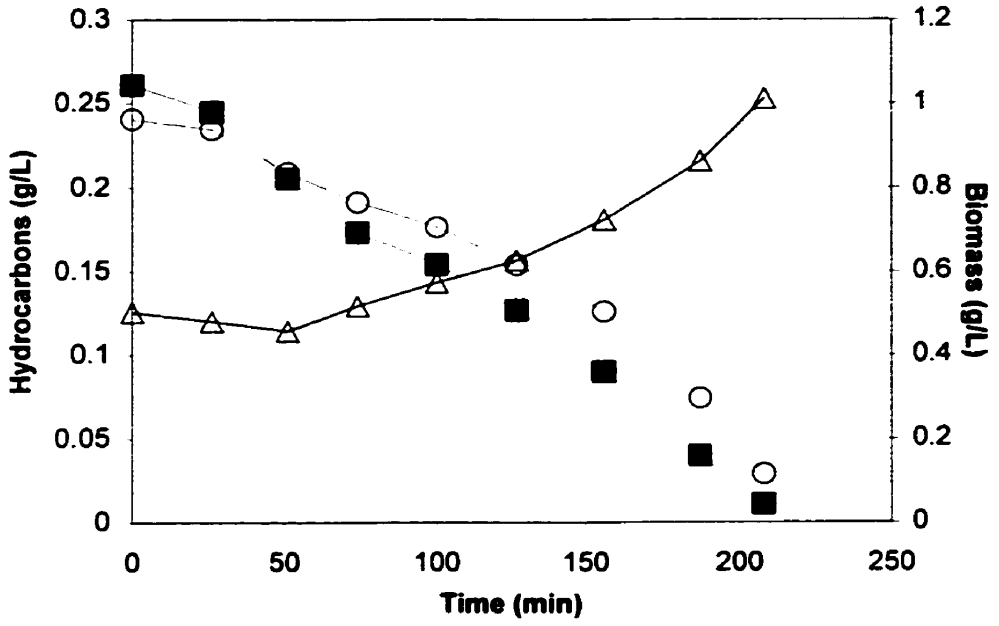

Figure 5-17: Concentration of hexadecane (■), heptadecane (○) and biomass (Δ), run #7, cycle 16, *Rhodococcus* IS01.

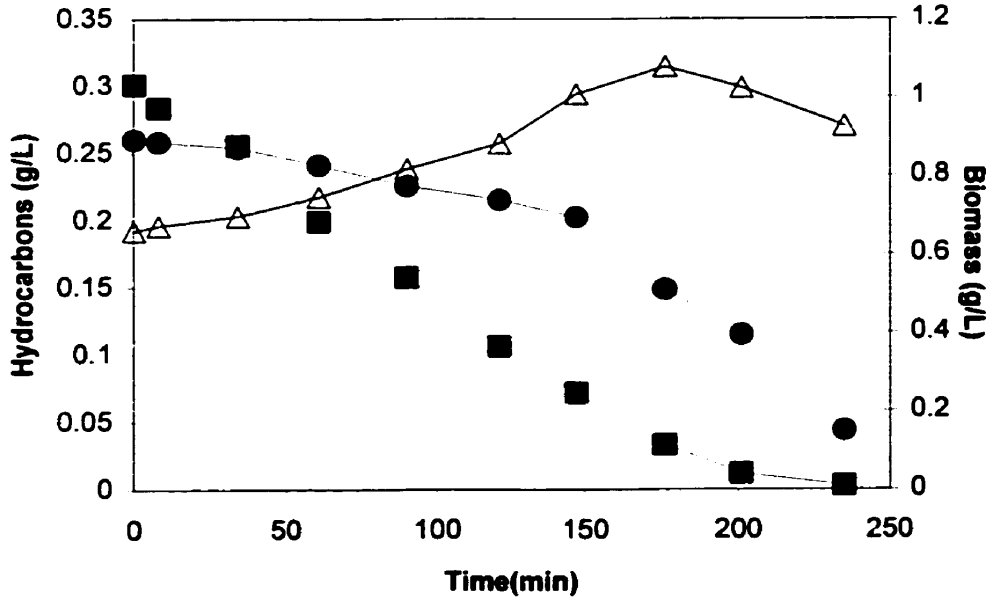

Figure 5-18: Concentration of hexadecane (■), eicosane (●) and biomass (Δ), run #7, cycle 22, *Rhodococcus* IS01.

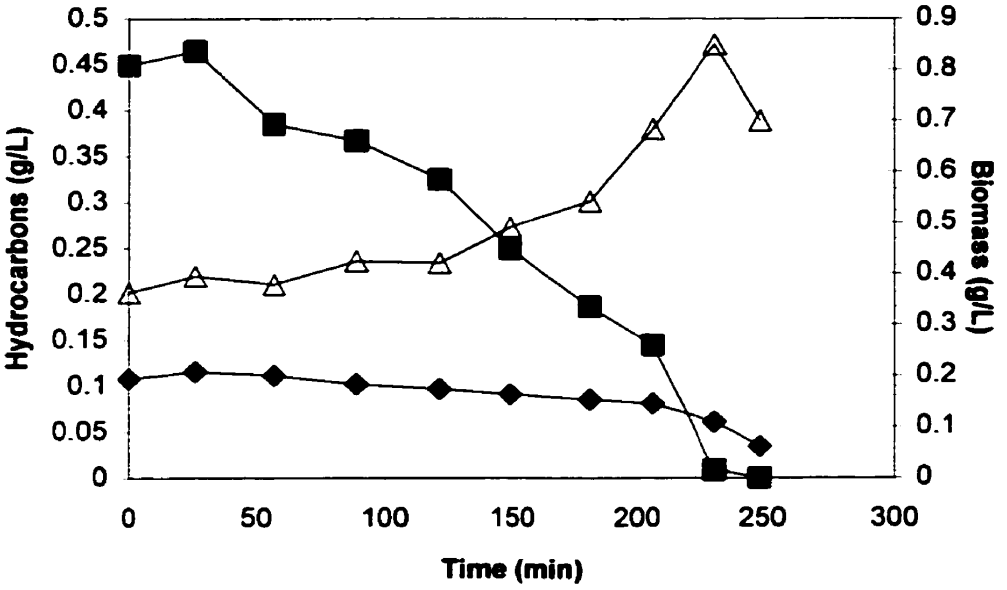

Figure 5-19: Concentration of hexadecane (■), pentacosane (◆) and biomass (Δ), run #7, cycle 28, *Rhodococcus* IS01.

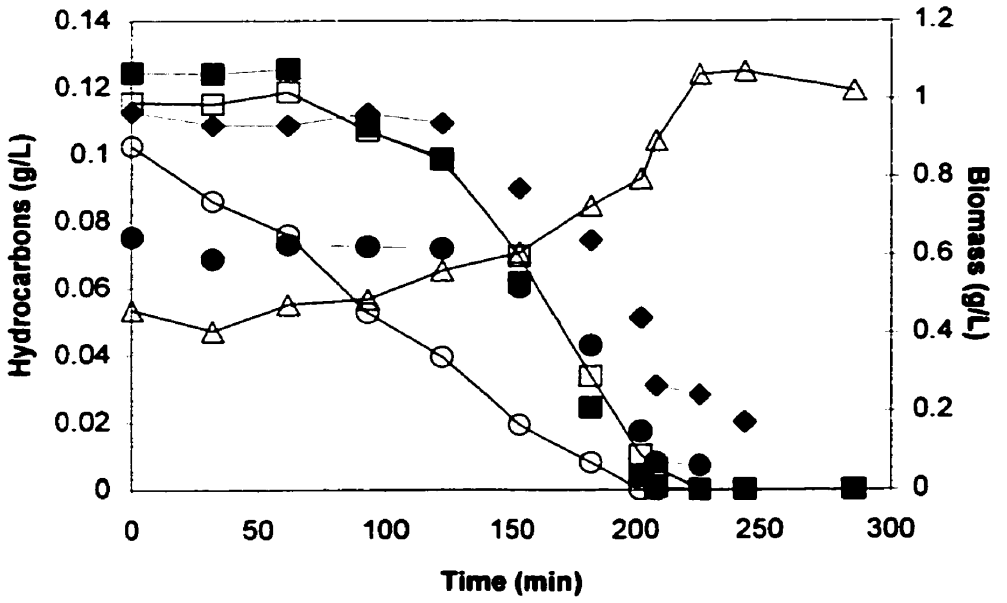

Figure 5-20: Concentration of dodecane (O), hexadecane (■), heptadecane (□), eicosane (●), pentacosane (◆) and biomass (Δ), run #7, cycle 32, *Rhodococcus* IS01.

The next 7 figures present the results for the fermentations using pristane was the olubilizing hydrocarbon. Except for cycle 57, no biomass measurements were obtained for this set of fermentations. Figure 5-21 shows the concentrations of $C_{12}H_{26}$ and pristane over time for cycle 38. Figure 5-22 shows the degradation of $C_{16}H_{34}$ and pristane for cycle 43. Figure 5-23 shows the concentrations of $C_{20}H_{42}$ and pristane over time for cycle 48. Figure 5-24 shows the concentrations of $C_{25}H_{52}$ and pristane over time for cycle 52. Figure 5-25 shows the concentrations for mixture#1 which consisted of $C_{12}H_{26}$, $C_{17}H_{36}$, $C_{20}H_{42}$, $C_{25}H_{52}$, pristane and biomass *versus* time for cycle 57. Figure 5-26 shows the results for the fermentation of the *n*-alkane mixture#2 which has the same composition as mixture#1 except for the initial concentration of $C_{12}H_{26}$ which was halved. And finally, figure 5-27 show the concentrations of pristane and the solid *n*-alkanes $C_{20}H_{42}$, $C_{25}H_{52}$ and $C_{30}H_{62}$ over time for cycle 66. In each of the above seven cases, the concentration of pristane in the fermentation remained constant. No degradation was apparent. If oxidation of pristane did take place, it was negligible. After the end of cycle 66, no additional hydrocarbons were added to the SCF and the fermentation was left to continue for another 12 hrs. At that point, the only hydrocarbon detectable in the SCF was pristane. In 12 hrs, the concentration of pristane in the reactor decreased from 3.4 g/L to 1.4 g/L suggesting that *Rhodococcus* IS01 has the ability to degrade pristane when more favored carbon source is not available.

Figure 5-28 shows the carbon dioxide evolution by *Rhodococcus* IS01 when it was growing on pristane and $C_{16}H_{34}$ and then followed by pristane and $C_{20}H_{42}$. The profiles correlated well with the dissolved oxygen traces. The CO_2 production reached its maximum when the O_2 demand also reached its maximum.

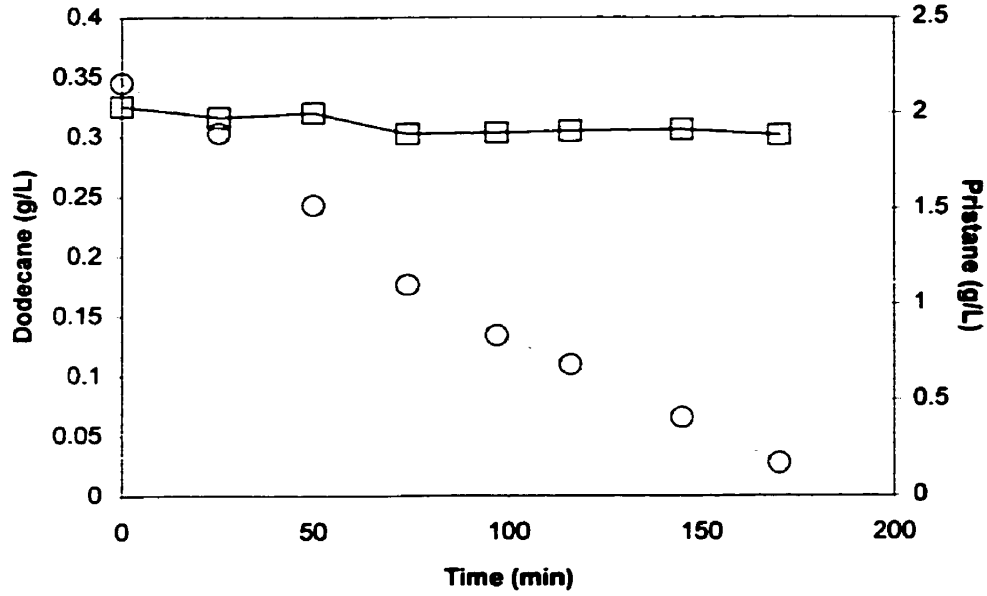

Figure 5-21: Concentration of dodecane (O) and pristane (□), run #7, cycle 38, *Rhodococcus* IS01.

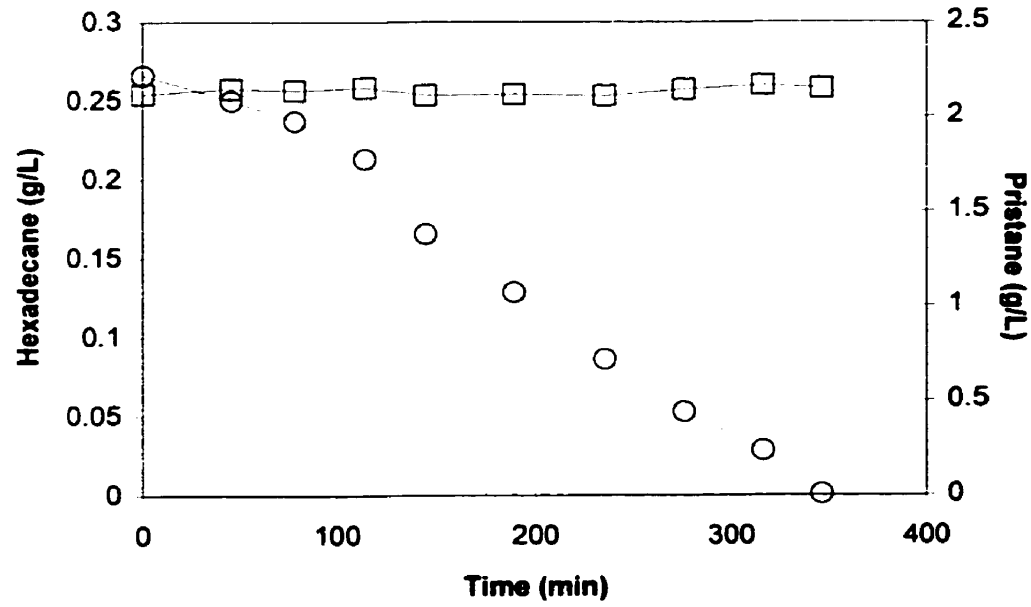

Figure 5-22: Concentration of hexadecane (O) and pristane (□), run #7, cycle 43, *Rhodococcus* IS01.

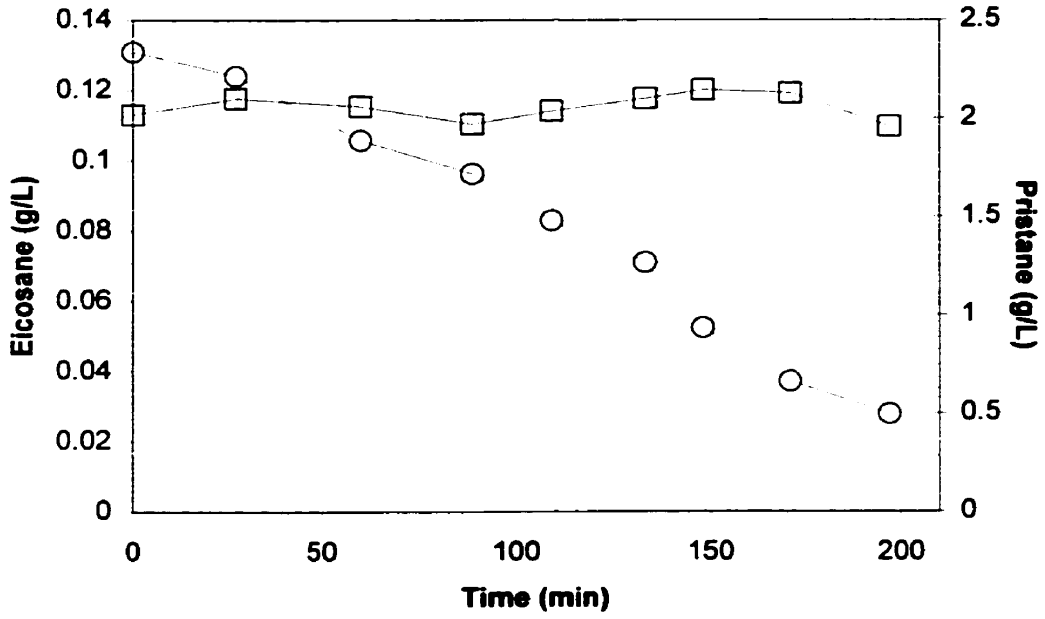

Figure 5-23: Concentration of eicosane (O) and pristane (□), run #7, cycle 48, *Rhodococcus* IS01.

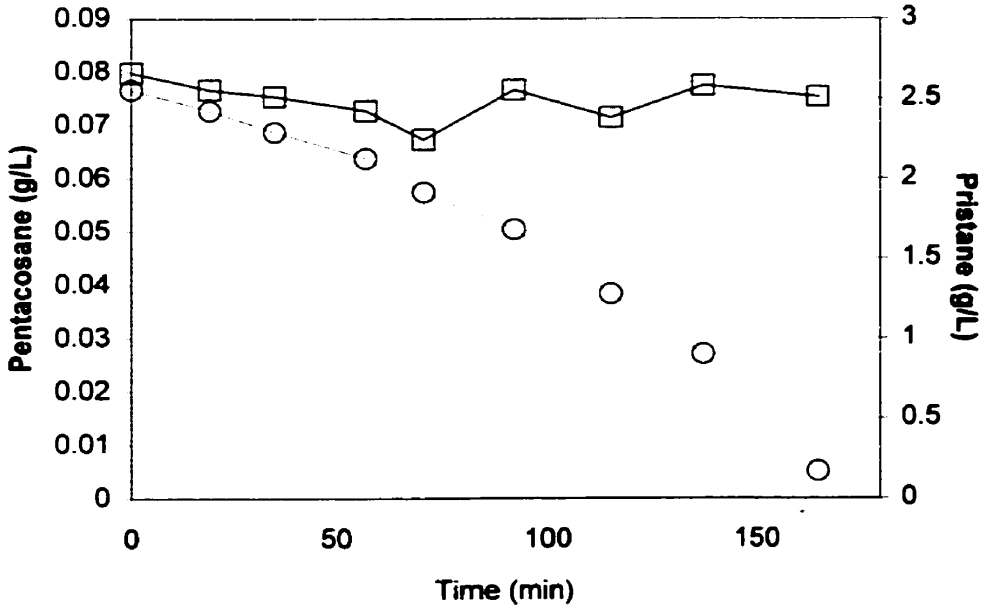

Figure 5-24: Concentration of pentacosane (O) and pristane (□), run #7, cycle 52, *Rhodococcus* IS01.

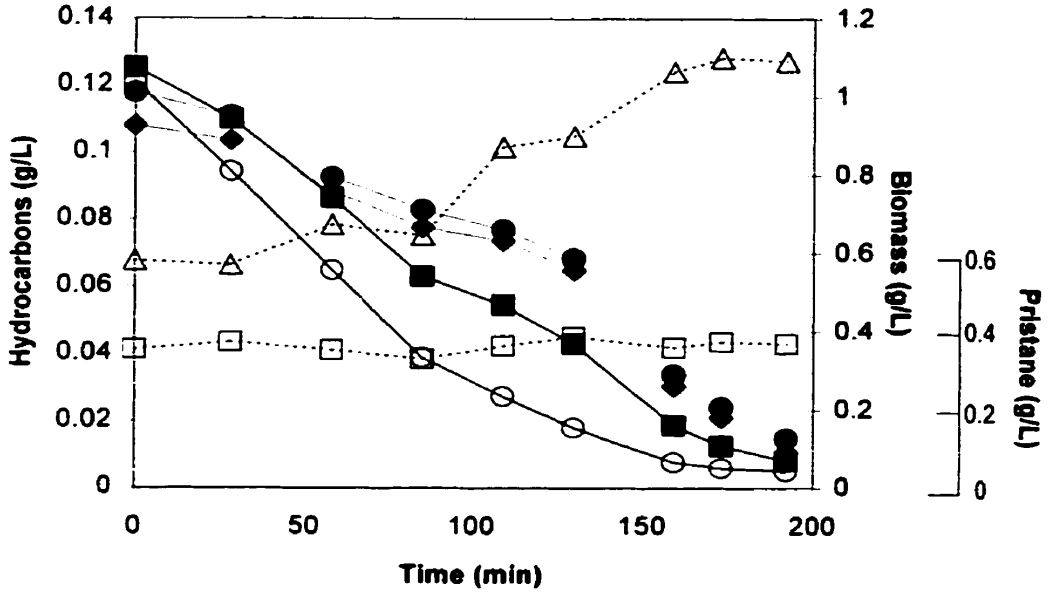

Figure 5-25: Concentration of mixture #1 of dodecane (○), heptadecane (■), eicosane (●), pentacosane (◆), pristane (□) and biomass (Δ), run #7, cycle 57, *Rhodococcus* IS01.

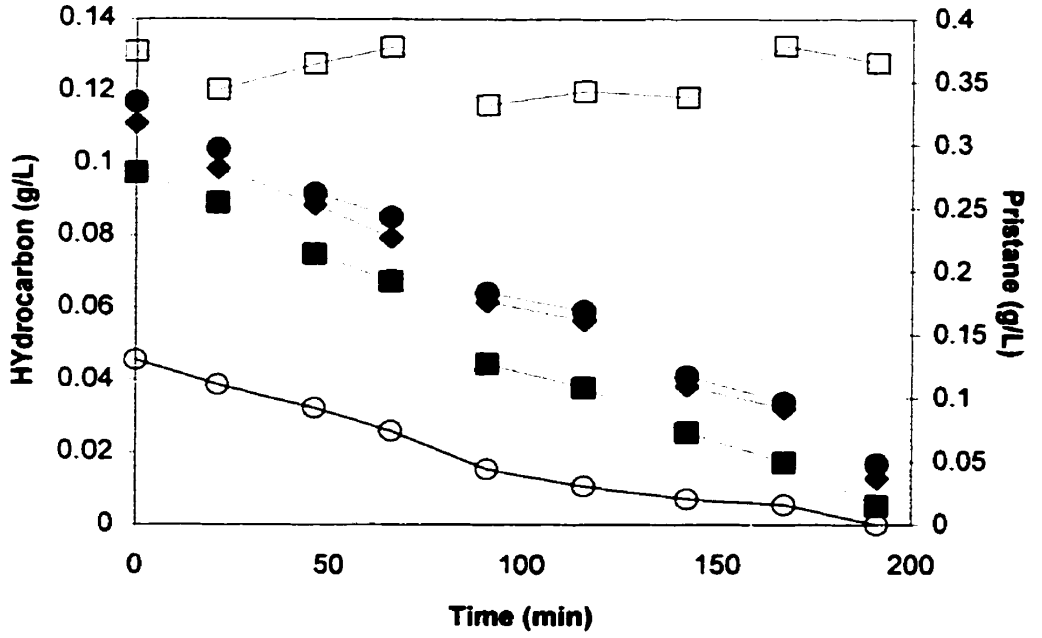

Figure 5-26: Concentration of mixture #2 of dodecane (○), heptadecane (■), eicosane (●), pentacosane (◆) and pristane (□), run #7, cycle 62, *Rhodococcus* IS01.

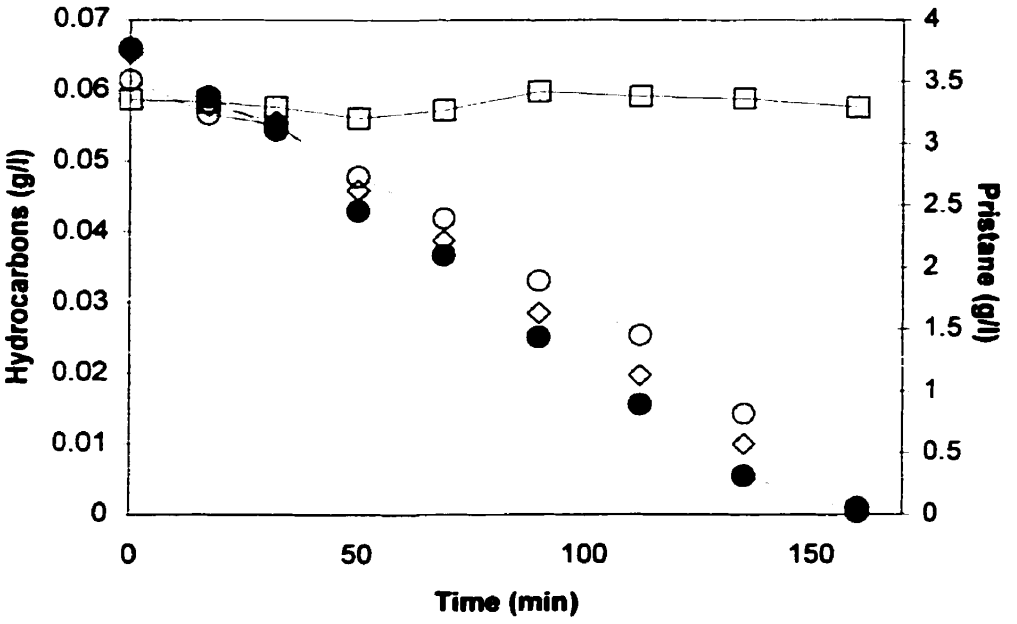

Figure 5-27: Concentration of eicosane (●), pentacosane (◊), triacontane (○) and pristane (□), run #7, cycle 66, *Rhodococcus* IS01.

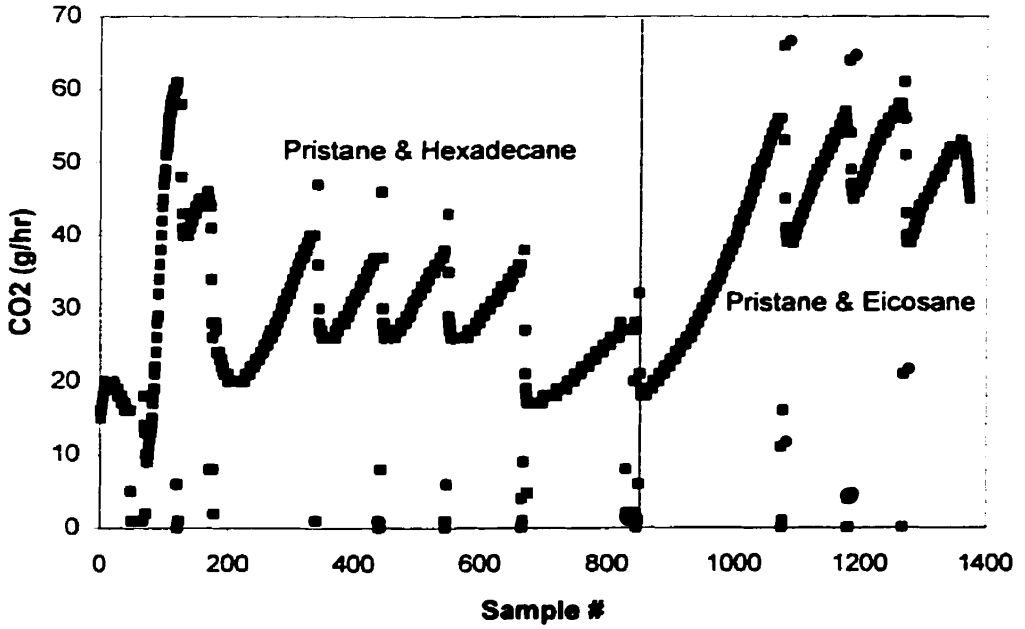

Figure 5-28: Carbon dioxide evolution for pristane and $C_{16}H_{34}$ run and pristane and $C_{20}H_{42}$, run#7, *Rhodococcus* IS01.

5.3 Abiotic Run

To determine if the disappearance of the hydrocarbons observed in the Self-Cycling fermentations mentioned above was solely due to microbiological factors or if it was due partially to other factors such as the volatility of the hydrocarbons, a mixture of *n*-alkanes ($C_{12}H_{26}$, $C_{16}H_{34}$, $C_{17}H_{36}$, $C_{20}H_{42}$ and $C_{25}H_{52}$) and pristane were added to the cyclone reactor under abiotic conditions. Figure 5-29 shows the concentrations of the *n*-alkanes of the mixture in the SCF after 16 hrs. The decrease in hydrocarbons during that period was negligible indicating that the disappearance of the *n*-alkanes was due to the microorganisms and not to stripping by the stream of air.

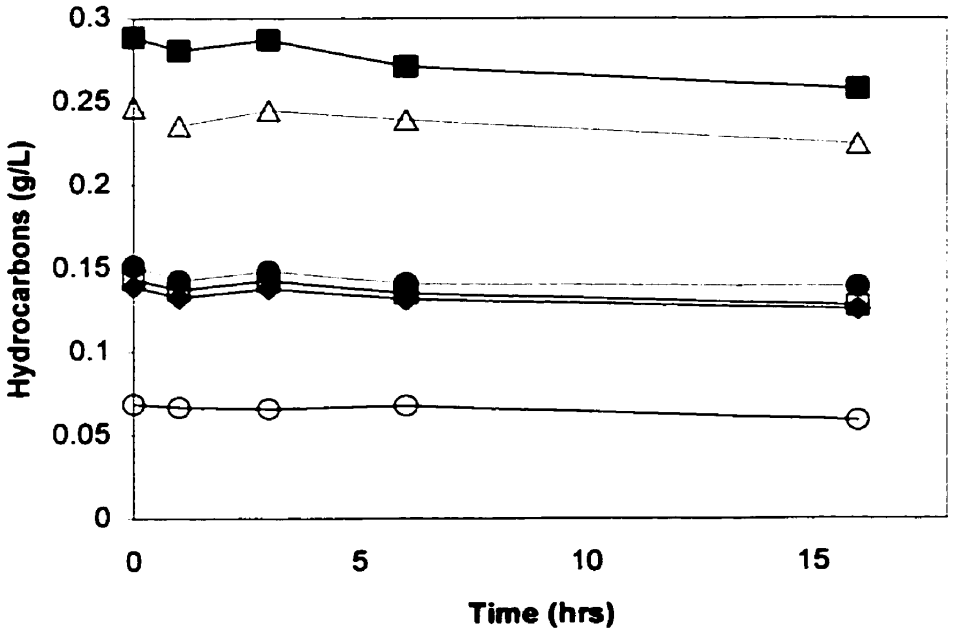

Figure 5-29: Concentration of dodecane (○), hexadecane (■), heptadecane (□), eicosane (●), pentacosane (◆) and pristane (Δ), Abiotic run .

5.4 First-order oxidation rate constants k

A first-order system implies that the degradation rate of the substrate is only dependant on the substrate concentration. The Monod growth equation can be simplified to a first-order system if 2 conditions are met: 1) the biomass concentration must be constant and 2) the half saturation constant Ks must be much larger than the substrate concentration.

Condition 1 was met by looking at the biomass concentration. The biomass concentration generally started to increase after the 4th sample. Therefore for those first 4 samples, it can be assumed that the biomass was more or less constant.

Condition 2 was met by looking at non-linear regression and a genetic algorithm results obtained when fitting the Monod kinetics model to the data obtained with the SCF. Both methods gave the same results. Except for dodecane, Ks was consistently found to be much larger than the concentrations used in the fermentations (see table 2).

Table 5-2: Initial substrate concentrations and Ks values for run#7.

Hydrocarbon	Ks (g/L)	So (g/L)
Pristane +...		
$C_{30}H_{62}$	0.978	0.061
$C_{25}H_{52}$	2.063	0.076
$C_{20}H_{42}$	1.278	0.131
$C_{17}H_{36}$	5.491	0.345
$C_{12}H_{26}$	0.517	0.266
Hexadecane +...		
$C_{25}H_{52}$	0.931	0.108
$C_{20}H_{42}$	15.17	0.261
$C_{17}H_{36}$	3.911	0.241
$C_{16}H_{34}$	13.25	0.777
$C_{12}H_{26}$	0.388	0.236

Since the two criteria required to assume a first-order system were met, the first-order oxidation constants k were determined by finding the slope of the natural logarithm of the ratio of the concentration of the hydrocarbon under study over it's initial concentration when plotted against time. Only the first four of five data of each experiment were used to compute the constants.

Figure 5-30 shows the results of the 1st order oxidation constants *versus* the number of carbons in the *n*-alkane molecule for the set of experiments using pristane as the solubilizing agent. Figure 5-31 shows the 1st order oxidation constants *versus* the carbon number for the set of experiments using $C_{16}H_{34}$ as the solubilizing hydrocarbons. The 1st order oxidation constants were also calculated for the $C_{16}H_{34}$ and wax degradation data recorded during cycle 36 and are shown in figure 5-32.

5.5 Maximum specific growth rate μ_{max}

The two parameters μ_{max} and Ks were obtained by fitting the Monod kinetics mathematical model to the SCF data using non-linear regression and a genetic algorithm. In all cases, the maximum specific growth rate μ_{max} was found to be the same by both methods. Both methods gave the same results for Ks as well. Figure 5-33 shows the maximum specific growth rate μ_{max} *versus* the carbon number for the pristane experiments. Figure 5-34 shows the maximum specific growth rate μ_{max} *versus* the carbon number for the hexadecane experiments.

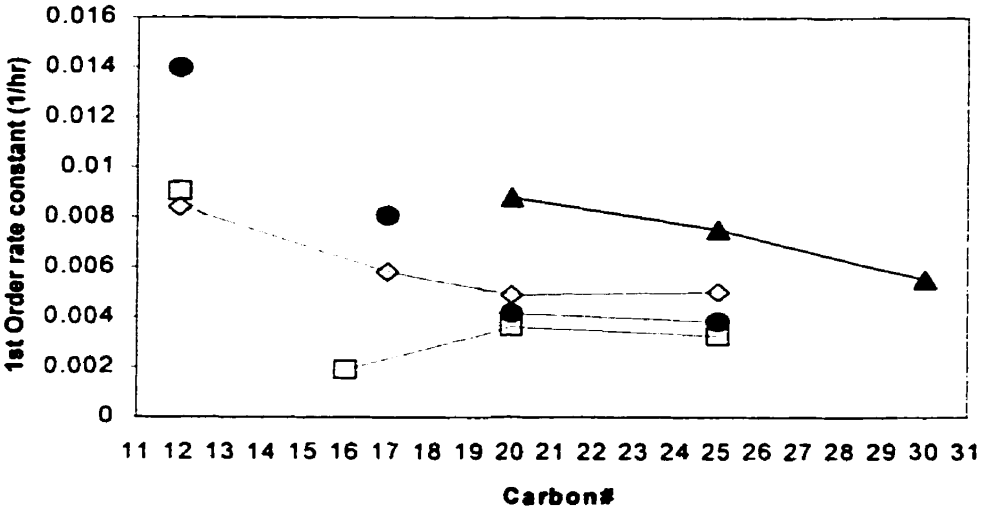

Figure 5-30: First-order oxidation rate constants *versus*. carbon number. Pristane and individual *n*-alkanes (□), pristane and mixture of $C_{12}H_{26}$, $C_{17}H_{36}$, $C_{20}H_{42}$ & $C_{25}H_{52}$ #1 (●), pristane and mixture of $C_{12}H_{26}$, $C_{17}H_{36}$, $C_{20}H_{42}$ & $C_{25}H_{52}$ #2 (◊), pristane and mixture of $C_{20}H_{42}$, $C_{25}H_{52}$ and $C_{30}H_{62}$ (▲).

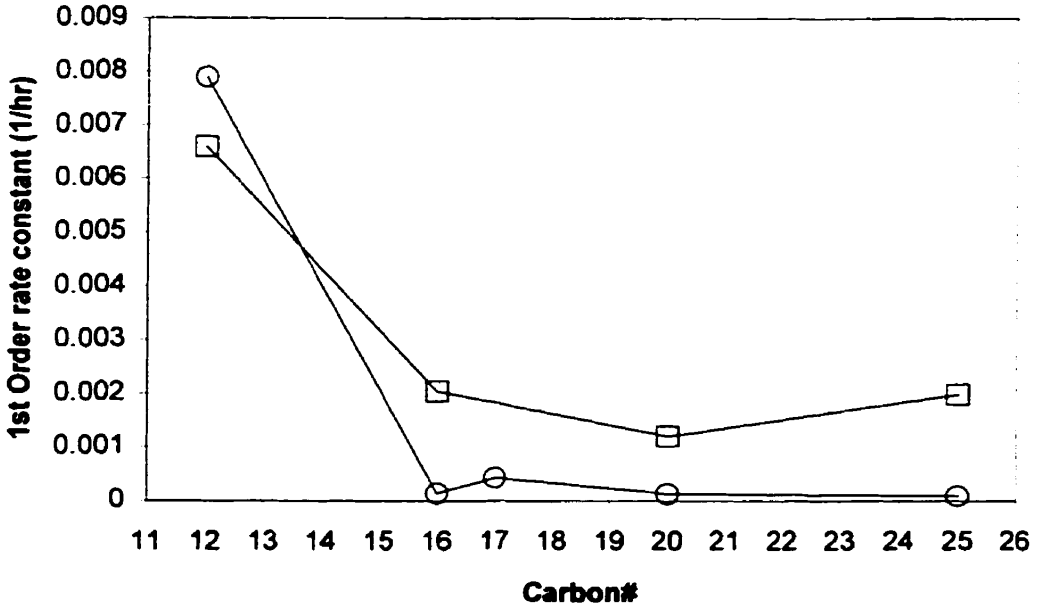

Figure 5-31: First-order oxidation rate constants *versus*. carbon number. Hexadecane and individual *n*-alkanes (□), hexadecane with mixture of $C_{12}H_{26}$, $C_{17}H_{36}$, $C_{20}H_{42}$ & $C_{25}H_{52}$ (○).

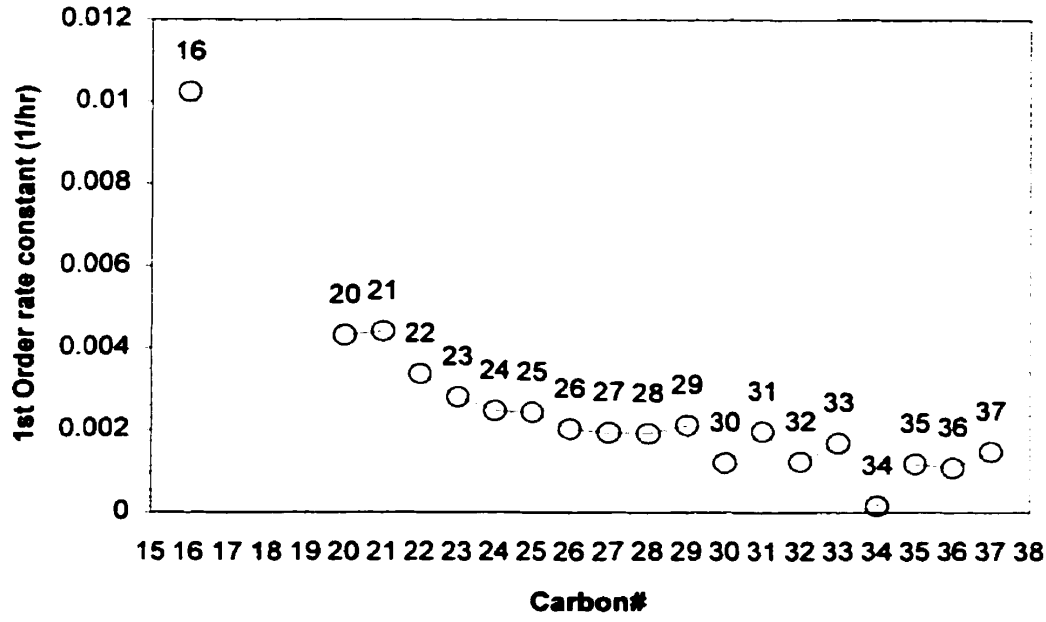

Figure 5-32: First-order oxidation rate constants *versus*. carbon number. Hexadecane and individual *n*-alkanes from paraffin wax (O), run #7, cycle 36, *Rhodococcus* IS01

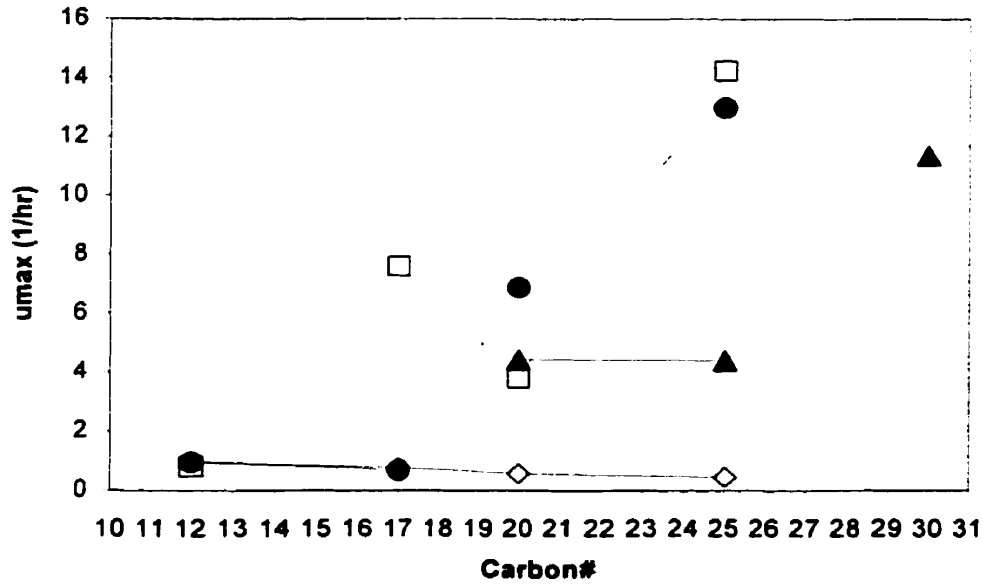

Figure 5-33: Maximum specific growth rate μ_{max} *versus*. carbon number. Pristane and individual *n*-alkanes (□), pristane and mixture of $C_{12}H_{26}$, $C_{17}H_{36}$, $C_{20}H_{42}$ & $C_{25}H_{52}$ #1 (●), pristane and mixture of $C_{12}H_{26}$, $C_{17}H_{36}$, $C_{20}H_{42}$ & $C_{25}H_{52}$ #2 (◊), pristane and mixture of $C_{20}H_{42}$, $C_{25}H_{52}$ and $C_{30}H_{62}$ (▲).

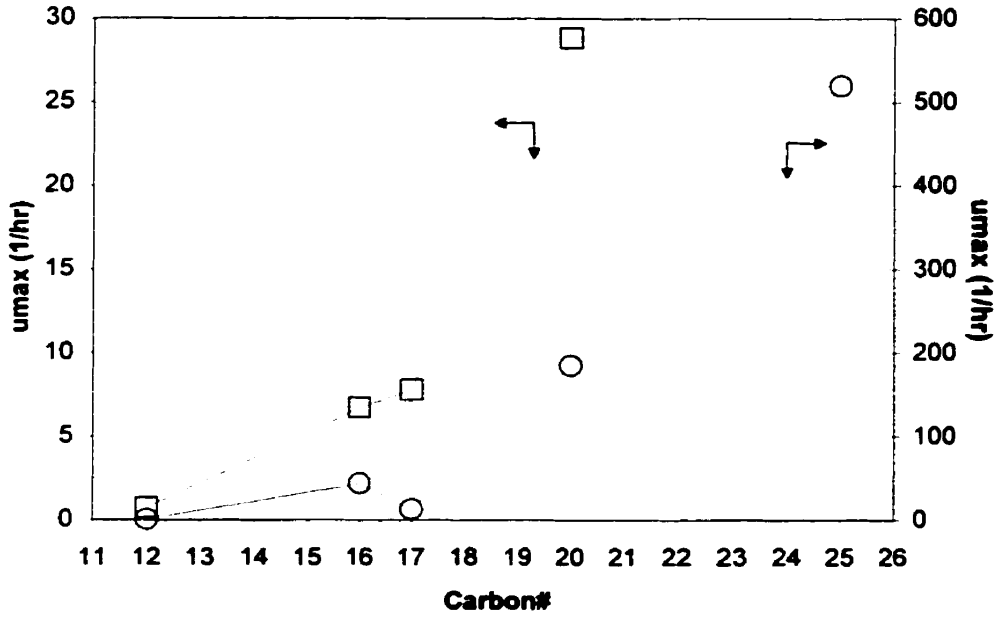

Figure 5-34: Maximum specific growth rate μ_{max} *versus* carbon number. Hexadecane and individual *n*-alkanes (□), hexadecane with mixture of $C_{12}H_{26}$, $C_{17}H_{36}$, $C_{20}H_{42}$ & $C_{25}H_{52}$ (○).

5.6 Hydrocarbon metabolite

An extra peak appeared in the chromatograms of samples analyzed by gas chromatography when *Rhodococcus* IS01, *Mycobacterium* OFS and *Arthrobacter paraffineus* ATCC 19558 were grown on paraffin wax and/or hexadecane. The peak also appeared when *Rhodococcus* IS01 was grown on individual *n*-alkanes ranging from dodecane to triacontane. The position of this peak did not correspond to the position of any of the hydrocarbons added. Figure 5-35 shows the gas chromatogram of sample 2 of cycle 36 of run#7 when *Rhodococcus* IS01 was grown on wax and hexadecane. This compound was present in small quantities at the beginning of the cycle (possibly residuals from the previous cycle). It reached a maximum concentration in sample 9 (see fig. 5-36) before decreasing in concentration toward the end of the cycle. Figure 5-37 shows the area ratio of the peak unknown compound to the internal standard (pentadecane) *versus* time for cycle 36 (paraffin wax and hexadecane). The area ratio is directly proportional to the concentration. Figures 5-38 to 5-41 show the concentration of the unknown compound for cycle 28, 32, 57 and 52 respectively *versus* time. In some of the fermentations, the concentration of the unknown compound varied dramatically as shown by figures 5-37 to 5-41. For example, a sudden increase in concentration followed by a sudden decrease in concentration was observed for the growth of *Rhodococcus* IS01 on a mixture of dodecane, hexadecane, heptadecane, eicosane and pentacosane (cycle 32, run#7, fig 5-39). The time of the sudden increase and decrease correspond to the time at which the hexadecane, the heptadecane, the eicosane and the pentacosane start being degraded at a faster rate (see fig 5-20). A similar trend was observed with the degradation of paraffin wax and hexadecane by *Rhodococcus* IS01 (cycle 36, run#7, fig. 5-11). The concentration of the unknown compound reached a maximum and then suddenly decreased when the hexadecane was depleted (see fig. 5-37). When the fermentations were performed with only a single *n*-alkane, the concentration of the unknown compound remain somewhat constant (see fig. 5-41).

The GC peaks of this compound did not correspond to a simple hydrocarbons or fatty acids ranging from lauric acid to pentacosanic acid. Mass spectrometry of the

unknown compound was performed in an attempt to identify it. The mass spectrograph is shown in figure 5-42. The pattern is consistent with a monounsaturated hydrocarbon with a formula $C_{24}H_{48}$.

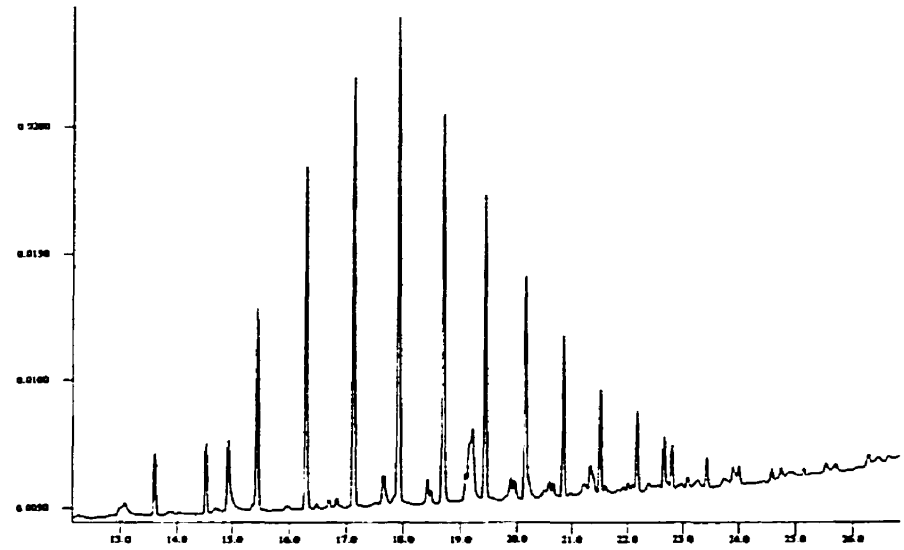

Figure 5-35: Gas chromatogram of paraffin wax, run#7, cycle 36, sample 2, *Rhodococcus* IS01.

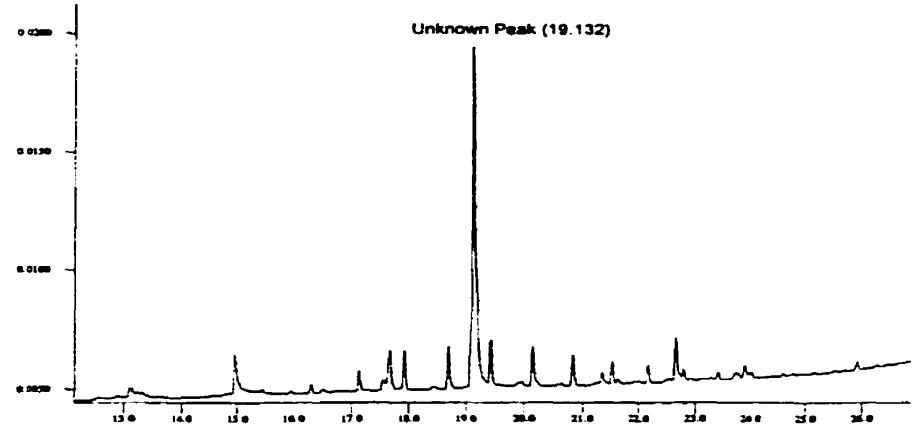

Figure 5-36: Gas chromatogram of paraffin wax, run#7, cycle 36, sample 9, *Rhodococcus* IS01. The unknown peak appears at 19.132 minutes.

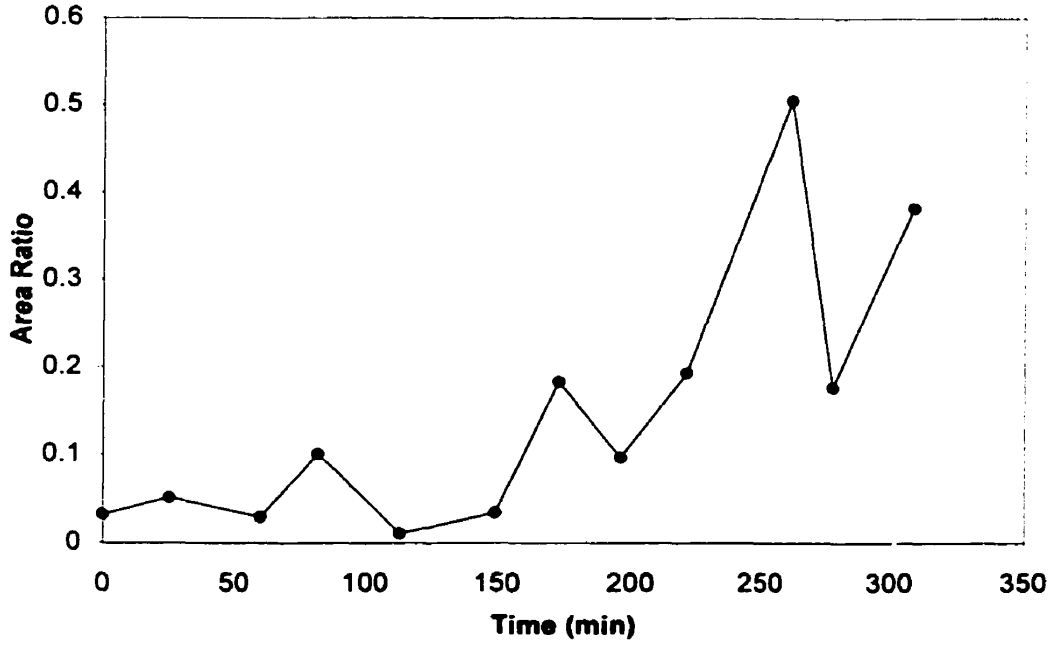

Figure 5-37: Unknown peak concentration over time, run#7, cycle 36, *Rhodococcus* IS01.

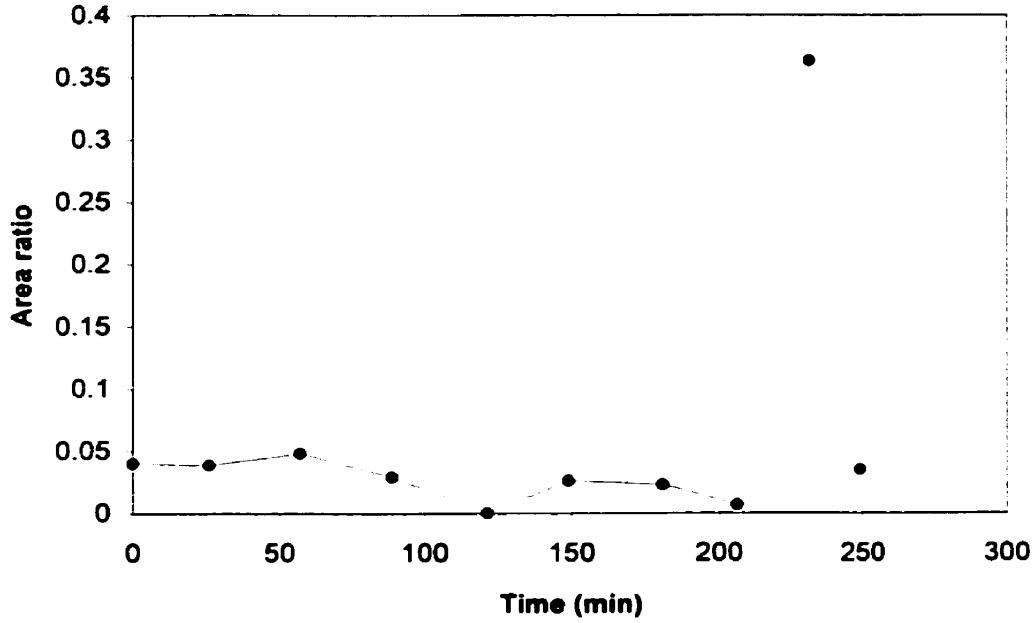

Figure 5-38: Concentration of unknown peak during growth on hexadecane and pentacosane, run #7, cycle 28, *Rhodococcus* IS01.

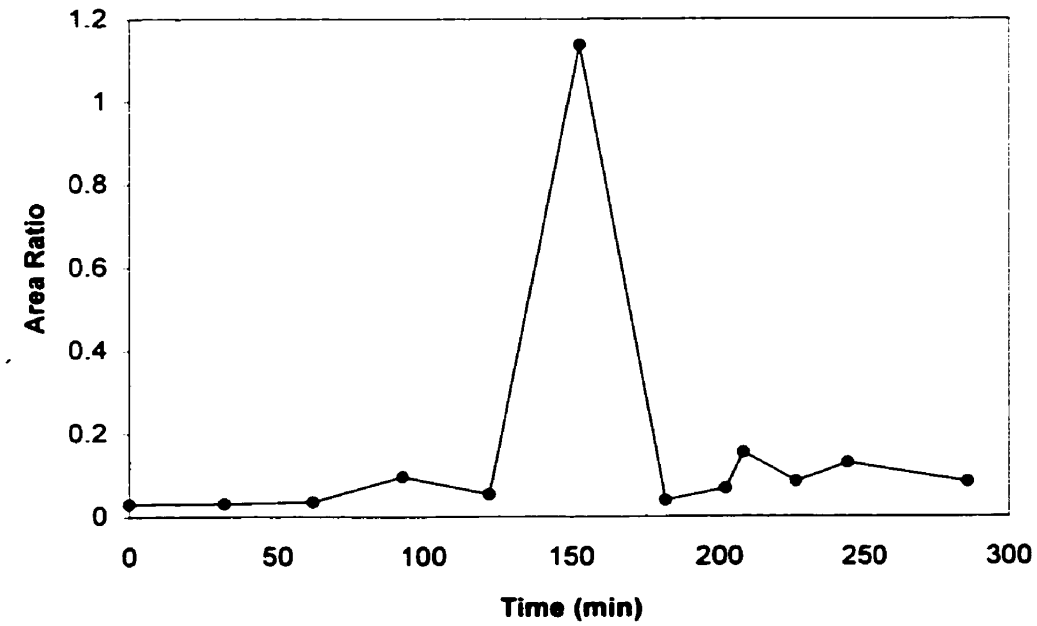

Figure 5-39: Concentration of unknown peak during growth on dodecane, hexadecane, heptadecane, eicosane and pentacosane, run #7, cycle 32, *Rhodococcus* IS01.

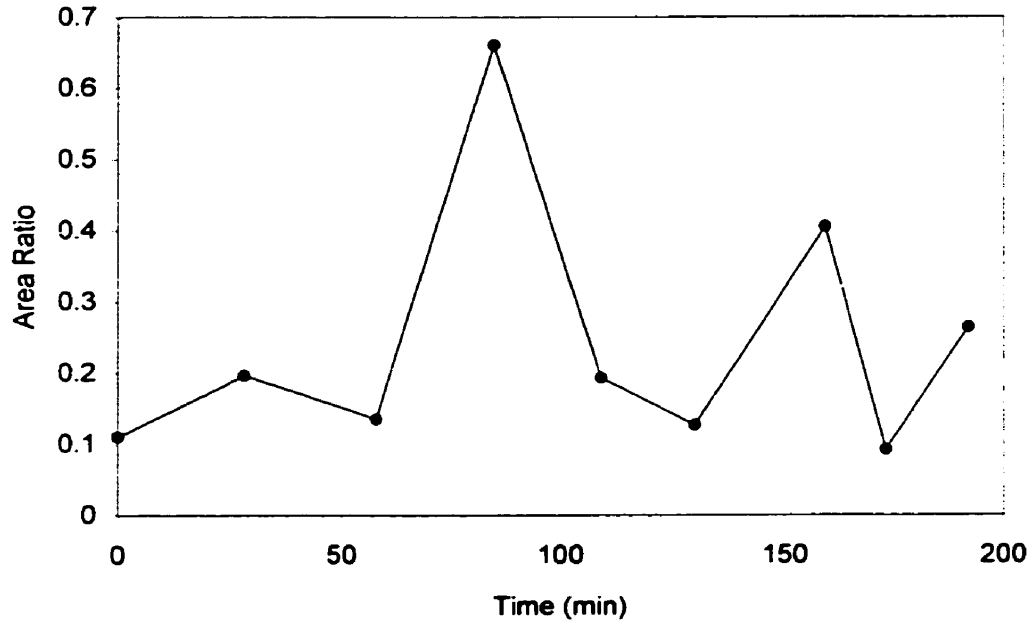

Figure 5-40: Concentration of unknown peak during growth on mixture #1 composed of dodecane, heptadecane, eicosane, pentacosane and pristane, run #7, cycle 57, *Rhodococcus* IS01.

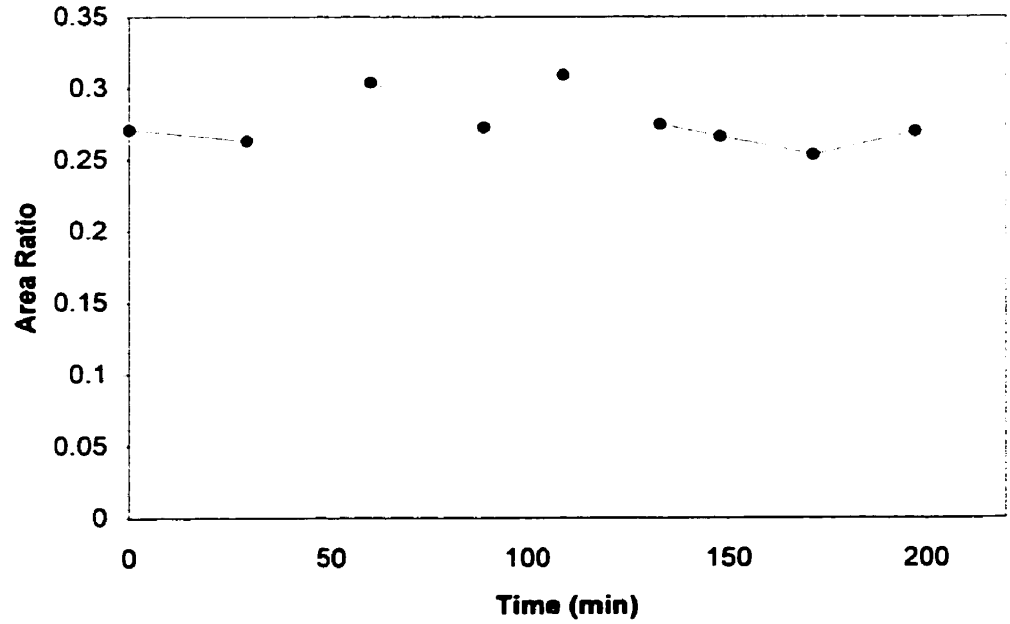

Figure 5-41: Concentration of unknown peak during growth on pentacosane and pristane, run #7, cycle 52, *Rhodococcus* IS01.

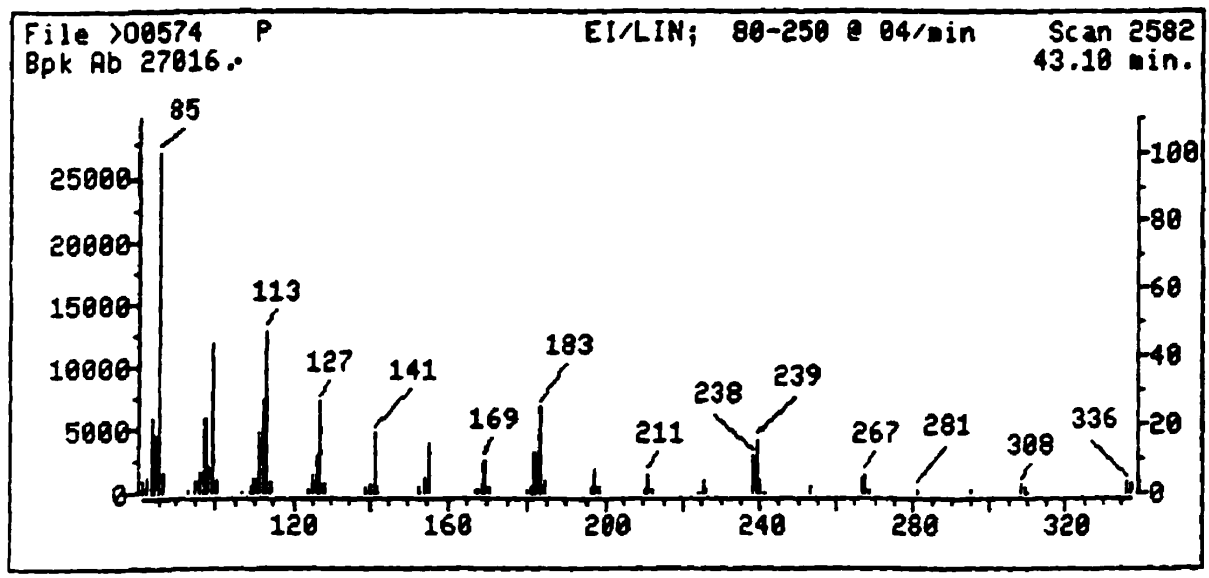

Figure 5-42: Mass spectrograph of unknown compound.

6.0 DISCUSSION

6.1 Bioremediation of paraffin wax

When the bacteria *Rhodococcus* IS01 and *Mycobacterium* OFS were grown on solid wax alone, the pieces of wax became coloured with the pigment that was characteristic of each of the bacteria (orange for *Mycobacterium* OFS and beige for *Rhodococcus* IS01). This suggested that the bacteria were adhering to the solid pieces of wax and growing on it. In all cases, by the end of seven days all of the solid wax was dispersed throughout the medium suggesting that these two bacteria produced some surface-active compound.

In a control experiment, the growth of the bacteria on the solid phase was slow. This limitation was due to the relatively small surface area available to the microbes to attack the substrate[28]. In order to have degradation of the paraffin wax in the Self-Cycling Fermenter in a reasonable period of time, it was necessary to have this substrate in a liquid phase. Hexadecane was used as the liquefying agent because it is relatively inexpensive and relatively little is required, it is widely used as a substrate in the literature and most importantly it is biodegradable.

In the work presented here, paraffin wax dissolved in hexadecane was completely biodegraded by *Rhodococcus* IS01. Kinetic studies of the biodegradation of *n*-alkanes varying from dodecane to heptatriacontane showed that shorter chains were utilized by the bacteria earlier than longer ones. The results also indicated that the initial first-order oxidation constant decreased with increasing chain length possibly due to an enzyme specificity constraint. The growth is suspected to follow some form of diauxie.

During run#7, with *Rhodococcus* IS01, the paraffin wax and the hexadecane were completely degraded. Half a g/L of hexadecane and 0.15 g/L of wax were added to the reactor at the beginning of every cycle. After only 300 minutes, no detectable residual hydrocarbons remained in the SCF. *Rhodococcus* IS01 has the ability to utilize *n*-alkanes ranging from $C_{12}H_{26}$ to $C_{37}H_{76}$. The SCF allowed fast and complete removal of the paraffin wax and the hexadecane. Several biodegradation studies have been performed using crude oil as a substrate, but few studies examined the biodegradation of paraffin

wax. Several biodegradation studies with conventional methods such as batch reactors showed that crude oil could be degraded by mixed or pure cultures. However, the rate of biodegradation was in general much slower than the rates observed in this work[33,5,13,47,56,95]. Partial degradation could be achieved rapidly in some cases, but complete degradation typically took much longer to occur (in the order of days).

In some cases, the oxygen demand for hydrocarbon fermentation has been shown to be up to 3 times greater than that of carbohydrate fermentation[39]. This high oxygen demand was a limiting factor for the amount of paraffin wax and hexadecane that was added in at the beginning of every cycle. Run#3 with *Mycobacterium* OFS and run#4 with *Arthrobacter paraffineus* ATCC 19558 were partially successful (see section 5.2 and 5.3). Fifty-five percent of the hexadecane and 54% of the paraffin wax was degraded during run#3 and 69% of the hexadecane and 53% of the paraffin wax were degraded during run#4. The SCF technique is a self-regulated system, therefore the residual hydrocarbon is due to the nature of the fermentation. It is unclear why the biomass stopped respiring before the limiting substrate (the hydrocarbon) was depleted. Figure 5-9 shows the DO profile for cycles using hexadecane as the liquefying agent in run#7. As soon as the minimum in DO was reached, the cells stopped respiring and the dissolved oxygen increased sharply, at which time, the computer initiated the harvesting phase. The sharp rise in DO indicated that the limiting nutrient was suddenly exhausted and that the biomass stopped growing at once. This pattern of limiting nutrient depletion was unique to *Rhodococcus* ISO1. Interestingly, in this work, *Rhodococcus* ISO1 was the only bacterial species able to completely degrade hexadecane and paraffin wax within one cycle. The cycles during the SCF with *Rhodococcus* ISO1 were self-regulated to deplete all of the hydrocarbons, therefore it was not necessary to extend the cycles beyond their natural length of time to get additional biodegradation. However, the results from run#3 and run#4 showed a different DO pattern than run#7 (see fig. 5.2 and 5.5). During run#3 and run#4, after reaching a minimum, the DO did not increase sharply, but instead gradually increased until the computer initiated the phasing step. For these two runs, the hexadecane and the paraffin wax were not degraded to completion. In Self-Cycling Fermentations with *n*-alkanes, the DO pattern could indicate if the limiting nutrient was

completely utilized or not. A sharp increase in DO indicates the exhaustion of the limiting nutrient while a smooth increase in DO after the minimum is reached indicate incomplete biodegradation of the limiting *n*-alkane substrate.

The reason why the oxygen demand of the bacteria, and hence the growth of the biomass, decreased before the microorganisms fully utilized the carbon source or why there is residual hydrocarbons at all is unclear. It has been reported that some bacteria, when grown on insoluble compounds, form intracytoplasmic inclusions or vacuoles containing hydrocarbons that can be observed by X-ray diffraction or by electron microscopy[12,22]. Perhaps when the inclusions reach a certain size, they become detrimental to the cells and growth is slowed down or halted. This could explain the gradual decrease in oxygen demand. Or perhaps during the SCF, the cells created reserves of carbon source and become saturated with intracellular hydrocarbon and simply start using this reserve of carbon source as opposed to the substrate present outside the cells in the medium. It certainly would be an energetically favorable utilization of the hydrocarbons, the need for transport would be suppressed and utilization could be faster. This could help explaining the residual hydrocarbon. At the beginning of the SCF, *Rhodococcus* IS01 was highly hydrophobic with an adhesion factor of close to 0.32[77]. As the cycle continued, after roughly 150 minutes, the cells showed a lower hydrophobicity with an adhesion factor of 0.64. It was also proposed that residual hydrocarbon could be due to a certain portion of the insoluble substrate binding to the hydrophobic cell wall[41].

6.2 Metabolites

Many microorganisms have been reported to produce solubilizing agents such as biosurfactants and bioemulsifiers when grown on hydrocarbons to facilitate their uptake[94]. Surfactants are believed to increase the bioavailability of insoluble compounds to the microorganisms[1,4,9,20,42]. Of the four bacteria used in this study, three of them (*Arthrobacter paraffineus* ATCC 19558, *Rhodococcus* IS01 and *Mycobacterium* OFS) showed surface tension lowering properties to a certain extent (none of them showed extensive bioemulsifying abilities). All four bacteria degraded and grew well on *n*-

alkanes suggesting that biosurfactants could be helpful but not essential for growth on insoluble substrates. The three bacteria demonstrating surface-active properties where all highly hydrophobic (they stuck to the *n*-alkanes) and two of them (*Rhodococcus* IS01 and *Mycobacterium* OFS) showed evidence of cell-associated biosurfactants. When *Rhodococcus* IS01 and *Mycobacterium* OFS were grown in excess hexadecane and paraffin wax, a significant lowering of the surface tension was observed. Under SCF conditions, no significant surface tension reduction was observed for any of the three bacteria probably because the concentrations of hydrocarbons used were much lower than those used in shake-flasks experiments. Of the three bacteria, only fermentations with *Arthrobacter paraffineus* ATCC 19558 have been reported in the literature to have surface active properties. Duvniak *et al.* reported that *Arthrobacter paraffineus* ATCC 19558 produced a cell-associated biosurfactant capable of lowering the surface tension of the medium down to 31 mN/m[20]. All attempts to reproduce these results were unsuccessful, the lowest surface tension that was reached when following the same procedure were between 53 and 60 mN/m (see fig. 5-6). In the case of *Rhodococcus* IS01, the biosurfactant was suspected to be a glycolipid[73].

While looking for evidence of a biosurfactant, it was observed that the same compound appeared in the fermentations of *Rhodococcus* IS01, *Arthrobacter paraffineus* ATCC 19558 and *Mycobacterium* OFS. The mass spectrometry analysis indicated that the unknown compound was an unsaturated long chain hydrocarbon ($C_{24}H_{48}$).

6.3 Kinetic studies

After the preliminary work, it was decided to do the kinetic studies with *Rhodococcus* IS01. Pristane was the logical choice as the agent to dissolve the long chain hydrocarbons. It was added to all the experiments, even those with the shorter liquid *n*-alkanes to ensure standard conditions. A second set of experiments used hexadecane as the liquefying agent. Even though the hexadecane was readily metabolized, the kinetic parameters obtained were similar. This is an important observation because it shows that the rates of utilization of the various alkanes were not affected in simple mixtures. To be able to compare the kinetics of liquid (dodecane, hexadecane, heptadecane) and solid

(eicosane, pentacosane, triacontane) hydrocarbons with the same growth conditions, all the *n*-alkanes had to be in the liquid state. Since the bacteria could all grow on hexadecane, two highly branched hydrocarbons were tested as liquefying agents. Pristane was used because of its branched nature which renders it recalcitrant to mineralization and because of its reported effects when grown with more favoured alkanes[15]. Hepta-methyl nonane (HMN) was also tested. Initially, *Pseudomonas fluorescens* Texaco did not grow at all on pristane or hepta-methyl nonane (HMN) as the sole source of carbon. After 4 transfers (8 weeks), *Pseudomonas fluorescens* Texaco could grow on pristane but not on HMN, indicating that it had been acclimated to pristane by producing the necessary enzymes needed to utilize pristane. Acclimation is an important aspect of bioremediation[21,83]. In many studies, cell transfers to fresh media with *n*-alkanes are performed periodically to acclimatize the bacteria to the substrate and select for bacteria that grew as well and as fast as possible on the hydrocarbons. In the current work, the same type of acclimation was occurring but it was undesirable. *Arthrobacter paraffineus* ATCC 19558, *Rhodococcus* IS01 and *Mycobacterium* OFS were all growing on pristane and HMN nine days after the first transfer. It only took three days after the initial inoculation for all of them to grow on a mixture of pristane and hexadecane. This suggests that the bacteria were also acclimated to pristane and HMN, but in this case the acclimation was much faster.

There are essentially two constraints on the biodegradation of hydrocarbons by microorganisms: mass transfer and enzyme specificity. In the first case, the insoluble substrate cannot enter the cells. The hydrocarbon being in a separate phase creates additional barriers to the transport of the *n*-alkanes into the cells. The uptake and transport of hydrocarbons by microbes is an important limitation of the growth rates[27]. Miller and Bartha used a liposome encapsulation experiment to demonstrate that there was a transport limitation to explain the difficulty their *Pseudomonas* sp. had growing on hexatriacontane[34]. They showed that the Ks of a culture growing on liposome encapsulated hexatriacontane was up to 60 times lower than the Ks of cells growing on hexatriacontane alone. The half-saturation constant Ks reflects the concentration of available substrate. A large Ks indicates a poor availability while a low Ks indicates a high bioavailability. The obvious extremely small area available for growth and the

extremely low solubility of $C_{36}H_{74}$ in the medium were two of the difficulties the cells experienced while growing on solid $C_{36}H_{74}$. These are characteristic of solid *n*-alkanes. Liposome encapsulated $C_{36}H_{74}$ behaved similarly to a liquid hydrocarbon in the culture. They did not measure the Ks for cells growing on liquefied hexatriacontane. The Ks for such a culture would have certainly been much smaller than the value they reported for growth on solid $C_{36}H_{74}$. Also, they used a protein assay to measure the biomass concentration. To perform this assay, they needed samples from the cell suspensions. If the cells were highly hydrophobic and adhered to the solid substrate, they could not take into account the biomass bound to the cells which could have decreased the Ks. Finally, it is possible that the substrate transport limitation the cells experienced was particular to the *Pseudomonas* sp. they used.

The other limitation to the use of hydrocarbons by microorganisms is the enzyme specificity. The cells are unable to metabolize the hydrocarbons because of the absence of the appropriate transforming enzymes[54]. If the microorganisms cannot produce the necessary enzymes to degrade the substrate, obviously no growth or biodegradation can occur. It has been observed for several cases, that some bacteria could degrade hexadecane but could not utilize eicosane showing that the bacteria produced enzymes only able to metabolize *n*-alkane of a specific length.

6.3.1 First-order oxidation rate constant

It is widely accepted in the literature that several hydrocarbon biodegradation follows first-order kinetics[58,60,61,64]. When a low concentration of substrate is used (S<<Ks) and the cell concentration is initially high or constant throughout the fermentation, the Monod equation can be simplified from equation 1 to equation 2.

$$r_s = \frac{-1}{Y} \cdot \frac{\mu \max \cdot S}{Ks + S} \cdot X \qquad (1)$$

to

$$r_s = k \cdot S \qquad (2)$$

where $k = -\frac{\mu max \cdot X}{Y \cdot Ks}$

The variable k is the first-order oxidation rate constant. The variable X is the biomass concentration, S is the substrate and t is the time. The maximum specific growth rate is μ_{max}, Ks is the half-saturation constant for growth and Y is the yield coefficient. If the biodegradation is a first-order reaction, the rate of biodegradation will be dependent only on the substrate concentration[65]. First-order rates can often be misused when applied to biodegradation. Unless the two assumptions (biomass, X, constant and Ks>>S) are valid, first-order kinetics are not valid. To know if Ks>>S the Monod model has to be fit to experimental degradation data. In general, a concave profile of log concentration *versus* time is evidence that a Monod model applies[71]. This profile can often be mistaken for two different first-order rates (an initial rate and a final rate) as seen in fig#6-1. This misconception is based on the fact that the first assumption (X is constant) is not respected, hence first-order kinetics do not apply. During the early stages of SCF, the biomass was relatively constant during which time we could assume first-order kinetics. As the cells started to grow, the biomass increased and the first-order kinetics assumption was no longer valid. Both of these assumptions were used in the treatment of the data presented here.

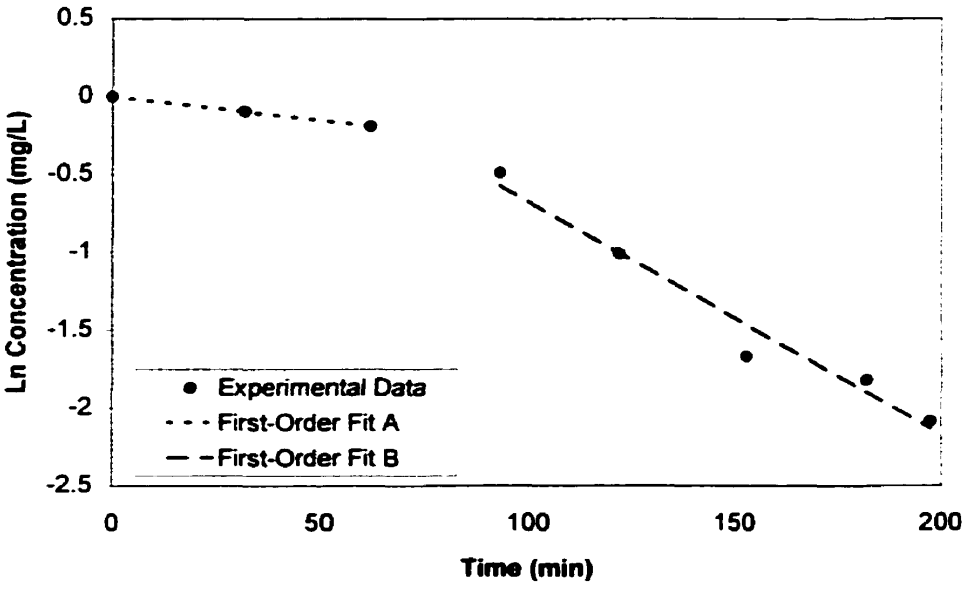

Figure 6-1: Example of a concave-down profile fit with two first-order fits.

Some authors advocated that k should be described as a pseudo-first-order constant as opposed to a first-order constant. They argue that the degradation of the pollutant is not truly first-order because other factors such as diffusion of the substrate in the cells makes the degradation reaction dependent on factors other than S[58,60]. In this work, k is regarded as a first-order constant because it comprises the half-saturation constant and the yield constant which are both assumed to be dependent on the mass transfer and consequently account for the mass transfer of the hydrocarbons into the cells.

Several studies investigated the degradation rates of *n*-alkanes[3,53,55,56,,58,62,66,67,68]. In general, it has been observed that the degradation rate of *n*-alkanes decreases with increasing chain length[53,55,58]. Some others reported the opposite[66]. Dostálek *et al.* showed that the biodegradation rates for *Candida lipolytica* initially decreased with increasing chain length (decane to pentacosane) and after most of the shorter chains were consumed the rates increased with increasing chain lengths[62]. Initial assimilation rates decrease with increasing molecular weight due to differences in the degradation kinetics

such as the selectivity of the cell wall (uptake) and/or the specific reactivity of the *n*-alkanes[54].

For the work presented here, the term "oxidation" is used preferentially to the term "degradation" because the parameter that was monitored during the SCF was the disappearance of the initial form of the substrate (as seen using a gas chromatograph). This happens with the first oxidation of the original alkane. The next steps lead to complete mineralization or "degradation". In fact, most of the reported studies of biodegradation rates also used gas chromatography and did not follow the fate of the contaminant to complete mineralization[3,53,55,56,57,62,63,67,68,93].

The kinetic studies using hexadecane and pristane as a liquefying agent showed the trend that has been generally observed: the first-order oxidation constant k decreased with increasing chain length. The exact same trend is observed for the hexadecane and paraffin wax biodegradation experiment. Hexadecane showed the largest first-order constant and as the number of carbon atoms increased, the value of the first-order oxidation constant k decreased. The value of the rate constants decreased sharply between dodecane and hexadecane and/or heptadecane and between hexadecane and/or heptadecane and eicosane. Above eicosane, the difference between the higher hydrocarbons was not as pronounced. This is in agreement with Dostálek's assimilable groups. He stated that assimilable *n*-alkanes can be classified into three groups. The first group consists of $C_{12}H_{26}$ to $C_{14}H_{30}$. The second group consists of $C_{15}H_{32}$ to $C_{17}H_{36}$ and the third group consists of $C_{18}H_{38}$ and up. The first-order oxidation rate constants obtained from the studies using hexadecane as a solvent seem to indicate that k is not dependent on the initial substrate concentration (see fig.5-31).

Mass transfer into the cell could potentially explain the slower initial rates for longer chains. Assuming that the diffusion across the bacterial membrane for smaller *n*-alkanes is faster than for longer chains, as the shorter chains get degraded, the relative concentration across the cell membrane increases for the longer chains and their rate of entry into the cell, relative to that of the shorter molecules, will also increase. However, the results of this work show that the difference in the initial first-order oxidation rates

between heptadecane and eicosane is significant while the difference between eicosane and triacontane is not. If mass transfer was the main factor affecting the initial rates, the difference between eicosane and triacontane should have been significant. One could argue that it could be a "cut-off effect": only certain chain lengths can get in and the others are excluded. However, once in a while a longer chain could slip through and get degraded. Therefore, the degradation of certain chains would be faster than for shorter ones. If this were the case, a large difference in the first-order oxidation constant between eicosane and triacontane would be expected but this was not the case. Mass transfer probably plays a role but the results presented in this work seem to indicate that it is not a major one.

The degradation patterns obtained from the experiments performed with hexadecane are shown in figures 5-15 to 5-20. In all cases it is apparent that the shorter chain hydrocarbons were initially attacked by the bacteria faster then the longer ones. However, at the end of the fermentation, in almost all cases, all the *n*-alkanes were degraded to the same extent. When all the *n*-alkanes were grown together, it is clearly evident that the cells immediately utilized dodecane, hexadecane and heptadecane followed shortly after and the solid hydrocarbons were last to be attacked. Except for dodecane, all *n*-alkanes showed some kind of lag phase. In the SCF, lag phases should theoretically be eliminated. Since fifty percent of the cells remain in the reactor, the bacteria are already acclimated and should theoretically already have the enzymes necessary to degrade the alkanes. If the enzymatic system required to oxidize the different chains were inducible, the induction should have been rapid as the cells were deprived of the *n*-alkanes only for a short period of time (the SCF phasing time lasted between 7-10 min). The degradation patterns of the experiments performed with pristane are shown in figures 5-22 to 5-27. When mixtures of *n*-alkanes are degraded in the presence of pristane, though not as obvious, a scenario similar to the growth with hexadecane occurred. The shorter chain hydrocarbons were initially oxidized faster that the longer ones. One of the two mixtures of *n*-alkanes grown had half the concentration of dodecane. No significant differences between the two degradation patterns were evident indicating that the concentration of dodecane had no effect on the oxidation rates

of the longer chain hydrocarbons. The initial rates of the solid hydrocarbons (eicosane, pentacosane and triacontane) decreased as the number of carbon increased but were close to each other. This suggests that these three *n*-alkanes may belong to the same assimilable group proposed by Dostálek.

The uptake of alkanes can be separated into two stages. First, the time required for the molecules to penetrate the cell wall. This can last 1 to 2 minutes in both induced and non-induced systems. Second, the time required for active uptake associated with metabolic processes (i.e. transport across the cytoplasmic membrane). In non-induced systems, this step can take a long time (on the order of hours to days depending on the conditions). However, in induced systems this step can be much faster (in the order of minutes)[54]. Suomalainen found that shorter-chain fatty acids cross the membrane faster than longer chains[54]. Therefore, if the rate-limiting step were the oxidation of the fatty acids, this would explain the faster assimilation of shorter chain alkanes. Except for pentacosane, the longest *n*-alkane, all hydrocarbons were completely utilized at intervals very close to each other. Pentacosane was the last one to be used up completely (see fig. 5-20).

6.3.2 Maximum specific growth rate constant

The Monod equation is used extensively to model the growth of microorganisms and their substrate utilization. The maximum specific growth rate μ_{max}, the yield Y and the half-saturation constant Ks are the three kinetic constants that are needed to fit the model to the experimental data. The Monod model describes the utilization of a single rate limiting substrate and the resulting microbial growth by a pure culture of microorganisms in a liquid medium at constant temperature[69]. The Monod model has no mechanistic basis but it is useful as a tool for rough predictions. The values of μ_{max} and Ks should be mostly used as a mean of comparing kinetic constant values between fermentations[72].

In this work, two assumptions were made before fitting the experimental kinetic data to the model. First, except for the studies with pristane and individual *n*-alkanes, all

the experiments used more than one rate limiting substrate. Therefore, it was assumed that the contribution of each substrate to bacterial growth was directly proportional to the initial concentration of the substrates in question (e.g. if the hydrocarbon mixture fed to the cells at the beginning of the SCF contained 40% hexadecane, then hexadecane contributed to 40% of the final biomass). Second, in many cases, it was not possible to obtain intracycle biomass data. Therefore, the kinetic parameters were estimated by non-linear regression using only the substrate depletion curves and the Robinson method[70].

The trend observed when looking at the maximum specific growth rate μ_{max} is the reverse of the trend observed for the first-order oxidation constant k. The maximum specific growth rate μ_{max} increased with increasing chain length (see fig 5-33 and 5-34). This trend would be reasonable if μ_{max} were treated as the maximum potential growth rate that the cells can achieve when not limited by factors like mass transfer or enzyme specificity.

One molecule of hexatriacontane contains more carbons than a molecule of dodecane and therefore has the potential of producing biomass more efficiently than three molecules of dodecane for example. A more efficient growth results in a faster specific growth rate. In some systems, the growth substrate was incorporated intact into higher cell fatty acids by an elongation mechanism. When *Candida lipolytica* was grown on *n*-alkanes between tetradecane to octadecane, there was evidence of elongation and/or intact incorporation[83]. If this were the case, then one longer chain molecule could result in a larger μ_{max} than a shorter chain *n*-alkane.

However, the opposite argument could also be used. If the *n*-alkanes molecules were metabolized using β-oxidation, three molecules of dodecane would be assimilated faster than one long chain of hexatriacontane assuming that the dodecane molecules was completely used through the TCA cycle in the form of acetyl-CoA. However evidence from the literature does not support the latter argument. It is apparent in the literature that the hydrocarbons were direct precursors of the fatty acids[83]. It was shown that acetyl-CoA carboxylase, the first enzyme in fatty acids biosynthesis, was repressed by *n*-alkanes in *Candida* species[83]. Also, experiments with bacteria growing on [^{14}C] labeled acetate and solid *n*-alkanes showed that *de novo* fatty acid synthesis was suppressed while the transport of [^{14}C] acetate was not inhibited[92].

6.4 Metabolism of *n*-alkanes

The reason for the difference in the initial oxidation rates between the different *n*-alkanes followed by the gradual "acceleration" in the biodegradation of the longer chains compared to the shorter chains is unclear. Two mechanisms could explain the results: a form of cometabolism or a form of diauxie.

During cometabolism, the non-specific enzymes of the bacteria can degrade other compounds somewhat structurally related to their growth substrate without deriving any energy for growth from these compounds[82]. The bacteria used in this work were all able to utilize *n*-alkanes ranging from dodecane to heptatriacontane. Since they were able to derive energy from these substrates, cometabolism probably did not play an important role in degrading the paraffins.

Generally, the degradation of aliphatic hydrocarbons has been shown to be inducible[83]. Figure 5-11 shows the degradation of hexadecane and the paraffin wax over time. The rate at which hexadecane was degraded seemed to be constant throughout the cycle. However, the degradation rate of the paraffin wax is constant until the system runs out of hexadecane, at which point, a sudden drop in the concentration of the wax was observed and the rate of biodegradation of the wax increased slightly until the complete utilization of the paraffin had been achieved. The biomass grew steadily until both substrates were consumed, at which point the cells stopped growing and the biomass reached a plateau because it ran out of limiting nutrient (see fig.5-10). It is unclear why there was a sudden drop and change in the rate of biodegradation of the paraffin wax. Pirnik suggested that the difference in initial oxidation rates between different *n*-alkanes followed by the gradual "acceleration" in the biodegradation of the longer chains compared to the shorter chains could be effected by diauxie[63]. It is possible that the hexadecane concentration (perhaps acting as a weak catabolite repressor characteristic of diauxic growth[83]) reached a threshold that triggered an increase in the production of enzymes able to utilize longer chains. Diauxic growth is characterized by the growth in two separate stages due to the preferential use of one carbon source over another; between these stages a temporary lag occurs[81]. Diauxic growth usually implies the induction of an enzymatic system. The apparent lag between the degradation of the

hydrocarbons could suggest that a form of diauxie is probable. Diauxie implies growth on two substrates. For the fermentation on hexadecane and paraffin wax, the system grows on a multiplicity of substrates. Therefore the term "diauxie" is not exact. The growth profile of the biomass did not show the step-like growth that is usually observed during diauxic growth. This could be explained by the smooth and gradual shift of degradation between the *n*-alkanes. Initially, smaller chain *n*-alkanes would be oxidized faster than the longer chains because of some kind of steric hindrance preventing the longer chains from easily accessing the active site of the enzymes preferentially degrading the shorter chains. However, occasionally, a longer chain hydrocarbon would be oxidized in the process. As the shorter chain *n*-alkanes become depleted, the concentration gradient becomes larger and the longer chains have statistically more chance of interacting with the oxidizing enzymes as well as being degraded by the induction of enzymes more specific to longer chains. This could explain the "acceleration" in the biodegradation observed as the shorter chain alkanes are disappearing. This form of diauxie could also explain the different initial first-order oxidation constants.

7.0 CONCLUSION

It was found that four of the nineteen bacteria tested grew well on paraffin wax. The bacteria were *Arthrobacter paraffineus* ATCC 19558, *Mycobacterium* OFS, *Pseudomonas fluorescens* Texaco and *Rhodococcus* IS01.

A mixture of paraffin wax liquefied in hexadecane was rapidly and completely biodegraded by *Rhodococcus* IS01 in the Self-Cycling Fermenter. *Rhodococcus* IS01 was found to be able to degrade *n*-alkanes ranging from dodecane to heptatriacontane as well as branched alkanes such as pristane and hepta-methyl-nonane. *Arthrobacter paraffineus* ATCC 19558 and *Mycobacterium* OFS only partially biodegraded the wax and the hexadecane in the SCF.

Kinetic studies performed with *Rhodococcus* IS01 growing on mixtures of *n*-alkanes showed that the shorter chains were initially degraded before the longer ones. The short lag period present between the degradation of the different chain length suggested that *Rhodococcus* IS01 followed some form of diauxic growth. It was also found from the kinetic studies that the initial first-order oxidation constant decreased with increasing *n*-alkane chain length. This trend is believed to be a consequence of an enzymatic specificity constraint rather than a mass transfer limitation. It was also found that the maximum specific growth rate constant (μ_{max}) increased with increasing *n*-alkane chain length.

Rhodococcus IS01 was found to produce a cell-associated biosurfactant.

8.0 REFERENCES

1. Churchill, P.F. and S.A. Churchill. Surfactant-Enhanced biodegradation of solid alkanes. J. Environ. Sci. Health. (1997), **A32**(1), 293-306.

2. Boethling, R.S. Biodegradation testing of insoluble chemicals. Env. Toxicol. Chem. (1984), **3**, 5-7.

3. Bosecker, K., Teschner, M. and H. Wehner. Biodegradation of crude oils. Dev. Geochem, (1991), **6**, 195-204.

4. Rouse, J.D., Sabatini, D.A., Suflita, J.M. and J.H. Harwell. Influence of surfactants on microbial degradation of organic compounds. Critical reviews in environmental science and technology. (1994), **4**, 325-370.

5. Ballerini, D. and J.P. Vandecasteele. Biodegradation of crude oils in a marine environment-general methodology. Energy and environmental chemistry. (1972), **1**, 185-197.

6. Sorkoh, N.A., Al-Hasan, R.H., Khanafer, M. and S.S. Radwan. Establishment of oil-degrading bacteria associated with cyanobacteria in oil-polluted soil. J. Appl. Bacteriol. (1995), **78**, 194-199.

7. Sorkoh, N.A., Ghannnoum, M.A., Ibrahim, A.S., Stretton, R.J. and S.S Radwan. Crude oil and hydrocarbon-degrading strains of *Rhodococcus rhodochrous* isolated from soil and marine environments in Kuwait. Env. Pol. (1990), **65**, 1-17.

8. Amund O.O. and I.J. Higgins. The degradation of 1-phenylalkanes by an oil-degrading strain of *Acinetobacter lwoffi*. Ant. Leeuw. (1985), **51**, 45-56.

9. Ramsay, B., McCarthy, J., Guerra-Santos, L., Kappelli, Fiechter, A. and A. Margaritis. Biosurfactant production and diauxic growth of *Rhodcoccus aurantiacus* when using n-alkanes as the carbon source. Can. J. Microbiol. (1988), **34**, 1209-1212.

10. Blasig, R., Huth, J., Franke, P., Borneleit, P., Schunck W-H. and H.-G. Müller. Degradation of long-chain *n*-alkanes by the yeast *Candida maltosa*. Appl. Microbiol. Biotechnol. (1989), **31**, 571-576.

11. Al-Mallah, M., Goutx, M., Mille, G. and J-C. Bertrand. Production of emulsifying agents during growth of a marine alteromonas in sea water with eicosane as carbon source, a solid hydrocarbon. Oil. Chem. Poll. (1990), **6**, 289-305.

12. Marin, M., Pedregosa, A., Rios, S., Ortiz, M.L. and F. Laborda. Biodegradation of diesel and heating oil by *Acinetobacter calcoaceticus* MMM5: it's possible applications on bioremediation. Intl. Biodet. Biodeg. (1995), 269-285.

13. Sepic, E., Leskovsek, H. and C. Trier. Aerobic bacterial degradation of selected polyaromatic compounds and *n*-alkanes found in petroleum. J.Chromat. (1995), **697**,515-523.

14. Wilson, N.G. and G. Bradley. Enhanced degradation of petrol (Slovene diesel) in an aqueous system by immobilized *Pseudomonas fluorescens*. J. Appl. Bacteriol. (1996), **80**, 99-104.

15. Miller, T.L. and M.J. Johnson. Utilization of normal alkanes by yeasts. Biotech. Biochem. (1966), **8**, 549-565.

16. Miller,, T.L. and M.J. Johnson. Utilization of gas oil by a yeast culture. Biotech. Biochem. (1966), **8**, 567-580.

17. Amin, P.M., Nigam, J.N., Lonsane, B.K., Baruah, B., Singh, H.D., Baruah, J.N. and M.S. Iyengar. Microbial biomass production on solid hydrocarbons. Folia Microbiol. (1973), **18**, 49-55.

18. Lonsane, B.K., Singh, H.D., Nigam, J.N. and Baruah, J.N. Fermentation studies on solid hydrocarbon utilizing bacterial isolates. Indian J. Exp. Biol. (1979), **17**, 1263-1264.

19. Fukui, S. and A. Tanaka. Production of useful compounds from alkane media in Japan. Adv. Bioch. Eng. (1980), **17**:1, 1-35.

20. Duvniak, Z., Cooper, D.G. and N. Kosaric. Production of surfactant by *Arthrobacter paraffineus* ATCC 19558. Biotech. Bioeng. (1982), **24**, 165-175.

21. Leahy, J.G and R.R. Colwell. Microbial degradation of hydrocarbons in the environment. Microbiol. Rev. (1990), **54**, 305-315.

22. Kennedy, R.S. and W.R. Finnerty. Microbial assimilation of hydrocarbons. Arch. Microbiol. (1975), **102**, 75-83.

23. Makula, R. and W.R Finnerty. Microbial assimilation of hydrocarbons. J. Bacteriol. (1968), **95**, 2102-2107.

24. Yoshida, F. and T. Yamane. Hydrocarbon uptake by microorganisms-A supplementary study. Biotech. Bioeng.(1971), **8**, 691-695.

25. H.W.D. Katinger. Influence of interfacial area and non-utilizable hydrocarbons on growth kinetics of *Candida* sp. in hydrocarbon fermentations. Biotech. Bioeng. Symp. (1973), **4**, 485-505.

26. Sutton, C and J.A. Calder. Solubility of higher-molecular-weight *n*-paraffins in distilled water and seawater. Env. Sci. Tech. (1974), **8**, 654-657.

27. Erikson, L.E. and T. Nakahara. Growth in cultures with two liquid phases: hydrocarbon uptake and transport. Proc. Biochem. (1975), **10**, 9-13.

28. Zilber, I.K., Gutnick, D. and E. Rosenberg. 32P Incorporation and growth of the hydrocarbon-degrading *Pseudomonad* UP-2. Curr. Microbiol. (1979), **2**, 163-167.

29. Rosenberg, M., Gutnick, D. and E. Rosenberg. Adherence of bacteria to hydrocarbons: a simple method for measuring cell-surface hydrophobicity. FEMS Microbiol. Lett. (1980), **9**, 29-33.

30. Neufeld, R.J., Zajic, J.E. and F. Gerson. Cell surface measurements in hydrocarbon and carbohydrate fermentations. Appl. Environ. Microbiol. (1980), **39**(3), 511-517.

31. Zilber, I.K., Rosenberg,E and D. Gutnick. Incorporation of 32P and growth of *Pseudomonad* UP-2 on *n*-tetracosane. Appl. Environ. Microbiol. (1980), **40**(6), 1086-1093.

32. Rosenberg, M. and E. Rosenberg. Bacterial adherence at the hydrocarbon-water interface. Oil. Pet. Poll. (1985), **2**, 155-162.

33. Thomas, J.M., Yordy,, J.R., Amador, J.A. and M. Alexander. Rates of dissolution and biodegradation of water-insoluble organic compounds. Appl. Environ. Microbiol. (1986), **52**(2), 290-296.

34. Miller, R.M. and R. Bartha. Evidence from liposome encapsulation for transport-limited microbial metabolism of solid alkanes. Appl. Environ. Microbiol. (1989), **55**(2), 269-274.

35. Goswami, P. and H.D. Singh. Different modes of hydrocarbon uptake by two *Pseudomonas* species. Biotech. Bioeng. (1990), **37**, 1-11.

36. Blenkinsopp, S.A., Jansen, W., Boivin, J. and J.W. Costerton. Paraffin removal down-hole. 419-425 (rest of reference unknown).

37. Husain, D.R., Goutx, M., Bezac, C., Gilewicz, M. and J.-C. Bertrand. Morphological adaptation of *Pseudomonas nautica* strain 617 to growth on eicosane and modes of eicosane uptake. Lett. Appl. Microbiol.(1997), **24**, 55-58.

38. Velankar, S.K., Barnett, S.M., Houston, C.W. and A.R. Thompson. Microbial growth on hydrocarbons-some experimental results. Biotech. Bioeng. (1975), **17**, 241-251.

39. Gutierrez, J.R. and L.E. Erickson. Hydrocarbon uptake in hydrocarbon fermentations. Biotech. Bioeng. (1977), **19**, 1331-1349.

40. Wang, D.I.C. and A. Ochoa. Measurements on the interfacial area of hydrocarbon in yeast fermentations and relationships to specific growth rates. Biotech. Bioeng. (1972), **14**, 345-360.

41. Hug, H., Blanch, H.W. and A. Fiechter. The functional role of lipids in hydrocarbon assimilation. Biotech. Bioeng. (1974), **16**, 965-985.

42. Rosenberg, E. Microbial biosurfactants. CRC critical reviews in Biotechnology. (1983), **3**, 109-132.

43. Goma, G., Pareilleux, A. and G. Durand. Aspects physicochimiques de l'assimilation des hydrocarbures par *Candida lipolytica*. Agric. Biol. Chem. (1974), **38**, 1273-1280.

44. Rosenberg, M., Bayer, E.A., Delrea, J. and E. Rosenberg. Role of thin fimbriae in adherence and growth of *Acinetobacter calcoaceticus* on hexadecane. Appl. Environ. Microbiol. (1982), **44**, 929-937.

45. Hommel, R. and H.-P. Kleber. A pyridine nucleotide-independent aldehyde dehydrogenase involved in the alkane oxidation of '*Acetobacter rancens*'. FEMS Microbiol. (1984), **22**, 139-42.

46. Fox, M.G.A., Dickinson, F.M. and C. Ratledge. Long-chain alcohol and aldehyde dehydrogenase activities in *Acinetobacter calcoaceticus* HO1-N. J. Gen. Microbiol. (1992), **138**, 1963-1972.

47. Sakai, Y., Maeng, J.H., Tani, Y, and N. Kato. Use of long-chain *n*-alkanes (C13-C44) by an isolate, *Acinetobacter* sp. M-1. Biosc. Biotechnol. Biochem. (1994), **58**(11), 2128-2130.

48. Sakai, Y., Maeng, J.H., Kubota, S., Tani, A., Tani, Y, and N. Kato. A non-conventional dissimilation pathway for long-chain *n*-alkanes in *Acinetobacter* sp. M-1 that starts with a dioxygenase reaction. J. Ferment. Bioeng. (1996), **81**(4), 286-291.

49. Maeng, J.H., Sakai, Y., Takeru I., Sakai, Y., Tani, Y, and N. Kato. Diversity of dioxygenases that catalyze the first step oxidation of long-chain *n*-alkanes in *Acinetobacter* sp. M-1. FEMS Microbiol. lett.

50. Makula, R and W.R. Finnerty. Microbial assimilation of hydrocarbons. 1. Fatty acids derived from normal alkanes. J. Bacteriol. (1968), **95**, 2102-2107.

51. Finnerty, W.R., Kallio, R.E., Klimstra, P.D. and S. Wawzonez. Utilization of 1-alkyl hydroperoxides by *Micrococcus cerificans*. Zeitschrift fur allgemeine Mikrobiologie. (1962), **2**, 263-266.

52. Zobell, C.E. Assimilation of hydrocarbons by microorganisms. Adv. Enzymol. (1950), **10**, 443-486.

53. Barua, P.K., Bhagat, S.D., Pillai, K.R., Singh, H.D., Baruah, J.N. and M.S. Iyengar. Comparative utilization of paraffins by a *Trichosporon* species. Appl. Microbiol. (1970), **20**(5), 657-661.

54. Eisele, A. and A. Fiechter. Liquid ans solid hydrocarbons. Adv. Biochem. Eng. (1971), **1**, 169-194.

55. Egli, M. and H. Wanner. Kinetics of the degradation of solid *n*-alkanes with *Actinomucor elegans* (CBS 104 29). Experientia. (1974), **30**(2), 148-149.

56. Oudot, J. Rates of microbial degradation of petroleum components as determined by computerized capillary gas chromatography and computerized mass spectrometry. Mar. Environ. Res. (1984), **13**(4), 277-302.

57. Li, K.Y., Kane, A.J., Wang, J.J. and W.A. Cawley. Measurement of biodegradation rate constants of a water extract from petroleum-contaminated soil. Wast. Manag. (1993), **13**, 245-251.

58. Sepic, E., Trier,, C. and H. Leskovsek. Biodegradation studies of selected hydrocarbons from diesel oil. Analyst. (1996), **121**, 1451-1456.

59. Geerdink, M.J., van Loosdrecht M.C.M. and K.Ch.A.M. Luyben. Biodegradation of diesel oil. Biodegradation. (1996), **7**, 73-81.

60. Doong, R.-A., Chen, T.-F. and W.-H. Chang. Effects of electron donor and microbial concentration on the enhanced dechlorination of carbon tetrachloride by anaerobic consortia. Appl. Microbiol. Biotechnol. (1996), **46**, 183-186.

61. Song, H.-G., Wang, X. and R. Bartha. Bioremediation potential of terrestrial fuel spills. Appl. Environ. Microbiol. (1990), **56**(3), 652-656.

62. Dostálek, M., Munk, V., Volfova, O. and K. Pecka. Cultivation of the yeast *Candida lipolytica* on hydrocarbons. I. Degradation of *n*-alkanes in batch fermentation of gas oil. Biotech. Bioeng. (1968), **10**(1), 33-43.

63. Pirnik, M.P., Atlas R.M. and R. Bartha. Hydrocarbon metabolism by *Brevibacterium erythrogenes*: normal and branched alkanes. J. Bacteriol. (1974), **119**, 868-878.

64. Aggarwal, P., Fuller, M., Gurgas, M., Manning, J. and M. Dillon. Use of stable oxygen and carbon isotope analyses for monitoring the pathways and rates of intrinsic and enhanced in situ biodegradation. Environ. Sci. Technol. (1997), **31**, 500-596.

65. Laidler, K.J. Chemical kinetics, McGraw-Hill, International Student Edition, London, 2nd Edition, 1965.

66. Kost'al, J., Mackova, M., Pazlarova. J. and K. Demnerova. Alkane assimilation ability of *Pseudomonas* C12B originally isolated for degradation of alkyl sulfate surfactants. Biotech. Lett. (1995), **17**(1), 765-770.

67. Prince, R. Petroleum spill bioremediation in marine environments. Critical Reviews in Microbiology. (1993), **19**(4), 217-242.

68. Setti, L., Pifferi, P., and G. Lanzarini. Surface tension as a limiting factor for anaerobic *n*-alkane biodegradation. J. Chem. Tech. Biotechol. (1995), **64**, 41-48.

69. Monod, J. The growth of bacterial cultures. Annual review of microbiology. (1949), **3**, 371-394.

70. Robinson, J.A. and J.M. Tiedje. Nonlinear estimation of Monod growth kinetic parameters from a single substrate depletion curve. Appl. Env. Microbiol. (1983), **45**(5), 1453-1458.

71. Bekins, B.A., Warren, E. and E.M. Godsy. A comparison of zero-order, first-order, and Monod biotransformation models. Ground Water. (1998), **36**, 261-268.

72. Szigeti, L. and R.D. Tanner. An error estimation of Michaelis-Menten (Monod)-type kinetics. Appl. Microbiol. Biotechnol. (1993), **38**, 610-614.

73. Desai, J.D and I.M. Banat. Microbial production of surfactants and their commercial potential. Microbiology and Molec. Biology Reviews. (1997), **61**, 47-64.

74. SUGAL Genetic Algorithm, written by Dr. A. Hunter, University of Sunderland, England.

75. Kiyohara, H., Nagao, K. and K. Yana. Rapid screen for bacteria degrading water-insoluble, solid hydrocarbon on agar plates. Appl. Environ. Microbiol. (1982), **43**(2), 454-457.

76. Koch, A.L. 1994. Growth measurement. Methods for general and molecular bacteriology, American society for microbiology, Gerhardt (ed.), Washington, D.C. 248-277.

77. Marino, F., Karp, J.M. and D.G. Cooper. Biomass measurements in hydrocarbon fermentations. Biotech. tech. (1998), **12**(5), 385-388.

78. Barriga, J., Characterization of the emulsifying mannoprotein of *Saccharomyces cerevisiae*. Master's Thesis, (1995), McGill University, Montr9al, Canada.

79. May, M. Production of lipase by *Candida bombicola* in a self-cycling fermenter (SCF)., Master's. Thesis, (1997), McGill University, Montr9al, Canada.

80. Brown, W.A., Self-Cycling Fermentation (SCF) of *Acinetobnacter calcoaceticus* RAG-1. Master's. (1991), Thesis, McGill University, Montréal, Canada.

81. Pelczar, M.J, Chan, E.C.S and N.R. Krieg. Microbiology. McGraw-Hill.5th edition. 1986.

82. Baker, K.H. and D.S. Herson. Bioremediation. McGraw-Hill. 1994.

83. Britton, L.N. Microbial degradation of aliphatic hydrocarbons. Microbiology series. Microbial degradation of organic coumpound. (1984), **13**, 89-129.

84. Alexander, M. Biodegradation of chemicals of environmental concern. Science. (1980), **211**(9), 132-138.

85. CNN website. www.cnn.com. Oil spills stories.

86. Brown, W.A. and D.G. Cooper. Self-Cycling Fermentation applied to *Acinetobacter calcoaceticus* RAG-1. Appl. Environ. Microbiol. (1991), **57**, 2901-2906.

87. Yamada, K. and Morio Yogo. Studies on the utilization of hydrocarbons by microorganisms. Agr.Biol. Chem. (1970), **34**, 296-301.

88. Atlas, R.M. Petroleum microbiology. Mcmillian Publishing Co., New York. 1984.

89. Benedek,A. and W.J.Heideger.Effect of additives on mass transfer in turbine aeration. Biotech. Bioeng. (1971), **13**, 663-684.

90. Sheppard, J.D., Feedback control and the continuous phasing of microbial cultures. Ph.D. Thesis,(1989), McGill University, Montr9al, Canada.

91. Brown, W.A, Real-time control strategies for cyclical biological reactors. Ph.D. Thesis, (1998), McGill University, Montr9al, Canada.

92. Hallas, L.E. and J.R. Vestal. The growth of Mycobacterium convolutum on solid *n*-alkane substrates: effect on cellular lipid composition. Can. J. Microbiol. (1978), **24**, 1197-1203.

93. Radwan, S.S., Sorkoh, N.A., Felzmann, H. and A.F. El-Desouky. Uptake and utilization of *n*-octacosane and *n*-nonacosane by Arthrobacter nicotianae KCC B35. J. Appl. Bacteriol. (1996), **80**, 370-374.

94. Zajic, J.E. and C.J. Panchel. Bio-emulsifiers. Crit. Rev. Microbiol. (1976), **5**, 39-66.

95. Jobson, A., Cook, F.D. and D.W.S. Westlake. Microbial utilization of crude oil. Appl. Microbiol.(1972), **23**(6),1082-1089.

9.0 APPENDIX A

Intracycle biomass measurement technique.

Marino, F., Karp, J.M. and D.G. Cooper. Biomass measurements in hydrocarbon fermentations. Biotech. tech. (1998), 12(5), 385-388.

Biotechnology Techniques, Vol 12, No 5, May 1998, pp. 385–388

Biomass measurements in hydrocarbon fermentations

F. Marino, J.M. Karp and D.G. Cooper

Department of Chemical Engineering, 3610 University Street, McGill University, Montréal, Que., Canada, H3A 2B2
Fax: 514-398-6678

A rapid and accurate method to determine biomass concentration of cultures growing on hydrocarbons is presented. The technique is based on turbidity. The method eliminates the common problem of inaccurate biomass measurements due to the presence of hydrocarbons affecting the readings or because of the adherence of the cells to the hydrocarbons phase. The method uses small samples (<5ml), is non-destructive and the results do not depend on the age of the culture under study.

Introduction

When hydrocarbons such as alkanes are being used as a carbon source, the biomass measurements can become unreliable because of several factors. Dry weight, in which culture samples are washed and dried, remains the standard method to obtain biomass (Agar, 1985; Gaudy and Gaudy, 1980). However, when hydrocarbons are present, the values obtained from dry weight measurements may be increased. Turbidity is also widely used as a technique to determine biomass, but samples containing hydrocarbons cannot be used to obtain accurate biomass values because the hydrocarbons droplets can interfere with such measurements (Koch, 1994; McCaffrey, 1992). Therefore any non-microbial compounds such as particulates, as well as hydrocarbons and salts, that could potentially bias the measurements, must be removed prior to analysis (Agar, 1985).

Other, less common methods to measure biomass are available. Total organic carbon (TOC), volatile suspended solids (VSS) and chemical oxygen demand (COD) can all be used as an indicator of biomass. However they could be adversely affected by the presence of the hydrocarbons since they can directly or indirectly measure the carbon content of the hydrocarbons as well as biomass (Gaudy and Gaudy, 1980).

Adherence of bacteria to liquid hydrocarbons may also affect the biomass measurements. When microorganisms of interest are metabolizing hydrocarbons, they often adhere to the hydrocarbons phase (Rosenberg *et al.*, 1980). With dry weight, this bacteria-hydrocarbon adherence would decrease the biomass value. If this phenomenon was occurring during turbidity measurements, the biomass reading could be either increased or decreased.

For a typical biological experiment with a small operating volume, the sample size must be kept to a minmum to prevent any disruptions. In many instances, it is necessary to perform rapid biomass measurements using the least amount of broth possible. Dry weight measurements are slow and require large samples (~25 ml) (Agar, 1985; Pirt, 1975). Turbidometric methods are widely used to estimate biomass. They require small volumes, and are quick and non-destructive (Koch, 1994). TOC requires a large volume (~20 ml) and takes about 1 hour to analyze the samples (Brown *et al.*, 1997). VSS is also an indicator of biomass and require a smaller volume (~11 ml) but requires more than 24 hours for analysis (Brown *et al.*, 1997; Gaudy and Gaudy, 1980). COD requires small samples (~2 ml) but requires between 3 and 5 hours for analysis (Brown *et al.*, 1997; Bullock *et al.*, 1995).

The method presented in this paper correlates turbidity and biomass values by quantifying the adherence and eliminating the contribution of the hydrocarbons.

Materials and methods

Organism and culture conditions

Pseudomonas fluorescens Texaco originally isolated from a contaminated metal working fluid was grown in 500 ml shake flasks (Beech and Gaylarde, 1989). Each flask was inoculated with 5 ml of cells in the exponential growth phase and agitated in 150 ml medium at 250 rpm on a temperature-controlled gyratory shaker at 30°C. *Pseudomonas putida* ATCC 23973 and *Rhodococcus* sp. ATCC 29671 were also grown under the same conditions. The inorganic basal medium from Sorkhoh *et al.* (1990) had the following composition (g l^{-1}): 0.85, $NaNO_3$; 0.56, KH_2PO_4; 0.86, Na_2HPO_4; 0.17, K_2SO_4; 0.37, $MgSO_4 \cdot 7H_2O$; 0.007, $CaCl_2 \cdot 6H_2O$; 0.004, Fe(III)EDTA; 2.5 ml of a trace element solution consisting of (g l^{-1}): 2.32 $ZnSO_4 \cdot 7H_2O$;

1.78, $MnSO_4$-$4H_2O$; 0.56, H_3BO_3; 1.0 $CuSO_4$-$5H_2O$; 0.39, Na_2MoO_4-$2H_2O$; 0.66, KI; 1.0 EDTA; 0.4, $FeSO_4$-$7H_2O$; 0.004, $NiCl_2$-$6H_2O$. The carbon source consisted of 1% (v/v) hexadecane (A&C, USA) and 0.3% (w/v) paraffin wax (Consomex, Canada).

Bacterial adherence to hydrocarbon

A modification of Rosenberg's assay was performed in triplicate with samples of *Pseudomonas putida* ATCC 23973, *Rhodococcus sp.* ATCC 29671 and *Pseudomonas fluorescens* Texaco (Rosenberg *et al.*, 1980). 20 ml samples of broth were centrifuged at 9000 g for 10 min at 4°C. The solidified hydrocarbon layer at the medium/air interface was carefully removed. The pellet was washed twice with 20 ml medium and resuspended in 20 ml medium. The turbidity was determined at 600 nm ($Turbidity_{600}$). 5 ml of the washed cell suspension supplemented with 1% (v/v) hexadecane and 0.3% (w/v) paraffin wax were incubated in a test tube for 10 minutes at 30 °C. The mixture was vortexed for 120 seconds and left to settle for 15 minutes to allow the phases to separate. The turbidity of the bottom phase was determined.

Biomass assay

Each of the following assays were performed in triplicate using *Pseudomonas fluorescens* Texaco.

Turbidity measurement before extraction

A 5 ml sample of broth was centrifuged with 15 ml medium at 9000 g for 12 min. Most of the supernatant, including the hydrocarbon layer, was removed with a pipette. The remaining supernatant was decanted. Occasionally, some hydrocarbons remained on the side of the centrifuge tube after pouring out the supernatant. When this occurred, the inside of the centrifuge tube was thoroughly wiped with a tissue paper (Kimwipe) to remove any visible hydrocarbon. The pellet was resuspended in 20 ml medium and the above washing procedure was repeated. The final pellet was resuspended in 5 ml medium and vortexed for 30 s. The turbidity was measured at 600 nm.

Turbidity measurement after extraction

2.5 ml iso-octane (A&C, USA) was added to a 5 ml sample of broth in a separatory funnel (1% pentadecane (A&C, USA) was used as an internal standard). The solution was vigorously shaken for 1 min and left to stand for 15 min. The aqueous phase from of the separatory funnel was centrifuged at 9000 g for 12 min. The cell pellet was washed (see above), resuspended in 5 ml medium and vortexed for 30 s. The turbidity at 600 nm was obtained.

Dry weight measurement before extraction

A 20 ml sample of broth was centrifuged for 12 min at 9000 g. The cell pellet was washed (see above), resuspended in 3 ml distilled water and vortexed for 30 s. The solution was poured into a tared foil pan for dry weight analysis.

Dry weight measurement after extraction

50 ml iso-octane was added to a 20 ml sample of broth in a separatory funnel. The solution was vigorously shaken for 1 min and left to stand for 15 min. The content of the separatory funnel was centrifuged at 9000 g for 12 min. The cell pellet was washed (see above), resuspended in 3 ml distilled water and vortexed for 30 s. The solution was poured into a tared foil pan for dry weight analysis.

Residual hydrocarbon

The following procedure was performed to measure the residual hydrocarbon after washing. 0.5 ml pentadecane was added to 150 ml of cell broth as an external standard. A 20 ml sample of the solution was centrifuged. The supernatant was poured into a flask for later analysis. A tissue paper was used to remove any visible hydrocarbons on the side of the centrifuge tube. The tissue paper was also added to the flask containing the supernatant. The pellet was resuspended in 20 ml medium and centrifuged. The supernatant was poured into the flask. 100 ml iso-octane (0.33% heptadecane (A&C, USA) was used as an internal standard) was added to the flask, shaken for 1 min and left to stand for 15 min for the phases to separate. The top organic layer was analyzed by gas chromatography using a non-polar capillary column. The remaining pellet was resuspended in 20 ml medium and an extraction was performed using 50 ml of iso-octane. The organic layer was analyzed by gas chromatography.

Results and discussion

The adherence of bacteria to hydrocarbon is a function of the culture age and growth conditions. Bacteria will adhere to a different extent depending on which growth phase they are in (Rosenberg and Rosenberg, 1985). This difference is due to changes in the surface energy of the cells that can occur during growth such as variations in the cell surface hydrophobicity or the production of cell-surface components such as biosurfactants (Rosenberg and Rosenberg, 1985). Adherence is measured by the ratio of the $turbidity_{600}$ after incubating the cells with the alkanes ($Turbidity_{after}$) to the turbidity before the incubation ($Turbidity_{before}$). A ratio value of 0 indicates complete adherence while a ratio of 1 indicated no adherence. The ratio for *P. fluorescens* Texaco at three different growth stages did not show a large difference in adherence (Table 1) suggesting a stable surface energy during its growth. This stability

Table 1 Bacterial Adherence to Hydrocarbons

Bacterium	$Turbidity_{after}/Turbidity_{before}$		
	Mid growth phase	*Late growth phase*	*Stationary phase*
P. fluorescens Texaco	0.63	0.63	0.56
Rhodococcus sp. ATCC 29671	ND	ND	0.32
P. putida ATCC 23973	ND	ND	1.08

ND, not determined.

allows for the development of an accurate and consistent assay to measure biomass. Direct observation of *P. putida* ATCC 23973 showed very low adherence to the hydrocarbons while *Rhodococcus* sp. ATCC 29671 showed high adherence hence they can be used to provide comparisons. They demonstrate the range of values possible for this test. The adherence values for these two bacteria corroborates those visual observations (Table 1). The ratios obtained give the adherence factor (AF).

The residual hydrocarbon in the broth was determined by solvent extraction. Hexane and pentane are commonly used as solvents to perform hydrocarbon extractions. However, liquid alkanes with less than 8 C atoms are toxic to many microorganisms because they can dissolve the lipids of the cellular membranes (Einsele and Fiechter, 1971). This damage decreases the weight of the biomass. To keep the damage to the cells to a minimum, iso-octane was used as the solvent because it has good extracting properties, limited toxicity and is relatively inexpensive. It was therefore necessary to obtain the biomass after the extraction procedure to determine the percentage of cells lost during the procedure. Figure 1 shows that there exists a linear relationship between the dry weight before and after extraction with Iso-octane. The slope is 0.615 and will be used later as the extraction factor (EF) for the biomass.

Figure 2 shows the dry weight plotted against the $Turbidity_{600}$. Each datum corresponds to a different culture age and different residual hexadecane and wax concentration. Through regression analysis, dry weight and $Turbidity_{before}$ were found to be related by a factor 1.14g dry weight/AU (absorbancy units)($R^2 = 0.980$) while dry weight and $Turbidity_{after}$ gave a factor 0.865g dry weight/AU ($R^2 = 0.968$). The lipid loss caused by the extraction is linear suggesting that it does not depend on the age of the culture and/or on the concentration of hydrocarbons remaining in the broth. If the age of the culture or the residual hydrocarbon in the broth affected the dry weight or the $Turbidity_{600}$, the data points would show a random distribution. The biomass present in the samples that were extracted showed a 25.1 ± 3.5% reduction (95% confidence interval) in $Turbidity_{600}$ due to a loss of cells after the solvent extraction. This number falls well within the 95% confidence interval for the curve shown on Figure 1.

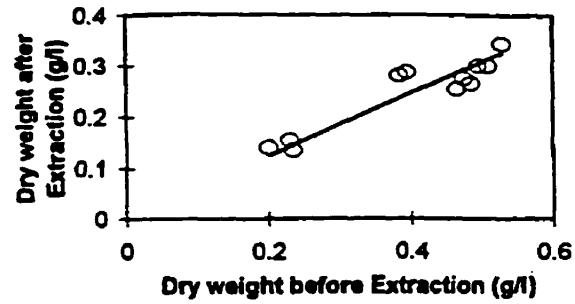

Figure 1 Dry weight before extraction with iso-octane *vs.* dry weight after extraction for *P. fluorescens* Texaco growing on hexadecane and paraffin wax. The solid line represents the best fit curve ($R^2 = 0.87$, Slope = 0.615). The slope corresponds to the extraction factor (EF).

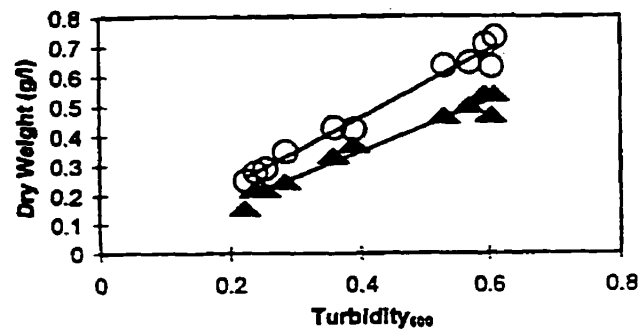

Figure 2 Turbidity vs. dry weight before extraction (○) and *vs.* dry weight after extraction with iso-octane (▲) for *P. fluorescens* Texaco growing on hexadecane and paraffin wax. The data were obtained from broth samples of different ages and different residual hydrocarbon concentrations.

It was important to determine the amount of hydrocarbon remaining in the pellet and hence contributing to the biomass measurement after the washing procedure. The system under study being heterogeneous, the ratio of hydrocarbons to bacteria in the sample may not have been representative of the contents in the shake-flasks from which the samples were obtained. 301 ± 156 μg pentadecane (95% confidence interval) and 695 ± 135 μg hexadecane (95% confidence interval) was detected in the pellet after the washing procedure constituting 1.4% and 3.2% of the biomass respectively. No wax was detected in the pellet. These results indicate that the washing effi-

ciently removed most of the alkanes from the samples. The rest of the hydrocarbons ended up in the washings. They contained 1.1 ± 0.03 ml pentadecane/ml, 2.15 ± 0.28 ml hexadecane/l (95% confidence interval) and 0.46 ± 0.03 g wax/l (95% confidence interval).

The results suggest that the procedure proposed above is adequate to obtain accurate quick biomass measurements using small broth samples from bacteria growing on hydrocarbons. Once the adherence factor, the extraction factor and the relationship between the turbidity and the dry weight are known for a given organism and given hydrocarbons, it is a simple matter to determine the biomass concentration. To correct for the biomass lost because of the adherence, the dry weight value (DW) obtained from $Turbidity_{600}$ is divided by the adherence factor (see equation 1) (If the adherence were different at each growth stage, the appropriate adherence factor would need to be a function of the age and the growth phase of the culture).

$$Biomass = \frac{DW}{AF} \quad (1)$$

To correct for the biomass lost during the extraction procedure, the dry weight value (DW) obtained from $Turbidity_{600}$ is divided by the extraction factor (EF). The loss caused by the adherence is compensated for by further dividing the corrected biomass value by the adherence factor (AF) as seen in equation 2. The final value corresponds to the true biomass.

$$Biomass = \frac{DW}{AF \cdot EF} \quad (2)$$

Conclusion

A rapid and accurate method for measuring small samples (<5ml) growing on hydrocarbons was established. The same sample can be used to obtain the residual hydrocarbon content by extraction as well as an accurate measurement for the biomass. The method eliminates the common problem of inaccurate biomass measurements due to the presence of hydrocarbons. It also takes into consideration any adherence effect that could decrease the biomass measurement. It is possible that the method could be used with other water insoluble substrates if the appropriate adherence factor were determined.

References

Agar, D.W. (1985). Microbial Growth Rate Measurement Techniques. In: *Comprehensive Biotechnology*, C.W. Robinson and J.A Howell, eds. vol.4. pp.305–327, Oxford: Pergamon Press.

Beech, I.B. and Gaylarde, C. (1989). *J. Appl. Bacteriol.* 67, 201–207.

Bullock, C.M., Bicho, P.A., Zhang, Y. and Saddler, J.N. (1995). Wat.Res. 30, 1280–1284.

Brown, W.A., Pinchuk, R. and Cooper, D.G. (1997). *Biotechnol.Tech.* 11, 213–216.

Einsele, A. and Fiechter, A. (1971). *Adv. Biochem. Engin.* 1, 169–194.

Gaudy, A.F., Jr., and Gaudy, E.T. (1980). *Microbiology for Environmental Scientists and Engineers*, pp. 35, 225–230, New York: McGraw-Hill Book Company.

Koch, A.L. (1994) Growth measurement. In: *Methods for General and Molecular Bacteriology*. P. Gerhardt, ed., pp. 261–267. Washington DC: American Society for Microbiology.

McCaffrey, W.C. (1992). *Secondary metabolite production using self-cycling fermentation. Master's thesis.* Department of Chemical Engineering, McGill University, Montreal, Que., Canada, p.30.

Pirt, J.S. (1975). *Principles of Microbe and Cell Cultivation*, pp.15–21, Oxford: Blackwell Scientific Publications.

Rosenberg, M., Gutnick, D. and Rosenberg E. (1980), *FEMS Microbiol. Lett.* 9, 29–33.

Rosenberg, M. and Rosenberg, E. (1985). *Oil & Petrochem. Pol.* 2, 155–162.

Sorkhoh, N.A., Ghannoum, M.A., Ibrahim, A.S., Stretton, R.J. and Radwan, S.S. (1990). *Environ. Pol.* 65, 1–17.

Received: 2 March 1998
Revisions requested: 4 March 1998
Revisions received: 26 March 1998
Accepted 26 March 1998

10.0 APPENDIX B

Modeling of run#7 with a Genetic Algorithm.

The modeling of the bacterial growth and the substrate consumption was attempted for the SCF of *Rhodococcus* IS01 growing on hexadecane and paraffin wax (run#7, cycle 36).

Three assumptions were made to obtain a working model of this system: first, since the yield of each *n*-alkanes was theoretically very close, the overall yield was calculated and was assumed to be identical for each *n*-alkane. For cycle 36, the yield, Y, was 1.1 g Biomass/g Substrate. Second, each substrate was assumed to have a unique maximum specific growth rate (μ_{max}) and a unique half-saturation constant (Ks) (equations 1,2,3 and 4). Third, the overall mu was equal to the sum of all the individual mu (equation 5). Be advised that this model has no mechanistic basis and is only an attempt to model this system.

The system was described by the following equations derived from the Monod equation:

$$mu_1 = \left(\frac{\mu_{max1} \cdot S_1}{Ks_1 + S_1} \right) \qquad (1)$$

$$\vdots$$

$$mu_n = \left(\frac{\mu_{maxn} \cdot S_n}{Ks_n + S_n} \right) \qquad (2)$$

$$\frac{dS_1}{dt} = \frac{-1}{Y} \cdot mu_1 \cdot X \qquad (3)$$

$$\vdots$$

$$\frac{dS_n}{dt} = \frac{-1}{Y} \cdot mu_n \cdot X \qquad (4)$$

$$\frac{dX}{dt} = \sum_{i=1}^{n} mu_i \cdot X \qquad (5)$$

During the growth of *Rhodococcus* IS01 on hexadecane and paraffin wax, the bacteria were growing on nineteen different substrates ($C_{16}H_{34}$ and $C_{20}H_{42}$ to $C_{37}H_{76}$). Therefore the substrates contributed nineteen equations and the biomass contributed 1 equation.

The model consisted of twenty differential equations describing the transient behavior of the biomass and of the nineteen *n*-alkanes. Since each substrate equations required two parameters each (μ_{max} and Ks), thirty-eight parameters had to be fit to the experimental data shown on figures 5-10 to 5-14.

The model parameters were estimated from the experimental data using a Genetic Algorithm (GA). The estimation was performed using the SUGAL Genetic Algorithm package written by Dr. A. Hunter of the University of Sunderland, England. The modeling of a bacterial system growing on multiple substrates is very ambitious and probably constitutes a graduate degree in itself. It is obvious that the fit obtained is far from ideal and much work needs to be done to achieve a better fit. Table A-1 shows the values obtained for μ_{max} and Ks with the GA for each *n*-alkane. The figures 10-1 to 10-4 were obtained by using The student edition of Matlab version 5.

Table 10-1: Values of parameters obtained with GA.

Compound	μ_{max}	Ks
Hexadecane	1.892353	155.117647
Eicosane	0.316294	30.411765
Heneicosane	0.401	43.745098
Docosane	0.198647	21.784314
Triacosane	0.316294	42.176471
Tetracosane	0.349235	50.803922
Pentacosane	0.316294	47.666667
Hexacosane	0.176686	30.411765
Heptacosane	0.073157	13.54902
Octacosane	0.273941	49.627451
Nonacosane	0.192373	35.901961
Triacontane	0.342961	81
Hentriacontane	0.204922	37.862745
Dotriacontane	0.176686	47.27451
Tritriacontane	0.364922	87.27451
Tetratriacontane	0.164137	56.686275
Pentatriacontane	0.143745	30.411765
Hexatriacontane	0.233157	27.666667
Heptatriacontane	0.270804	13.54902

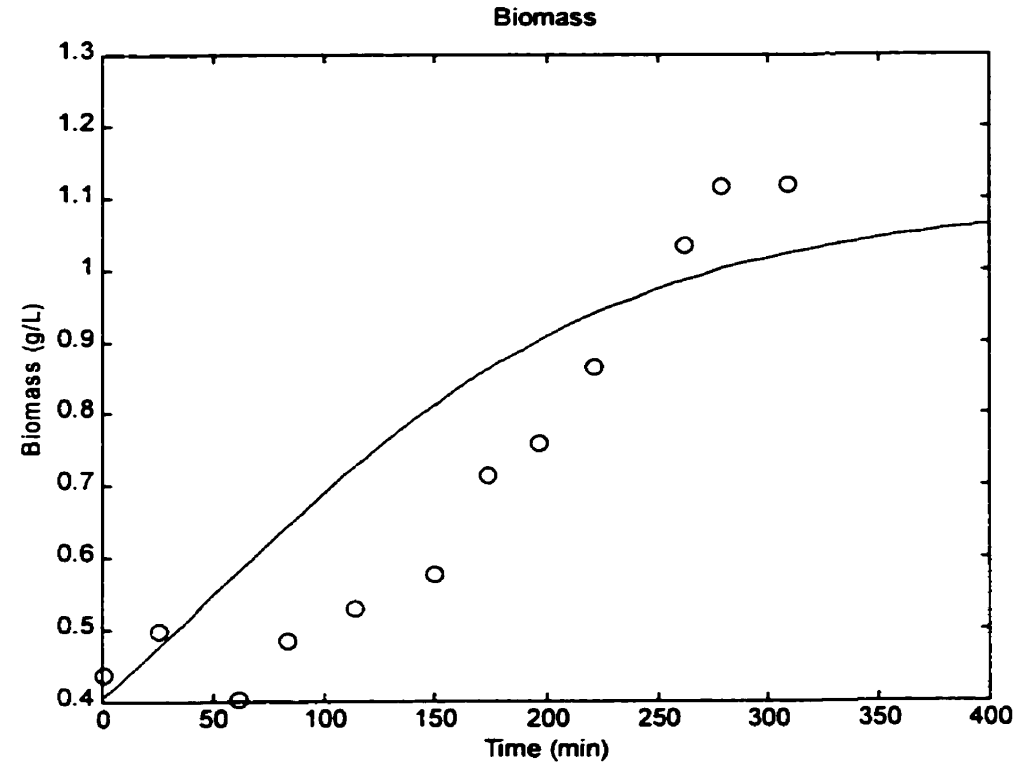

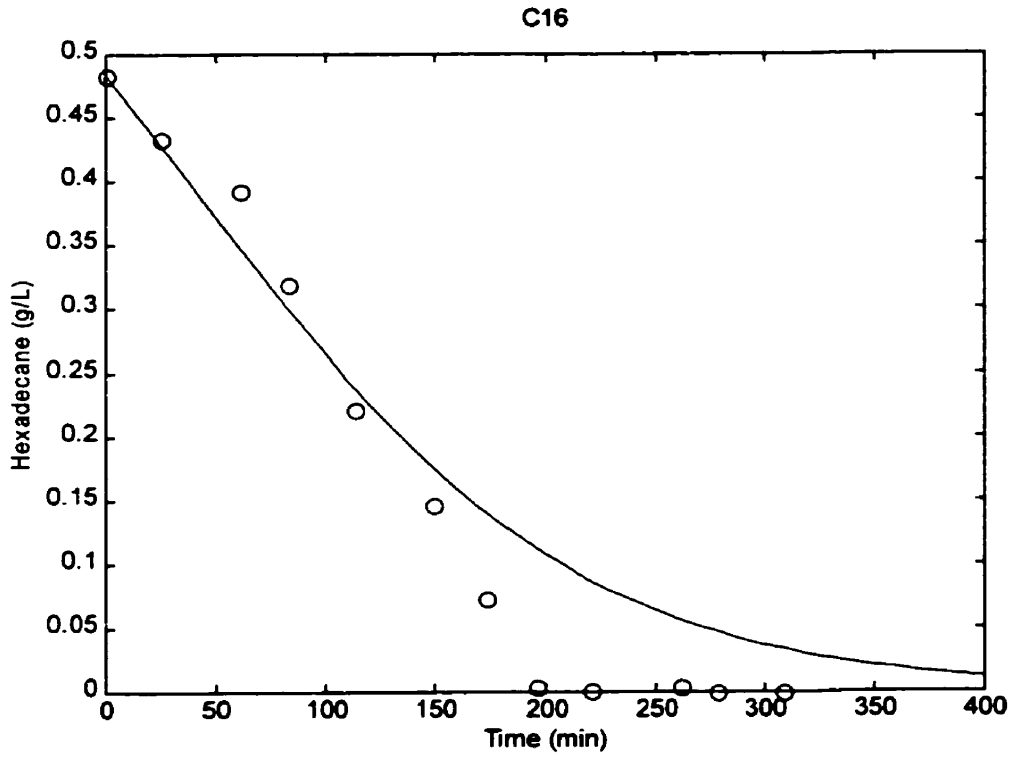

Figure 10-1: Biomass and hexadecane concentrations *versus* time. Experimental data (o), model prediction (—).

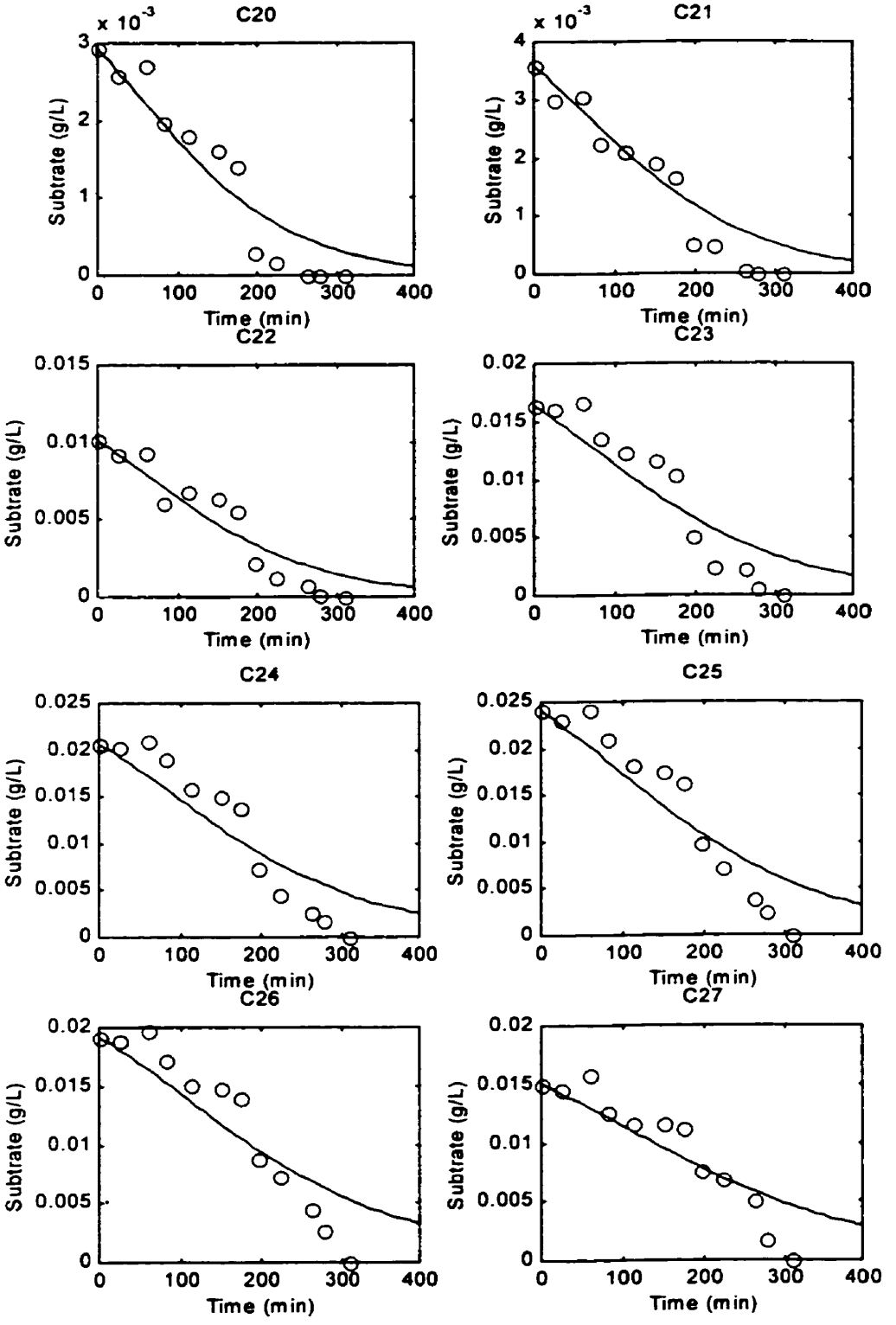

Figure 10-2: Eicosane to heptacosane concentrations *versus* time.
Experimental data (o), model prediction (—).

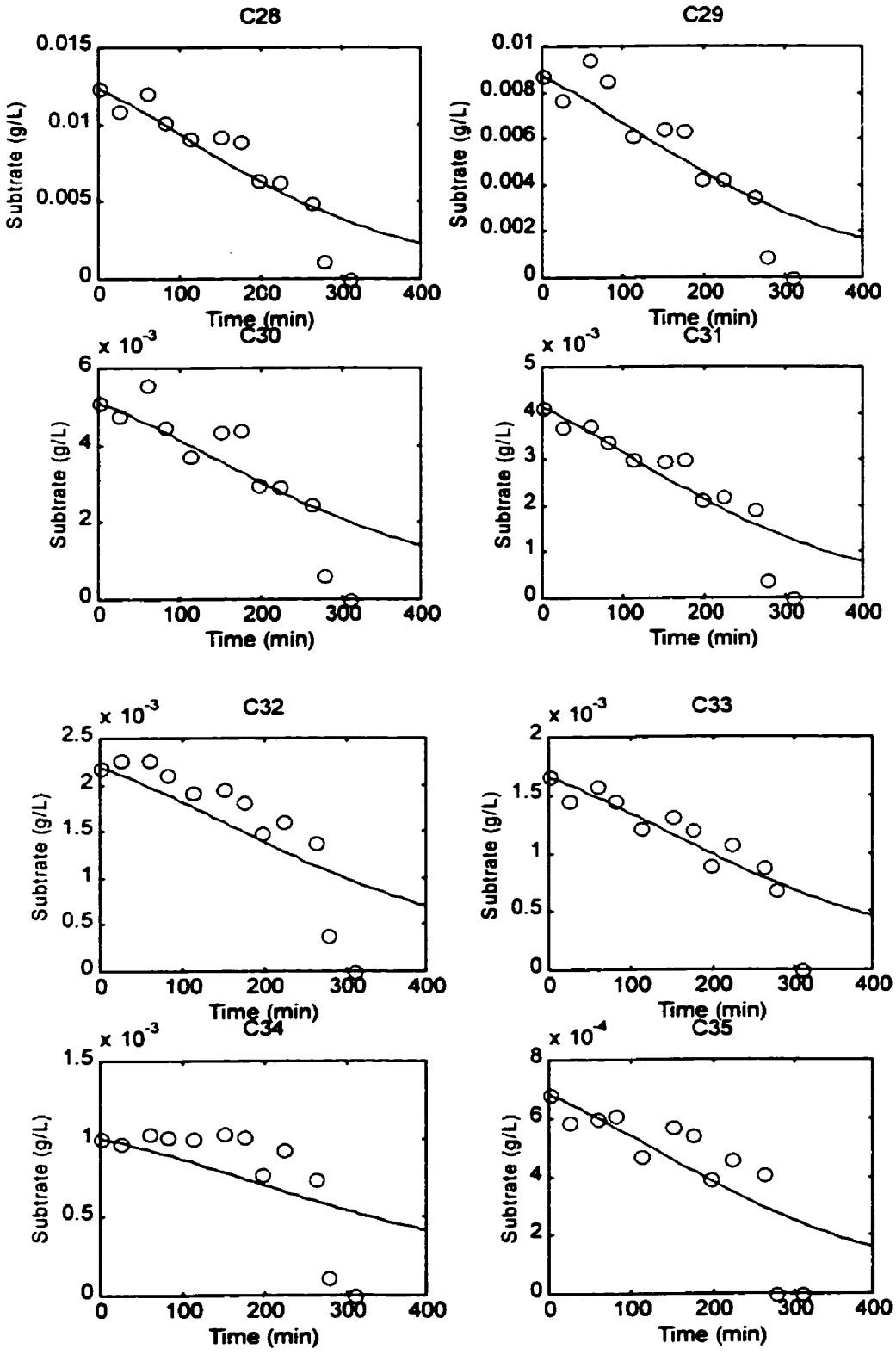

Figure 10-3: Octacosane to pentatriacontane concentrations *versus* time. Experimental data (o), model prediction (—).

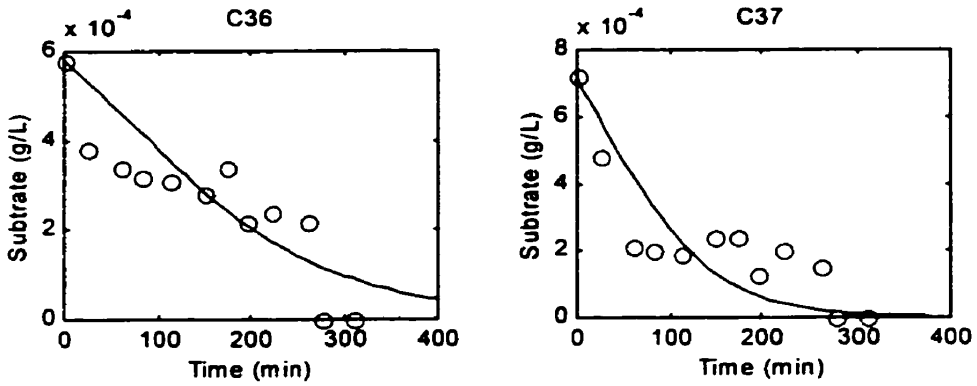

Figure 10-4: Hexatriacontane and heptatriacontane concentrations *versus* time. Experimental data (o), model prediction (—).

This is the GA program file used to solve the equations. Part of this program was written by Robert Pinchuk.

```
/*****************************************
        File: massrun7.c  yield=1.1
*****************************************/

#include <stdio.h>
#include "c:\sugal\sugal.h"
#include <stdlib.h>
#include <math.h>
#include <direct.h>

#define MAX_SETS 2 //max number of data sets
#define MAX_DATA 20 // max number of points per set
#define NO_PARAMS 38 //no of model parameters
#define NO_VAR 20 //no of equations

int Cset,Dset,last[MAX_SETS];
float
*t[MAX_SETS],*b[MAX_SETS],*C16[MAX_SETS],*C20[MAX_SETS],*C21[MAX_SETS],*C22[MA
X_SETS],*C23[MAX_SETS],*C24[MAX_SETS],*C25[MAX_SETS],*C26[MAX_SETS]*C27[MAX_S
ETS],*C28[MAX_SETS],*C29[MAX_SETS],*C30[MAX_SETS],*C31[MAX_SETS],*C32[MAX_SETS
],*C33[MAX_SETS],*C34[MAX_SETS],*C35[MAX_SETS],*C36[MAX_SETS],*C37[MAX_SETS],*b
_weight[MAX_SETS],*C16_weight[MAX_SETS],*C20_weight[MAX_SETS],*C21_weight[MAX_SETS
],*C22_weight[MAX_SETS],*C23_weight[MAX_SETS],*C24_weight[MAX_SETS],*C25_weight[MAX
_SETS],*C26_weight[MAX_SETS],*C27_weight[MAX_SETS],*C28_weight[MAX_SETS],*C29_weigh
t[MAX_SETS],*C30_weight[MAX_SETS],*C31_weight[MAX_SETS],*C32_weight[MAX_SETS],*C33
_weight[MAX_SETS],*C34_weight[MAX_SETS],*C35_weight[MAX_SETS],*C36_weight[MAX_SETS
],*C37_weight[MAX_SETS];float  Max_b[MAX_SETS],Max_C16[MAX_SETS],
max_C20[MAX_SETS],
max_C21[MAX_SETS],Max_C22[MAX_SETS],Max_C23[MAX_SETS],Max_C24[MAX_SETS],Max_
C25[MAX_SETS],Max_C26[MAX_SETS],Max_C27[MAX_SETS],Max_C28[MAX_SETS],Max_C29[
MAX_SETS],Max_C30[MAX_SETS],Max_C31[MAX_SETS],Max_C32[MAX_SETS],Max_C33[MAX_
SETS],Max_C34[MAX_SETS],Max_C35[MAX_SETS],Max_C36[MAX_SETS],Max_C37[MAX_SETS]
;

const float dt_max = 1;
double parameters[NO_PARAMS];
long double X[NO_VAR],res;

//parameters
long double
umax16,umax20,umax21,umax22,umax23,umax24,umax25,umax26,umax27,umax28,umax29,umax30,um
ax31,umax32,umax33,umax34,umax35,umax36,umax37,Ks16,Ks20,Ks21,Ks22,Ks23,Ks24,Ks25,Ks26,Ks
27,Ks28,Ks29,Ks30,Ks31,Ks32,Ks33,Ks34,Ks35,Ks36,Ks37;

/* Function prototypes */
int bitwise_crossover(int length);
int SuGetCrossoverPoint(int length);
int evaluate(SuChromosome *chrom, double *fitness);
void FitEval(void);
double rungekutta(float,float,long double*);
long double model(long double*,int);
void export(double*,int);
```

```
SuActionPair my_crossover_actions[] =
{
 "bitwise", bitwise_crossover,
 "normal", SuGetCrossoverPoint,
 NULL, NULL
};
SuAction my_crossover_action =
{
 1, &SuaGetCrossoverPoint, my_crossover_actions
};
SuParameter my_parameters[] =
{
 "crossover_granularity", &my_crossover_action, NULL, SU_ACTION,

 /* NULL-terminate the list; otherwise, program crash
        guaranteed! */
 NULL, NULL, NULL, NULL
};

/* bitwise crossover routine */
int bitwise_crossover(int length)
{
 return ( SuRandIntUpTo(length) );
}

/*******************************************************
        The Main Function
*******************************************************/

main(int argc, char *argv[])

{
float *minute,*Bio,*S16,*S20,*S21,*S22,*S23,*S24,*S25,*S26,*S27,
                    *S28,*S29,*S30,*S31,*S32,*S33,*S34,*S35,*S36,*S37,
                    *w_S16,*w_S20,*w_S21,*w_S22,*w_S23,*w_S24,*w_S25,*w_S26,
                    *w_S27,*w_S28,*w_S29,*w_S30,*w_S31,*w_S32,*w_S33,*w_S34,
                    *w_S35,*w_S36,*w_S37,*w_Bio;
int i, First_Pass, End_of_File,ind;
FILE *datain;

_chdir("c:\\sugal");  //active directory
minute=calloc(MAX_DATA,sizeof(float));
S16=calloc(MAX_DATA,sizeof(float));
S20=calloc(MAX_DATA,sizeof(float));
S21=calloc(MAX_DATA,sizeof(float));
S22=calloc(MAX_DATA,sizeof(float));
S23=calloc(MAX_DATA,sizeof(float));
S24=calloc(MAX_DATA,sizeof(float));
S25=calloc(MAX_DATA,sizeof(float));
S26=calloc(MAX_DATA,sizeof(float));
S27=calloc(MAX_DATA,sizeof(float));
S28=calloc(MAX_DATA,sizeof(float));
S29=calloc(MAX_DATA,sizeof(float));
S30=calloc(MAX_DATA,sizeof(float));
```

```
S31=calloc(MAX_DATA,sizeof(float));
S32=calloc(MAX_DATA,sizeof(float));
S33=calloc(MAX_DATA,sizeof(float));
S34=calloc(MAX_DATA,sizeof(float));
S35=calloc(MAX_DATA,sizeof(float));
S36=calloc(MAX_DATA,sizeof(float));
S37=calloc(MAX_DATA,sizeof(float));
Bio=calloc(MAX_DATA,sizeof(float));
w_S16=calloc(MAX_DATA,sizeof(float));
w_S20=calloc(MAX_DATA,sizeof(float));
w_S21=calloc(MAX_DATA,sizeof(float));
w_S22=calloc(MAX_DATA,sizeof(float));
w_S23=calloc(MAX_DATA,sizeof(float));
w_S24=calloc(MAX_DATA,sizeof(float));
w_S25=calloc(MAX_DATA,sizeof(float));
w_S26=calloc(MAX_DATA,sizeof(float));
w_S27=calloc(MAX_DATA,sizeof(float));
w_S28=calloc(MAX_DATA,sizeof(float));
w_S29=calloc(MAX_DATA,sizeof(float));
w_S30=calloc(MAX_DATA,sizeof(float));
w_S31=calloc(MAX_DATA,sizeof(float));
w_S32=calloc(MAX_DATA,sizeof(float));
w_S33=calloc(MAX_DATA,sizeof(float));
w_S34=calloc(MAX_DATA,sizeof(float));
w_S35=calloc(MAX_DATA,sizeof(float));
w_S36=calloc(MAX_DATA,sizeof(float));
w_S37=calloc(MAX_DATA,sizeof(float));
w_Bio=calloc(MAX_DATA,sizeof(float));

 /*********************************************************
        Reads Experimental Measurements from a Data File
*********************************************************/
        i = 0;
        End_of_File=0;
        First_Pass = 1;
        Dset = 0;
        Max_C16[Dset] = 0;
        Max_C20[Dset] = 0;
        Max_C21[Dset] = 0;
        Max_C22[Dset] = 0;
        Max_C23[Dset] = 0;
        Max_C24[Dset] = 0;
        Max_C25[Dset] = 0;
        Max_C26[Dset] = 0;
        Max_C27[Dset] = 0;
        Max_C28[Dset] = 0;
        Max_C29[Dset] = 0;
        Max_C30[Dset] = 0;
        Max_C31[Dset] = 0;
        Max_C32[Dset] = 0;
        Max_C33[Dset] = 0;
        Max_C34[Dset] = 0;
        Max_C35[Dset] = 0;
        Max_C36[Dset] = 0;
        Max_C37[Dset] = 0;
        Max_b[Dset] = 0;
```

```
//*******************************This is the data file

datain = fopen("massrun7.dat","r"); //name of data file

fscanf(datain,"%f",minute+i);

while ((!End_of_File) && (Dset<MAX_SETS)) //Check for end of data file
{
                    if (*(minute+i)==-1) End_of_File=1;

                    if ( ((!First_Pass) && (*(minute+i)<*(minute+i-1))) || (i==MAX_DATA))
//Check for new data set
                    {
                                        b[Dset]=calloc(i,sizeof(float));
                                        C16[Dset]=calloc(i,sizeof(float));
                                        C20[Dset]=calloc(i,sizeof(float));
                                        C21[Dset]=calloc(i.sizeof(float));
                                        C22[Dset]=calloc(i,sizeof(float));
                                        C23[Dset]=calloc(i,sizeof(float));
                                        C24[Dset]=calloc(i.sizeof(float));
                                        C25[Dset]=calloc(i,sizeof(float));
                                        C26[Dset]=calloc(i,sizeof(float));
                                        C27[Dset]=calloc(i,sizeof(float));
                                        C28[Dset]=calloc(i,sizeof(float));
                                        C29[Dset]=calloc(i,sizeof(float));
                                        C30[Dset]=calloc(i,sizeof(float));
                                        C31[Dset]=calloc(i,sizeof(float));
                                        C32[Dset]=calloc(i,sizeof(float));
                                        C33[Dset]=calloc(i,sizeof(float));
                                        C34[Dset]=calloc(i,sizeof(float));
                                        C35[Dset]=calloc(i,sizeof(float));
                                        C36[Dset]=calloc(i,sizeof(float));
                                        C37[Dset]=calloc(i,sizeof(float));
                                        t[Dset]=calloc(i,sizeof(float));
                                        b_weight[Dset]=calloc(i,sizeof(float));
                                        C16_weight[Dset]=calloc(i,sizeof(float));
                                        C20_weight[Dset]=calloc(i,sizeof(float));
                                        C21_weight[Dset]=calloc(i,sizeof(float));
                                        C22_weight[Dset]=calloc(i,sizeof(float));
                                        C23_weight[Dset]=calloc(i,sizeof(float));
                                        C24_weight[Dset]=calloc(i,sizeof(float));
                                        C25_weight[Dset]=calloc(i,sizeof(float));
                                        C26_weight[Dset]=calloc(i,sizeof(float));
                                        C27_weight[Dset]=calloc(i,sizeof(float));
                                        C28_weight[Dset]=calloc(i,sizeof(float));
                                        C29_weight[Dset]=calloc(i,sizeof(float));
                                        C30_weight[Dset]=calloc(i,sizeof(float));
                                        C31_weight[Dset]=calloc(i,sizeof(float));
                                        C32_weight[Dset]=calloc(i,sizeof(float));
                                        C33_weight[Dset]=calloc(i,sizeof(float));
                                        C34_weight[Dset]=calloc(i,sizeof(float));
                                        C35_weight[Dset]=calloc(i,sizeof(float));
                                        C36_weight[Dset]=calloc(i,sizeof(float));
                                        C37_weight[Dset]=calloc(i,sizeof(float));
```

```
for (ind=0;ind<i;ind++)
{

        *(b[Dset]+ind)=*(Bio+ind);
        *(C16[Dset]+ind)=*(S16+ind);
        *(C20[Dset]+ind)=*(S20+ind);
        *(C21[Dset]+ind)=*(S21+ind);
        *(C22[Dset]+ind)=*(S22+ind);
        *(C23[Dset]+ind)=*(S23+ind);
        *(C24[Dset]+ind)=*(S24+ind);
        *(C25[Dset]+ind)=*(S25+ind);
        *(C26[Dset]+ind)=*(S26+ind);
        *(C27[Dset]+ind)=*(S27+ind);
        *(C28[Dset]+ind)=*(S28+ind);
        *(C29[Dset]+ind)=*(S29+ind);
        *(C30[Dset]+ind)=*(S30+ind);
        *(C31[Dset]+ind)=*(S31+ind);
        *(C32[Dset]+ind)=*(S32+ind);
        *(C33[Dset]+ind)=*(S33+ind);
        *(C34[Dset]+ind)=*(S34+ind);
        *(C35[Dset]+ind)=*(S35+ind);
        *(C36[Dset]+ind)=*(S36+ind);
        *(C37[Dset]+ind)=*(S37+ind);
        *(t[Dset]+ind)=*(minute+ind);
        *(b_weight[Dset]+ind)=*(w_Bio+ind);
        *(C16_weight[Dset]+ind)=*(w_S16+ind);
        *(C20_weight[Dset]+ind)=*(w_S20+ind);
        *(C21_weight[Dset]+ind)=*(w_S21+ind);
        *(C22_weight[Dset]+ind)=*(w_S22+ind);
        *(C23_weight[Dset]+ind)=*(w_S23+ind);
        *(C24_weight[Dset]+ind)=*(w_S24+ind);
        *(C25_weight[Dset]+ind)=*(w_S25+ind);
        *(C26_weight[Dset]+ind)=*(w_S26+ind);
        *(C27_weight[Dset]+ind)=*(w_S27+ind);
        *(C28_weight[Dset]+ind)=*(w_S28+ind);
        *(C29_weight[Dset]+ind)=*(w_S29+ind);
        *(C30_weight[Dset]+ind)=*(w_S30+ind);
        *(C31_weight[Dset]+ind)=*(w_S31+ind);
        *(C32_weight[Dset]+ind)=*(w_S32+ind);
        *(C33_weight[Dset]+ind)=*(w_S33+ind);
        *(C34_weight[Dset]+ind)=*(w_S34+ind);
        *(C35_weight[Dset]+ind)=*(w_S35+ind);
        *(C36_weight[Dset]+ind)=*(w_S36+ind);
        *(C37_weight[Dset]+ind)=*(w_S37+ind);

}

*(minute)=*(minute+i);
last[Dset] = i-1;
Dset++;
Max_b[Dset] = 0;
Max_C16[Dset] = 0;
Max_C20[Dset] = 0;
Max_C21[Dset] = 0;
Max_C22[Dset] = 0;
Max_C23[Dset] = 0;
```

```
Max_C24[Dset] = 0;
Max_C25[Dset] = 0;
Max_C26[Dset] = 0;
Max_C27[Dset] = 0;
Max_C28[Dset] = 0;
Max_C29[Dset] = 0;
Max_C30[Dset] = 0;
Max_C31[Dset] = 0;
Max_C32[Dset] = 0;
Max_C33[Dset] = 0;
Max_C34[Dset] = 0;
Max_C35[Dset] = 0;
Max_C36[Dset] = 0;
Max_C37[Dset] = 0;

i = 0;
}

if (!End_of_File)
{

fscanf(datain,"%f%f%f%f%f%f%f%f%f%f%f%f%f%f%f%f%f%f%f%f%f%f%f%f%f%f%f%
f%f%f%f%f%f%f%f%f%f%f%f",

Bio+i,S16+i,S20+i,S21+i,S22+i,S23+i,S24+i,S25+i,S26+i,S27+i,S28+i,S29+i,S30+i,S31+i,S32+i
,S33+i,S34+i,S35+i,S36+i,S37+i,w_Bio+i, w_S16+i, w_S20+i, w_S21+i, w_S22+i,w_S23+i, w_S24+i,
w_S25+i, w_S26+i, w_S27+i,w_S28+i, w_S29+i, w_S30+i, w_S31+i, w_S32+i,w_S33+i, w_S34+i,
w_S35+i, w_S36+i, w_S37+i);
if (*(S16+i) > Max_C16[Dset])
        Max_C16[Dset] = *(S16+i);
if (*(S20+i) > Max_C20[Dset])
        Max_C20[Dset] = *(S20+i);
if (*(S21+i) > Max_C21[Dset])
        Max_C21[Dset] = *(S21+i);
if (*(S22+i) > Max_C22[Dset])
        Max_C22[Dset] = *(S22+i);
if (*(S23+i) > Max_C23[Dset])
        Max_C23[Dset] = *(S23+i);
if (*(S24+i) > Max_C24[Dset])
        Max_C24[Dset] = *(S24+i);
if (*(S25+i) > Max_C25[Dset])
        Max_C25[Dset] = *(S25+i);
if (*(S26+i) > Max_C26[Dset])
        Max_C26[Dset] = *(S26+i);
if (*(S27+i) > Max_C27[Dset])
        Max_C27[Dset] = *(S27+i);
if (*(S28+i) > Max_C28[Dset])
        Max_C28[Dset] = *(S28+i);
if (*(S29+i) > Max_C29[Dset])
        Max_C29[Dset] = *(S29+i);
if (*(S30+i) > Max_C30[Dset])
        Max_C30[Dset] = *(S30+i);
if (*(S31+i) > Max_C31[Dset])
        Max_C31[Dset] = *(S31+i);
if (*(S32+i) > Max_C32[Dset])
        Max_C32[Dset] = *(S32+i);
```

```
                                        if (*(S33+i) > Max_C33[Dset])
                                                Max_C33[Dset] = *(S33+i);
                                        if (*(S34+i) > Max_C34[Dset])
                                                Max_C34[Dset] = *(S34+i);
                                        if (*(S35+i) > Max_C35[Dset])
                                                Max_C35[Dset] = *(S35+i);
                                        if (*(S36+i) > Max_C36[Dset])
                                                Max_C36[Dset] = *(S36+i);
                                        if (*(S37+i) > Max_C37[Dset])
                                                Max_C37[Dset] = *(S37+i);
                                        if (*(Bio+i) > Max_b[Dset])
                                                Max_b[Dset] = *(Bio+i);
                                        i++;
                                        fscanf(datain,"%f",minute+i);
                                        First_Pass = 0;
                                        }

}

//for(i=0;i<MAX_DATA;i++)
//{printf(datain,"%f\n",(minute+i));}

Dset--;
fclose(datain);
free(minute);free(S16);free(S20);free(S21);free(S22);free(S23);free(S24);
free(S25);free(S26);free(S27);free(S28);free(S29);free(S30);
free(S31);free(S32);free(S33);free(S34);free(S35);free(S36);
free(S37);free(Bio);free(w_Bio);free(w_S16);free(w_S20);
free(w_S21);free(w_S22);free(w_S23);free(w_S24);free(w_S25);free(w_S26);
free(w_S27);free(w_S28);free(w_S29);free(w_S30);free(w_S31);free(w_S32);
free(w_S33);free(w_S34);free(w_S35);free(w_S36);free(w_S37);

/**************************************
                Call to Sugal
**************************************/

SuRegisterParameters (my_parameters);
SuaEvaluationFunction = evaluate;
SuRun( "korna.cfg" , argc, argv );

export(parameters,NO_PARAMS);

for(i=0;i<=Dset;i++)
{free(b[i]);
free(C16[i]);
free(C20[i]);
free(C21[i]);
free(C22[i]);
free(C23[i]);
free(C24[i]);
free(C25[i]);
free(C26[i]);
free(C27[i]);
free(C28[i]);
free(C29[i]);
free(C30[i]);
```

```
        free(C31[i]);
        free(C32[i]);
        free(C33[i]);
        free(C34[i]);
        free(C35[i]);
        free(C36[i]);
        free(C37[i]);
        free(t[i]);
        free(b_weight[i]);
        free(C16_weight[i]);
        free(C20_weight[i]);
        free(C21_weight[i]);
        free(C22_weight[i]);
        free(C23_weight[i]);
        free(C24_weight[i]);
        free(C25_weight[i]);
        free(C26_weight[i]);
        free(C27_weight[i]);
        free(C28_weight[i]);
        free(C29_weight[i]);
        free(C30_weight[i]);
        free(C31_weight[i]);
        free(C32_weight[i]);
        free(C33_weight[i]);
        free(C34_weight[i]);
        free(C35_weight[i]);
        free(C36_weight[i]);
        free(C37_weight[i]);}

        return (0);
}
/*************************************************************************
                The Model Goes Here
*************************************************************************/
long double model(long double *X,int equation)
{
        /*****************************************
                X[0] = C16
                X[1] = C20
                X[2] = C21
                X[3] = C22
                X[4] = C23
                X[5] = C24
                X[6] = C25
                X[7] = C26
                X[8] = C27
                X[9] = C28
                X[10] = C29
                X[11] = C30
                X[12] = C31
                X[13] = C32
                X[14] = C33
                X[15] = C34
                X[16] = C35
                X[17] = C36
                X[18] = C37
```

```
            X[19] = Biomass
*****************************************/

long double mu1=umax16*X[0]/(Ks16+X[0]);
long double mu2=umax20*X[1]/(Ks20+X[1]);
long double mu3=umax21*X[2]/(Ks21+X[2]);
long double mu4=umax22*X[3]/(Ks22+X[3]);
long double mu5=umax23*X[4]/(Ks23+X[4]);
long double mu6=umax24*X[5]/(Ks24+X[5]);
long double mu7=umax25*X[6]/(Ks25+X[6]);
long double mu8=umax26*X[7]/(Ks26+X[7]);
long double mu9=umax27*X[8]/(Ks27+X[8]);
long double mu10=umax28*X[9]/(Ks28+X[9]);
long double mu11=umax29*X[10]/(Ks29+X[10]);
long double mu12=umax30*X[11]/(Ks30+X[11]);
long double mu13=umax31*X[12]/(Ks31+X[12]);
long double mu14=umax32*X[13]/(Ks32+X[13]);
long double mu15=umax33*X[14]/(Ks33+X[14]);
long double mu16=umax34*X[15]/(Ks34+X[15]);
long double mu17=umax35*X[16]/(Ks35+X[16]);
long double mu18=umax36*X[17]/(Ks36+X[17]);
long double mu19=umax37*X[18]/(Ks37+X[18]);


//Each differential equation goes under a case

        switch(equation){
                case 0:return(-1/(1.1)*mu1*X[19]);
                                        break;
                case 1:return(-1/(1.1)*mu2*X[19]);
                                        break;
                case 2:return(-1/(1.1)*mu3*X[19]);
                                        break;
                case 3:return(-1/(1.1)*mu4*X[19]);
                                        break;
                case 4:return(-1/(1.1)*mu5*X[19]);
                                        break;
                case 5:return(-1/(1.1)*mu6*X[19]);
                                        break;
                case 6:return(-1/(1.1)*mu7*X[19]);
                                        break;
                case 7:return(-1/(1.1)*mu8*X[19]);
                                        break;
                case 8:return(-1/(1.1)*mu9*X[19]);
                                        break;
                case 9:return(-1/(1.1)*mu10*X[19]);
                                        break;
                case 10:return(-1/(1.1)*mu11*X[19]);
                                        break;
                case 11:return(-1/(1.1)*mu12*X[19]);
                                        break;
                case 12:return(-1/(1.1)*mu13*X[19]);
                                        break;
                case 13:return(-1/(1.1)*mu14*X[19]);
                                        break;
                case 14:return(-1/(1.1)*mu15*X[19]);
```

```
                                        break;
                case 15:return(-1/(1.1)*mu16*X[19]);
                                        break;
                case 16:return(-1/(1.1)*mu17*X[19]);
                                        break;
                case 17:return(-1/(1.1)*mu18*X[19]);
                                        break;
                case 18:return(-1/(1.1)*mu19*X[19]);
                                        break;
                case
19:return((mu1+mu2+mu3+mu4+mu5+mu6+mu7+mu8+mu9+mu10+mu11+mu12+mu13+mu14+mu15+
mu16+mu17+mu18+mu19)*X[19]);
                                        break;
                                        }
return(0);
}

/*****************************************************************************
                        The Runge Kutta Procedure
*****************************************************************************/

double rungekutta(float t0,float h,long double *X)
{
double k[4][NO_VAR],X0[NO_VAR];
int i,n;

for (i=0;i<NO_VAR;i++)
        X0[i]=X[i];

for (n=0;n<3;n++){

        for (i=0;i<NO_VAR;i++)
                k[n][i]=h*model(X,i);

        for (i=0;i<NO_VAR;i++)
                X[i]=X0[i]+k[n][i]/2;

}
for (i=0;i<NO_VAR;i++)
        X[i]=X0[i]+k[2][i];

for (i=0;i<NO_VAR;i++)
        k[3][i]=h*model(X,i);

for (i=0;i<NO_VAR;i++)
        X[i]=X0[i]+(k[0][i]+2*k[0][i]+2*k[0][i]+k[0][i])/6.;

return(t0+h);
}

/*****************************************************************************
                        The Fitness Evaluation Procedure
*****************************************************************************/

void FitEval()
```

```
{
int i;
float dt,tt;
res = 0;
for (Cset=0;Cset<=Dset;Cset++)     // for each data set
        {
         i = 1;
         X[0] = *(C16[Cset]);   // C16
         X[1] = *(C20[Cset]);   // C20
         X[2] = *(C21[Cset]);   // C21
         X[3] = *(C22[Cset]);   // C22
         X[4] = *(C23[Cset]);   // C23
         X[5] = *(C24[Cset]);   // C24
         X[6] = *(C25[Cset]);   // C25
         X[7] = *(C26[Cset]);   // C26
         X[8] = *(C27[Cset]);   // C27
         X[9] = *(C28[Cset]);   // C28
         X[10] = *(C29[Cset]);   // C29
         X[11] = *(C30[Cset]);   // C30
         X[12] = *(C31[Cset]);   // C31
         X[13] = *(C32[Cset]);   // C32
         X[14] = *(C33[Cset]);   // C33
         X[15] = *(C34[Cset]);   // C34
         X[16] = *(C35[Cset]);   // C35
         X[17] = *(C36[Cset]);   // C36
         X[18] = *(C37[Cset]);   // C37
         X[19] = *(b[Cset]);   // Biomass
         tt = *(t[Cset]);              // Initial Time

         do
                 {
                         if (tt+dt_max<*(t[Cset]+i))
                                 {dt=dt_max;
                                 tt=rungekutta(tt,dt,X);
                                 continue;}
                         else
                                 {dt=*(t[Cset]+i)-tt+0.000001;
                                 tt=rungekutta(tt,dt,X);

                          res = res + 1000**(C16_weight[Cset]+i)*(*(C16[Cset]+i) -
X[0])*(*(C16[Cset]+i) - X[0])/(Max_C16[Cset]*Max_C16[Cset]);

                          res = res + 1000**(C20_weight[Cset]+i)*(*(C20[Cset]+i) -
X[1])*(*(C20[Cset]+i) - X[1])/(Max_C20[Cset]*Max_C20[Cset]);

                          res = res + 1000**(C21_weight[Cset]+i)*(*(C21[Cset]+i) -
X[2])*(*(C21[Cset]+i) - X[2])/(Max_C21[Cset]*Max_C21[Cset]);

                          res = res + 1000**(C22_weight[Cset]+i)*(*(C22[Cset]+i) -
X[3])*(*(C22[Cset]+i) - X[3])/(Max_C22[Cset]*Max_C22[Cset]);

                          res = res + 1000**(C23_weight[Cset]+i)*(*(C23[Cset]+i) -
X[4])*(*(C23[Cset]+i) - X[4])/(Max_C23[Cset]*Max_C23[Cset]);

                          res = res + 1000**(C24_weight[Cset]+i)*(*(C24[Cset]+i) -
X[5])*(*(C24[Cset]+i) - X[5])/(Max_C24[Cset]*Max_C24[Cset]);
```

```
                                res = res + 1000**(C25_weight[Cset]+i)*(*(C25[Cset]+i) -
X[6])*(*(C25[Cset]+i) - X[6])/(Max_C25[Cset]*Max_C25[Cset]);

                                res = res + 1000**(C26_weight[Cset]+i)*(*(C26[Cset]+i) -
X[7])*(*(C26[Cset]+i) - X[7])/(Max_C26[Cset]*Max_C26[Cset]);

                                res = res + 1000**(C27_weight[Cset]+i)*(*(C27[Cset]+i) -
X[8])*(*(C27[Cset]+i) - X[8])/(Max_C27[Cset]*Max_C27[Cset]);

                                res = res + 1000**(C28_weight[Cset]+i)*(*(C28[Cset]+i) -
X[9])*(*(C28[Cset]+i) - X[9])/(Max_C28[Cset]*Max_C28[Cset]);

                                res = res + 1000**(C29_weight[Cset]+i)*(*(C29[Cset]+i) -
X[10])*(*(C29[Cset]+i) - X[10])/(Max_C29[Cset]*Max_C29[Cset]);

                                res = res + 1000**(C30_weight[Cset]+i)*(*(C30[Cset]+i) -
X[11])*(*(C30[Cset]+i) - X[11])/(Max_C30[Cset]*Max_C30[Cset]);

                                res = res + 1000**(C31_weight[Cset]+i)*(*(C31[Cset]+i) -
X[12])*(*(C31[Cset]+i) - X[12])/(Max_C31[Cset]*Max_C31[Cset]);

                                res = res + 1000**(C32_weight[Cset]+i)*(*(C32[Cset]+i) -
X[13])*(*(C32[Cset]+i) - X[13])/(Max_C32[Cset]*Max_C32[Cset]);

                                res = res + 1000**(C33_weight[Cset]+i)*(*(C33[Cset]+i) -
X[14])*(*(C33[Cset]+i) - X[14])/(Max_C33[Cset]*Max_C33[Cset]);

                                res = res + 1000**(C34_weight[Cset]+i)*(*(C34[Cset]+i) -
X[15])*(*(C34[Cset]+i) - X[15])/(Max_C34[Cset]*Max_C34[Cset]);

                                res = res + 1000**(C35_weight[Cset]+i)*(*(C35[Cset]+i) -
X[16])*(*(C35[Cset]+i) - X[16])/(Max_C35[Cset]*Max_C35[Cset]);

                                res = res + 1000**(C36_weight[Cset]+i)*(*(C36[Cset]+i) -
X[17])*(*(C36[Cset]+i) - X[17])/(Max_C36[Cset]*Max_C36[Cset]);

                                res = res + 1000**(C37_weight[Cset]+i)*(*(C37[Cset]+i) -
X[18])*(*(C37[Cset]+i) - X[18])/(Max_C37[Cset]*Max_C37[Cset]);

                                res = res + 1000**(b_weight[Cset]+i)*(*(b[Cset]+i) - X[19])*(*(b[Cset]+i) -
X[19])/(Max_b[Cset]*Max_b[Cset]);

                                if (res>=powl(10,300)) return;
                                i++;}
                        }while (tt < *(t[Cset]+last[Cset]));
                }
                }

//*************************************************************************
//                      Chromosome evaluation
//*************************************************************************
int evaluate(SuChromosome *chrom, double *fitness)
{
double a[NO_PARAMS];
int i;
```

```
static double low=1e12;
        for (i=0; i < SuGenesInChromosome(chrom);i++)
                a[i] = SuGetGeneAsInt (chrom->string, i);
        //ranges of parameters
                umax16=0.01+3*a[0]/255.0;
                umax20=0.001+0.4*a[1]/255.0;
                umax21=0.001+0.4*a[2]/255.0;
                umax22=0.001+0.4*a[3]/255.0;
                umax23=0.001+0.4*a[4]/255.0;
                umax24=0.001+0.4*a[5]/255.0;
                umax25=0.001+0.4*a[6]/255.0;
                umax26=0.001+0.4*a[7]/255.0;
                umax27=0.001+0.4*a[8]/255.0;
                umax28=0.001+0.4*a[9]/255.0;
                umax29=0.001+0.4*a[10]/255.0;
                umax30=0.001+0.4*a[11]/255.0;
                umax31=0.001+0.4*a[12]/255.0;
                umax32=0.001+0.4*a[13]/255.0;
                umax33=0.001+0.4*a[14]/255.0;
                umax34=0.001+0.4*a[15]/255.0;
                umax35=0.001+0.4*a[16]/255.0;
                umax36=0.001+0.4*a[17]/255.0;
                umax37=0.001+0.4*a[18]/255.0;

                Ks16=1+300*a[19]/255.0;
                Ks20=1+100*a[20]/255.0;
                Ks21=1+100*a[21]/255.0;
                Ks22=1+100*a[22]/255.0;
                Ks23=1+100*a[23]/255.0;
                Ks24=1+100*a[24]/255.0;
                Ks25=1+100*a[25]/255.0;
                Ks26=1+100*a[26]/255.0;
                Ks27=1+100*a[27]/255.0;
                Ks28=1+100*a[28]/255.0;
                Ks29=1+100*a[29]/255.0;
                Ks30=1+100*a[30]/255.0;
                Ks31=1+100*a[31]/255.0;
                Ks32=1+100*a[32]/255.0;
                Ks33=1+100*a[33]/255.0;
                Ks34=1+100*a[34]/255.0;
                Ks35=1+100*a[35]/255.0;
                Ks36=1+100*a[36]/255.0;
                Ks37=1+100*a[37]/255.0;
        FitEval();
        if (res < low)
        {
         low = res;

         parameters[0]=umax16;
         parameters[1]=umax20;
         parameters[2]=umax21;
         parameters[3]=umax22;
         parameters[4]=umax23;
         parameters[5]=umax24;
         parameters[6]=umax25;
         parameters[7]=umax26;
```

```
                parameters[8]=umax27;
                parameters[9]=umax28;
                parameters[10]=umax29;
                parameters[11]=umax30;
                parameters[12]=umax31;
                parameters[13]=umax32;
                parameters[14]=umax33;
                parameters[15]=umax34;
                parameters[16]=umax35;
                parameters[17]=umax36;
                parameters[18]=umax37;
                parameters[19]=Ks16;
                parameters[20]=Ks20;
                parameters[21]=Ks21;
                parameters[22]=Ks22;
                parameters[23]=Ks23;
                parameters[24]=Ks24;
                parameters[25]=Ks25;
                parameters[26]=Ks26;
                parameters[27]=Ks27;
                parameters[28]=Ks28;
                parameters[29]=Ks29;
                parameters[30]=Ks30;
                parameters[31]=Ks31;
                parameters[32]=Ks32;
                parameters[33]=Ks33;
                parameters[34]=Ks34;
                parameters[35]=Ks35;
                parameters[36]=Ks36;
                parameters[37]=Ks37;

                //export(parameters,NO_PARAMS);
              }
              *fitness = res;
 return 0;
}
void export(double *parameters,int number)
{
double *ptr;
FILE *dataout;
dataout=fopen("mat2.out","w");
for (ptr=parameters;ptr<(parameters+number);ptr++)
fprintf(dataout,"%f\n",*ptr);
fclose(dataout);
}
```

These are the Matlab m-files used to solve and plot the figures 10-1 to 10-4.

mass7.m

```
function yprime=mass7(t,y);

format long;
load c:\sugal\mat2.out
load c:\sugal\yldrun7.dat
for i=1:19
  umax(i)=mat2(i);
end
s=1;
for j=20:38
  Ks(s)=mat2(j);
  s=s+1;
end
for i=1:19
  k=i+1;
  mu(i)=umax(i)*(y(k)/(Ks(i)+y(k)));
end
for l=1:18
  Y(l)=yldrun7(l);
end
yprime1=[(sum(mu))*y(1);
    -1/(1.1)*mu(1)*y(1);];
for g=1:18
  h=g+1;
  yprime2(g,:)=[-1/Y(g)*mu(h)*y(1);];
end
yprime=[yprime1;yprime2];
```

mass7run.m

```
[t,y]=ode45('mass7', [0 400], [0.404071 0.483748 0.002927 0.003587 0.01014 0.016403 0.020697
0.024069 0.019168 0.014981 0.012353 0.008748 0.005115 0.004141 0.002189 0.001656 0.001006
0.000682 0.000578 0.000716]);

format long;
% R E A L   D A T A
load c:\sugal\massrun7.dat;
load c:\sugal\mat2.out;
[R,C]=size(massrun7);
newmassive=massrun7;
newmassive(13,:)=[];
figure(1);
subplot(1,2,1);
xxxx=1:19;
bar(xxxx,mat2(1:19));
title('umax')
subplot(1,2,2);
yyyy=1:19;
bar(yyyy,mat2(20:38));
title('Ks')
```

```
%Biomass and C16
  figure(2);
  x1=newmassive(:,1);
  y1=newmassive(:,2);
  y2=newmassive(:,3);
  X=y(:,1);
  C16=y(:,2);
  plot(x1,y1,'o',t,X);
  xlabel('Time (min)'),ylabel('Biomass (g/L)');
  title('Biomass');
     figure(3);
  x1=newmassive(:,1);
  y1=newmassive(:,2);
  y2=newmassive(:,3);
  X=y(:,1);
  C16=y(:,2);
  plot(x1,y2,'o',t,C16);
  title('C16');
  xlabel('Time (min)'),ylabel('Hexadecane (g/L)');

C=20;
n=7;
m=4;
for z=4:8
  figure(z)
  k=1;
     for i=m:n
      q=i-1;
      xx=newmassive(:,1);
      yy=newmassive(:,i);
      w=y(:,q);
      subplot(2,2,k);
      plot(t,w,xx,yy,'o');
      xlabel('Time (min)'),ylabel('Subtrate (g/L)');
      B=['C'num2str(C)];
      title(B)
      k=k+1;
      C=C+1;
     end

  m=m+4;
  n=n+4;
  z=z+1;
end
```